INVESTIGATION OF THE INFLUENCE OF WATER PARAMETERS ON GALVANIC CORROSION OF LEAD AND THE ROLE OF ORTHOPHOSPHATE IN INHIBITION OF LEAD RELEASE IN DRINKING WATER DISTRIBUTION SYSTEM

NG DING QUAN

NATIONAL UNIVERSITY OF SINGAPORE

2013

INVESTIGATION OF THE INFLUENCE OF WATER PARAMETERS ON GALVANIC CORROSION OF LEAD AND THE ROLE OF ORTHOPHOSPHATE IN INHIBITION OF LEAD RELEASE IN DRINKING WATER DISTRIBUTION SYSTEM

NG DING QUAN

(B. Eng. (Hons.), NUS)

A THESIS SUBMITTED

FOR THE DEGREE OF DOCTOR OF PHILOSOPHY

DEPARTMENT OF CIVIL AND ENVIRONMENTAL ENGINEERING

NATIONAL UNIVERSITY OF SINGAPORE

2013

DECLARATION

I hereby declare that the thesis is my original work and it has been written by me in its entirety. I have duly acknowledged all the sources of information which have been used in the thesis.

This thesis has also not been submitted for any degree in any university previously.

Ng Ding Quan

3 August 2013

ACKNOWLEDGEMENTS

TABLE OF CONTENT

SUMMARY

Lead contamination in drinking water has raised concerns in many developed cities in recent years. Lead can be released into drinking water from lead pipes, brass and solder that contain lead, and lead-bearing corrosion products on the pipe inner surfaces. Addition of orthophosphate has been commonly employed to suppress lead levels in drinking water. Its detailed mechanism, however, has not been fully elucidated. Recent cases of lead contamination in drinking water have been found in cities with no lead pipes, suggesting the source of lead to other piping materials such as leaded solders and brass fittings. These findings led to the development of a series of studies involving galvanic corrosion in drinking water and drinking water sampling protocols.

To better understand how lead behaves in drinking water, namely lead release and lead corrosion inhibition, well-controlled batch experiments and a pilot study were conducted to provide essential information previously lacking in the literature. The objectives of this study are (1) to investigate the mechanistic role of orthophosphate in lead release from PbO_2 in chloraminated drinking water, (2) to examine the effects of pH, chloride, sulfate, free chlorine, monochloramine and orthophosphate on galvanic corrosion between lead and copper in drinking water and (3) to identify lead sources and evaluate the effects of free chlorine, monochloramine and orthophosphate on lead release in a simulated premise drinking water distribution system using a modified sampling method.

Firstly, the mechanistic role of orthophosphate as a corrosion inhibitor in controlling lead release from PbO_2 in chloraminated solutions was investigated. In all experiments with orthophosphate addition of at least 1 mg/L as P, peaking of soluble Pb(II) concentration within the first 24 h was observed. The variation of soluble Pb(II) concentration could be attributed to the dynamics between the rate of PbO_2 reductive dissolution and that of chloropyromorphite ($Pb_5(PO_4)_3Cl$) precipitation.

Secondly, the effects of various water parameters on galvanic corrosion between lead and copper were investigated. In stagnant conditions, reducing pH and increasing either chloride or sulfate concentrations promoted soluble lead release. The effect of chloride concentration on soluble lead release was similar to that of sulfate at the same molar concentration and the chloride-to-sulfate mass ratio (CSMR) did not provide a good indication for soluble lead release. Soluble lead release increased while soluble copper decreased as initial free chlorine or monochloramine concentration increased and the rate of disinfectant decay was slower. Total lead release increased with increasing orthophosphate concentrations while soluble lead release decreased.

Lastly, a modified sampling protocol was proposed and evaluated. The sampling protocol could detect lead contamination and locate the source of lead release more effectively than existing protocols. "Lead-free" brass fittings were identified as the source of lead in this study. Elevated lead levels persisted for as long as five months in newly installed piping systems. Physical disturbances such as tap installation caused short-term spikes in lead release. Orthophosphate was able to suppress total lead release, but caused "blue water" problem. Total lead levels were suppressed when either free chlorine or monochloramine was first introduced to the system.

LIST OF TABLES

LIST OF FIGURES

NOMENCLATURE

ASV	Anodic stripping voltammetry
BS	British Standard
CSMR	Chloride-to-sulfate mass ratio
C_T	Total dissolved inorganic carbon
DPD-FAS	N,N-diethyl-p-phenylene diamine-ferrous ammonium sulfate
EDX	Energy dispersive X-ray spectroscopy
FE-SEM	Field emission-scanning electron microscopy
FWHM	Full width half maximum
HCl	Hydrochloric acid
HOCl	Hypochlorous acid
IAP	Ion activity product
ICDD	International Center for Diffraction Data
ICP-OES	Inductively coupled plasma mass spectrometer optical emission spectrometry
K_{sp}	Solubility product
LCR	Lead and Copper Rule
LSLs	Lead service lines
MCLG	Maximum Contaminant Level Goal
MDL	Method detection limit
Na_2HPO_4	Sodium hydrogen phosphate

Na_2SO_4	Sodium sulfate
$NaCl$	Sodium chloride
$NaHCO_3$	Sodium bicarbonate
$NaOCl$	Sodium hypochlorite
$NaOH$	Sodium hydroxide
NH_2Cl	Monochloramine
NH_4Cl	Ammonium chloride
$NHCl_2$	Dichloramine
NOM	Natural organic matter
$Pb(NO_3)_2$	Lead nitrate
$Pb(OH)_2$	Lead hydroxide
$Pb_3(CO_3)_2(OH)_2$	Hydrocerussite
$Pb_3(PO_4)_2$	Secondary lead phosphate
$Pb_5(PO_4)_3Cl$	Chloropyromorphite
$Pb_5(PO_4)_3OH$	Hydroxypyromorphite
$PbCO_3$	Cerussite
$PbO:PbSO_4$	Larnakite
PDF	Powder Diffraction File
P_T	Total phosphate
PUB	Public Utilities Board
RDT	Random daytime
SI	Saturation index
USEPA	US Environmental Protection Agency

VA	Voltammetry
WHO	World Health Organization
XPS	X-ray photoelectron spectrometer
XRD	X-ray diffraction
Ω	Supersaturation ratio
α-PbO$_2$	Scrutinyite
β-PbO$_2$	Plattnerite

Chapter 1

Introduction and Background

1.1   Drinking water as a source of lead

Consumption of drinking water contaminated with lead can cause serious gastrointestinal and neurological problems, especially to children and fetus [1-3]. To safeguard public health, the use of lead pipes in the distribution system was banned under the Safe Drinking Water Act in 1986 in the US [4], followed by the implementation of the Lead and Copper Rule (LCR) in 1991, which set a Maximum Contaminant Level Goal (MCLG) of zero mg/L for lead and an action level for lead at 0.015 mg/L [5]. Compliance with the action level is determined by measuring lead concentration in a number of samples collected at the point of use using a first-draw 1-L sample after a stagnation period of at least 6 h with 90% of the samples below 0.015 mg/L [6]. The guideline value for lead in drinking water set by the World Health Organization (WHO) is 0.01 mg/L [7].

Lead concentration in drinking water is mainly regulated by chemical reactions that occur within service lines and premise plumbing. Lead can be released into drinking water from lead pipes, brass and solder that contain lead, and lead-bearing corrosion products on the pipe inner surfaces. Several studies have shown that lead corrosion products predominantly exist as Pb(II) and Pb(IV) solid phases, including hydrocerussite ($Pb_3(CO_3)_2(OH)_2$) and cerussite ($PbCO_3$) [8-12] and in cases where a high free chlorine residual is maintained, plattnerite (β-PbO_2) and scrutinyite (α-PbO_2), with the former more commonly found on the inner surfaces of lead pipes [10, 12]. More recently, Pb_3O_4, a Pb(II)/Pb(IV) solid intermediate was discovered in drinking water distribution system [12]. Their stability in the distribution system, however, is not fully understood and hence cannot be well controlled. For example, there was a dramatic increase of lead concentration in Washington D.C. drinking water from 2001 to 2004 due to the switch of disinfectant from free chlorine to monochloramine to reduce disinfection by-products formation [13, 14]. This

event was linked to an increase in blood lead levels in young children by more than 4 times from 2001-2003 compared to data collected in 2000 and drinking water was first recognized as a potential lead exposure route to human [15, 16].

The change of disinfectant destabilized PbO_2 that was previously formed on the pipe inner surfaces and resulted in high lead concentrations far above the action level [13, 14]. Although PbO_2 has a low solubility in water, its reductive dissolution is impacted by a variety of water quality parameters. It has been found that the presence of natural organic matter (NOM) and auto-decomposition of monochloramine can cause reductive dissolution of PbO_2 [17-20]. It has been proposed that monochloramine can simultaneously promote PbO_2 reductive dissolution by an unknown intermediate generated from its auto-decomposition [17] and reduce lead release from PbO_2 by increasing the redox potential of the system, with longer contact time favoring the former mechanism [21]. An increase in dissolved inorganic carbon concentration can also accelerate the dissolution of PbO_2 via ligand-induced dissolution, while an increase in pH reduces dissolution rates [22].

1.2 Lead corrosion in drinking water distribution systems (DWDSs)

Although lead pipes are no longer installed in the US, UK, Germany, Canada, Australia, the Netherlands and many other countries since the 1980s, many older districts still contain lead service lines pending replacement or have leaded solders used in their distribution systems [23-27]. In 2006, tap water in Durham, North Carolina, was found to contain more than 800 µg/L lead despite having no lead pipes in the city [16]. The source of elevated lead was traced to a lead solder and the lead release was attributed to a change in coagulant chemical used from aluminum sulfate to ferric chloride. The increased chloride-to-sulfate mass ratio (CSMR) was believed to trigger galvanic corrosion of the lead solder and caused hazardous levels of lead released into drinking water [28]. Anion exchange for arsenic and organic anions removal which releases chloride to the treated water can also result in high CSMR [29]. Galvanic corrosion was reported to occur during partial lead pipes replacement with copper pipes [23] and in brass materials which are commonly found in premise plumbing [30, 31]. Recent cases of elevated lead in tap water, mainly in places without lead pipes, have been attributed to galvanic corrosion of metal alloys such as brass. "Lead-free" brass may contain up to 8% lead by mass [4] and can contribute a significant amount of lead to drinking water. Lead is seldom used as a raw material in making brass, but it is usually present as a contaminant from the recycling of materials and during casting [32]. Elfland, et. al [31] showed that certified ball valves could contain a significantly higher lead mass ratio on the surface than the whole valve. In recent years, lead contamination in drinking water caused by galvanic corrosion in leaded solders, brass fittings and during partial replacement of lead pipes has raised concerns of the public. Many studies have been conducted using a more practical approach with pipes and fittings. However, some phenomena could not be explained due to the complex nature of these systems. For example, the use of brass fittings in lead release studies [14, 28] is highly dependent on the brass composition, exposure time and water quality [33].

1.3   Galvanic corrosion of lead in drinking water

Corrosion is the physiochemical interaction between a metal and its environment which results in changes in the properties of the metal [34]. Galvanic corrosion occurs when at least two metals are involved, with the more noble metal acting as the cathode and the less noble metal acting as the anode in an electrolyte. When lead and copper are galvanic connected, copper acts as the cathode and lead acts as the anode. Oxidation (corrosion) occurs at the lead anode with the production of free electrons while reduction occurs at the copper cathode where the free electrons are consumed. Elemental lead is oxidized to soluble Pb^{2+} at the anode while at the cathode, dissolved oxygen is reduced to produce hydroxide ions in alkaline conditions and water in neutral or acidic conditions (Figure 1.1). In the absence of dissolved oxygen, hydrogen ions will be reduced to produce hydrogen gas at the cathode instead.
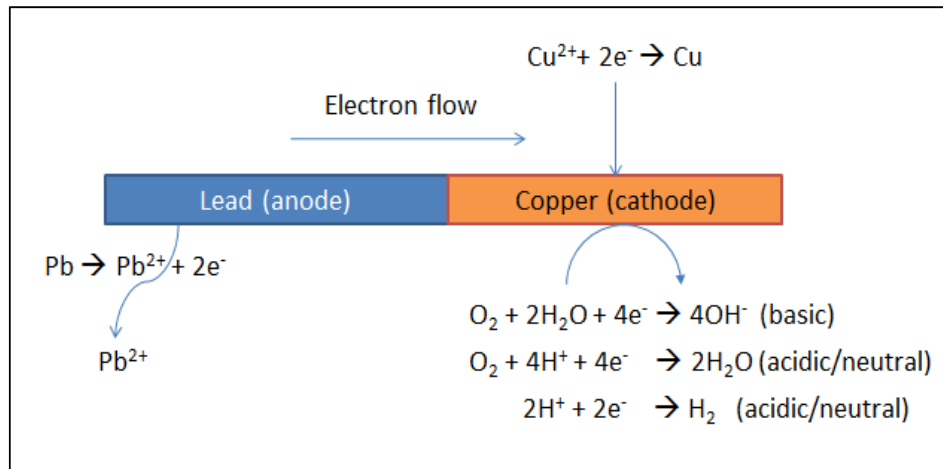
Figure 1.1 Galvanic corrosion between lead and copper in drinking water

Galvanic corrosion can be predicted by using the electromotive force (emf) or standard electrode potential series for metal reduction. The closer the standard potentials of the two metals are, the weaker the galvanic effect is and vice versa [35]. The relation between reaction Gibbs energy and the emf of the cell is given by equation 1.1:

$$-vFE = \Delta_r G \qquad (1.1)$$

where F is Faraday's constant, v is the stoichiometric coefficient of the electrons in the half-reactions. A positive emf gives a negative reaction Gibbs energy which corresponds to a spontaneous cell reaction. However, the above thermodynamic discussion only indicates whether a tendency to corrode exists and not the kinetics of the reactions involved [36].

Various methods such as measuring galvanic current, galvanic corrosion potential and soluble metal concentration have been employed to quantify the corrosion [28, 37-41]. Galvanic current is a direct measurement of the rate of corrosion. St. Clair, et. al [42] showed that galvanic current and total lead concentration decreased with the increasing distance between lead and copper pipes connected via an external grounding strap. Nguyen, et al. [43] observed that galvanic current increased with lead release using lead/tin solder-copper pipe couple, consistent with Faraday's law. However, it poses technical difficulty in application in real distribution systems because it is impossible to measure galvanic current between two metals with direct connection. Galvanic corrosion potential, which is dependent on the electrolyte conductivity, indicates if galvanic activity is occurring but does not provide information about the rate. An increase in galvanic corrosion potential due to an increase in electrolyte conductivity is insufficient to conclude that the rate of galvanic corrosion is increased [38]. The type of metal to be corroded and the rate of corrosion depend on factors such as changes in electrolyte composition and temperature that cause a shift in potential positioning in the galvanic series (Figure 1.2) [44].

```
Corroded end (anodic, or least noble)
Magnesium
Magnesium alloys
Zinc

Aluminum
Cadmium

Steel or iron
Cast iron

Iron alloys

Lead–tin solders
Lead
Tin

Nickel

Brasses
Copper
Bronzes

Titanium
Monel
Silver solder

Silver
Carbon (graphite)
Gold

Noncorroded end (cathodic, or most noble)
```

Figure 1.2 Galvanic series [45]

Oliphant [37] first reported that galvanic currents between lead solder and copper plates increased with increasing chloride concentrations. Similarly, Gregory [38] showed that an increase in chloride concentration increased both galvanic current and galvanic corrosion potential between lead solder and copper foil while an increase in sulfate concentration showed the reverse. Edwards and Triantafyllidou [28] demonstrated an increase in lead leaching with an increase in CSMR when lead-tin solder was connected to copper. The use of CSMR was proposed as an indicator for lead corrosion in drinking water. However, many related works were focused on the role of chloride with little emphasis placed on sulfate. In addition, lead-tin solder had been used in many studies and the role of tin in galvanic corrosion was often neglected. Hence, a simpler and more direct approach using pure metals can be used to compare the effects of chloride and sulfate.

Edwards & Dudi [14] observed that the presence of either monochloramine or free chlorine promoted more lead release from brass device than that without disinfectant and the promotion was higher in the presence of monochloramine than that of free chlorine. Free chlorine has also been observed to promote galvanic currents between lead-tin solder and copper joint [46]. Free chlorine is known to oxidize soluble Pb(II) ions and Pb(II) solids to form reddish-brown PbO_2 which is relatively insoluble in water [10, 14, 47-50]. In a study using a recirculating flow system, potential reversal was observed between lead and copper pipes in the presence of free chlorine, but not monochloramine [51]. The disadvantages of using a recirculating flow are the accumulation of contaminants and its impracticability due to the fact that drinking water only flows through the pipe once in real systems.

Stagnant and flow conditions have been employed in numerous studies to study galvanic corrosion between lead and copper [29, 40, 51-53]. Their results, however, have not all been in agreement. For example, Boyd, et. al [52] reported a transient increase in lead levels caused by galvanic corrosion under recirculating flow conditions but Wang, et. al [53] demonstrated that elevated lead levels due to galvanic corrosion persisted over 6 weeks under flow conditions. Arnold and Edwards [51] showed that continuous flow resulted in lower lead release than intermittent flow. Cartier, et. al [54] showed that after a stagnation period of 16 h, samples collected at high flow rate (32 L/min) had higher total lead, predominantly as particulate lead, than those collected at low flow rate (1.3 L/min). Stagnant condition represents the worst case scenario as it allows the accumulation of corrosion products such as lead(II) oxide, lead(II) carbonates and lead(IV) oxides in a localized region while flow condition represents the more frequently encountered scenarios [11, 12]. In stagnant water, the surface pH at the lead anode in a lead-copper couple decreases with time, hindering surface passivation and enhancing further lead release [44]. Household consumers are often exposed to long standing water, which is likely to contain exceeding high levels of lead, in the morning and in the evening after returning from school or work.

7

1.4   Orthophosphate as a corrosion inhibitor

The addition of orthophosphate has been considered as an economical approach for lead release control to suppress lead concentration below the action level [55-57]. It is well established in lead geochemistry that Pb^{2+} can react with orthophosphate to precipitate relatively insoluble lead phosphate minerals such as chloropyromorphite ($Pb_5(PO_4)_3Cl$) which is the most stable Pb mineral under normal environmental conditions [58]. Thermodynamically, other Pb solids should be transformed to chloropyromorphite via a dissolution-reprecipitation mechanism with adequate orthophosphate and chloride addition [58, 59]. The solubility product (K_{sp}) for chloropyromorphite was reported to be $10^{-84.4}$ (Eq (1.2 - 1.3)) [60].

$$Pb_5(PO_4)_3Cl = 5Pb^{2+} + 3PO_4^{3-} + Cl^- \tag{1.2}$$
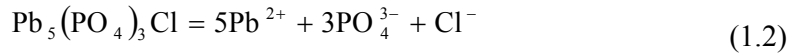
$$K_{sp} = \{Pb^{2+}\}^5 \{PO_4^{3-}\}^3 \{Cl^-\} = 10^{-84.4} \tag{1.3}$$

It has been reported that the addition of orthophosphate in drinking water can affect the type of corrosion products formed on pipe inner surfaces. For instance, free chlorine can oxidize Pb(II) ion and solids to form PbO_2 [10, 47, 49], but in the presence of orthophosphate, PbO_2 formation was inhibited [60]. Other lead phosphate minerals such as hydroxypyromorphite ($Pb_5(PO_4)_3OH$) and secondary lead phosphate ($Pb_3(PO_4)_2$) were formed instead [8, 61, 62]. These minerals, being less thermodynamically stable, should ideally transform to the more stable chloropyromorphite in the presence of chloride [10, 47, 49, 59-63]. The precipitation of chloropyromorphite has been observed at pH 7.0 and more acidic conditions with a chloride concentration of at least 35.5 mg/L [63-66] while hydroxypyromorphite formation has been reported at pH 8.0 with a lower chloride concentration of 6.8 mg/L [61]. It has been found that the effectiveness of using orthophosphate for lead release control in drinking water may depend on water chemistry and existing lead scales on pipe surfaces which could vary with pipe ages. Edwards and McNeill [56] observed that orthophosphate can reduce soluble lead release from old water pipes but promote lead release from new ones. In a separate

8

study by Edwards and Dudi [14], lead release from pure lead pipes in chloraminated waters was higher in the presence of orthophosphate than without. However, no detailed mechanism regarding the reactions of lead corrosion products was provided to explain the observations in both studies.

1.5   Sampling protocols

Under the LCR, a first-draw sample of 1 L is collected from household tap after at least six h of stagnation. This approach can detect lead release within the household, but it does not detect lead release in lead service lines (LSLs) [67]. In Europe, large numbers of random daytime (RDT) samples (without stagnation) and samples taken after a fixed stagnation time of 30 min were collected to provide a reasonable estimate of the average lead concentration at the tap [69, 69]. However, RDT sampling is not reproducible and a large number of samples would be required to gauge the effectiveness of corrosion control [70]. In Canada and France, sampling is conducted by a trained technician (30 min stagnation) while sampling is conducted by consumers (at least 6 h stagnation) in the United States [6, 71, 72].

In Singapore, the sampling protocol implemented by the Public Utilities Board (PUB) to detect lead in drinking water from tap has been found to be inadequate in safeguarding consumer health. According to the protocol, 1 L of water sample is collected by trained personnel after the tap has been flushed for about 3-5 min. The reason for flushing is because water after the water meter does not fall under PUB purview. No stagnation time is given to allow contaminants that may be released after the water meter to accumulate, hence potential lead release within the premise distribution system will likely be missed out. Table 1.1 shows the comparison between PUB and USEPA sampling protocol. To better protect public health, the sampling protocol in Singapore needs to be examined.

Table 1.1 Comparison between PUB and USEPA sampling protocol

	PUB	USEPA
Stagnation time	Not required	At least 6 h
Initial flush	3-5 min	-
1st draw sample volume	1 L	1 L

1.6   Objectives

To better understand how lead behaves in drinking water, namely its release and lead corrosion inhibition, well-controlled batch experiments were conducted to provide essential information previously lacking in the literature. The findings were then applied in a pilot study using simulated premise drinking water distribution system. The objectives of this study are as follow:

Objective 1:   To investigate the mechanistic role of orthophosphate in lead release from PbO_2 in chloraminated drinking water and its influence on the transformation of lead corrosion products to simulate systems experiencing disinfectant changeover.

Objective 2:   To examine the effects of pH, chloride, sulfate, free chlorine, monochloramine and orthophosphate on galvanic corrosion between lead and copper in drinking water.

Objective 3:   To identify lead sources and evaluate the effects of free chlorine, monochloramine and orthophosphate on lead release in a simulated premise drinking water distribution system using a modified sampling method.

1.7 Thesis organization

This thesis consists of six chapters. In Chapter 1, the background and objectives of this study are provided and relevant literatures are reviewed. In Chapter 2, the experimental setups and analytical methods employed are described. The results and discussion are presented in Chapters 3, 4 and 5. In Chapter 3, the mechanistic role of orthophosphate as a corrosion inhibitor in controlling lead release from tetravalent lead corrosion product PbO_2 in chloraminated solutions, a system representing distribution networks experiencing disinfectant changeover from free chlorine to monochloramine, was investigated. The effects of solution pH, monochloramine concentration and orthophosphate dosage on lead release were examined and the mineral composition and surface characteristics of the secondary solid phases formed in the experiments were determined. In Chapter 4, the effects of various water parameters such as pH, chloride, sulfate, free chlorine, monochloramine and orthophosphate, on galvanic corrosion between lead and copper in drinking water was examined. In Chapter 5, lead release in simulated premise drinking water distribution systems was examined using a modified sampling method. Three scenarios, namely orthophosphate addition, disinfectant switch from free chlorine to monochloramine and periodic free chlorine flushing were employed. Finally, Chapter 6 summarizes the findings of this study and provides recommendation for future studies.

Chapter 2

Materials and Methods

2.1   Reagents and chemicals

PbO_2 was prepared by adding concentrated NaOCl (~1M, Fisher Scientific) solution to 0.1 M $Pb(NO_3)_2$ (Sigma-Aldrich) solution with a $NaOCl/Pb^{2+}$ molar ratio of 1.1 according to the procedures described by Lin and Valentine [15]. The synthesized PbO_2 particles were freeze-dried and stored before use. Field emission-scanning electron microscopy (FE-SEM) image showed that the synthesized PbO_2 consisted of aggregates of nano-size particles and X-ray diffraction (XRD) spectra confirmed that it was plattnerite (Figure 2.1). The specific surface area measured using the 7-point N_2 BET was 25.1 m^2/g.

Stock monochloramine (NH_2Cl) solution of approximately 340 mg/L as Cl_2 was freshly prepared before each experiment by the addition of concentrated NaOCl to a carbonate ($NaHCO_3$, Sigma-Aldrich) buffered ammonium chloride (NH_4Cl, Sigma-Aldrich) solution with a Cl/N molar ratio of 0.7 [73]. The final solution was allowed to stand for 30 min for monochloramine formation to be complete before use. Concentrated NaOCl (~1M, Fisher Scientific) was used to obtain the desired free chlorine concentration. Stock solutions of Cl^- and SO_4^{2-} were prepared by dissolving reagent grade NaCl (Merck) and Na_2SO_4 (Sigma-Aldrich) in ultrapure water. Stock orthophosphate solution was prepared weekly at a concentration of 1000 mg/L as P using Na_2HPO_4 (Merck). The solution was kept in the dark at 4°C. All solutions were prepared using ultra-pure water obtained from a Millipore DirectQ system.
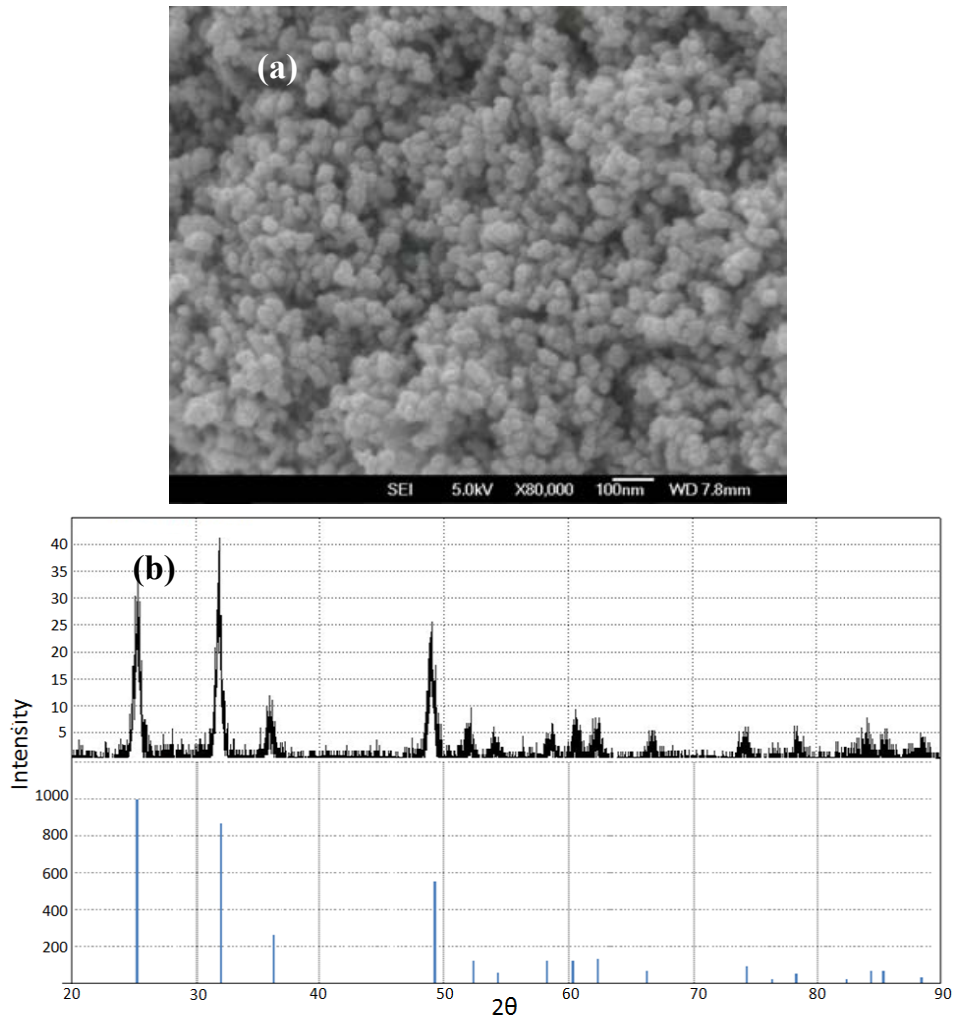
Figure 2.1 (a) FE-SEM image and (b) XRD patterns of synthesized PbO$_2$ and reference standard for plattnerite (β-PbO$_2$) obtained from PDF card: 01-089-2805.

2.2   Experimental setup

2.2.1 Investigation of role of orthophosphate as a corrosion inhibitor in chloraminated solutions containing tetravalent lead corrosion product PbO$_2$

All experiments were conducted in a batch mode using pre-acid washed 60 mL polyethylene bottles at 25°C with 20 mg/L PbO$_2$, 4 mM total dissolved inorganic carbon (C$_T$) and various solution pH values (6.0, 7.0, 8.0 and 9.0), initial NH$_2$Cl concentrations (1, 2 and 5 mg/L as Cl$_2$), and orthophosphate concentrations (0.5, 1, 2 and 5 mg/L as P). These bottles were filled with carbonate-buffered NH$_2$Cl solutions with pH adjusted to the desired value using 1 N HCl and NaOH followed by the addition of orthophosphate and PbO$_2$. These bottles were then sealed without headspace, covered with aluminum foil to prevent light-induced NH$_2$Cl decomposition and placed on a shaking table rotating at 200 rpm. Solid samples were collected periodically over a 7-d period by passing the solution through a nylon membrane filter with a 0.2 μm pore size (Whatman). The filtrate was analyzed for soluble Pb(II) concentration and NH$_2$Cl residual. The solution pH values were measured prior to filtration and the variations during the 7-d period were within the initial pH value ± 0.3 unit.

2.2.2 Evaluation of various water parameters on galvanic corrosion between lead and copper in drinking water

To simulate lead release due to galvanic corrosion caused by a copper/lead couple on the surface of brass or at the regions where lead and copper pipes are in contact during partial lead pipe replacement, 5 cm of pure lead (99.9%, 1 mm dia., Alfa Aesar) and copper wires (99.9%, 1 mm dia., Alfa Aesar) were connected together by tying the lead wire around the copper wire into various total effective lengths (3 cm, 6 cm and 8 cm), while ensuring that both copper and lead wires had the same length exposed to the water (Figure 2.2). The wires were rinsed 3 times with ultrapure water (Millipore DirectQ), dried and weighed using a microbalance with an accuracy of 0.001 mg before use. The connected wires were suspended using polyester thread and immersed in the experimental solution in pre-acid-washed 500-mL polyethylene bottles. For stagnant conditions, the bottles were stored in a cupboard for 7 d with periodic sampling. For completely-mixed conditions, the bottles were placed on a magnetic stirring plate and the solutions were stirred at 250 rpm. Tap water (Table 2.1) from the laboratory was used. Different amounts of chemicals were dosed to examine the effects of initial pH (6.0, 7.0, 7.8, 8.0 and 9.0), chloride concentration (60, 120 and 250 mg/L as Cl^-), sulfate concentration (60, 120 and 250 mg/L as SO_4^{2-}), varying chloride and sulfate concentrations at a constant CSMR of 1 (60, 120 and 250 mg/L as Cl^- and SO_4^{2-}), free chlorine concentration (0.5. 1, 2, 4 and 8 mg/L as Cl_2), monochloramine concentration (0.5. 1, 2, 4 and 8 mg/L as Cl_2) and orthophosphate concentration (1, 2 and 5 mg/L as P). Solution pH was adjusted using 1N HCl and 1N NaOH. The solution was then stirred with a glass rod to ensure homogeneity before placing the wires into the solution. Each bottle contained one pair of copper/lead wires and the solution was discarded after sampling to ensure independency of each data point. For each condition, duplicates were conducted at selected sampling times. The wires were left to air-dry at room temperature for at least 24 h prior to weighing and surface scaling analysis.
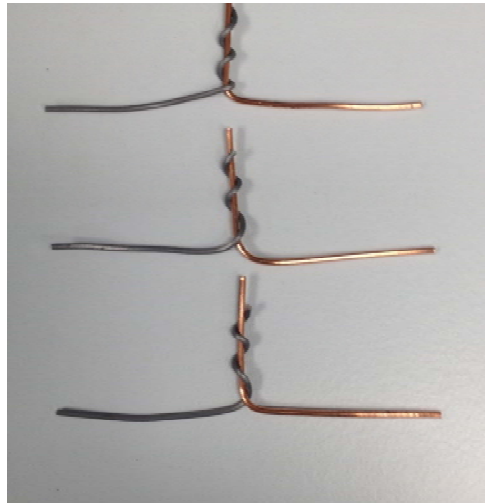
Figure 2.2 Copper and lead wires with a total effective length of 6 cm

Table 2.1 Tap water parameters

Water parameter	
pH	7.7 ± 0.3
Total alkalinity	16 ± 0.9 mg/L as $CaCO_3$
Chloride	35 ± 2.7 mg/L as Cl^-
Sulfate	18 ± 2.0 mg/L as SO_4^{2-}
Copper	17.2 ± 0.4 μg/L
Lead	2.0 ± 0.6 μg/L
Free chlorine residual	< 0.01 mg/L as Cl_2
monochloramine residual	0.02 ± 0.01 mg/L as Cl_2

2.2.3 Examination of lead release in simulated premise drinking water distribution systems

To determine whether lead contamination in drinking water will occur in a "lead-free" distribution system, three flow systems were built using lead-free materials to simulate premise drinking water distribution systems. The first stage of the experiment is to identify potential lead source in the systems using a modified sampling method as existing sampling protocols are unable to locate the source accurately. The second stage is to examine the effects of chemicals commonly added to drinking water on the lead release from the identified lead source. Three different scenarios, namely orthophosphate addition (System A), disinfectant switch from free chlorine to monochloramine (System B) and periodic flushing with free chorine (System C), experienced in distribution systems were investigated (Figures 2.3 and 2.4). Each flow system consists of approximately 20 m of copper pipes (0.5 inch dia) that were BS EN1057:2006 certified. Certified (BS EN1254-2:1998) brass fittings were used to connect segments of the pipes and stainless steel taps. The required copper pipe length is estimated based on the average household floor area of about 95 m^2 (Typical size of 4-room housing units) [74]. Three stainless steel taps were installed in Systems B and C to represent taps found in the kitchen, main toilet and master bedroom toilet while only 2 taps were installed in System A. A 25 L plastic container was used to hold supply water for each flow system. Plastic tubings were used to connect the plastic container to the copper pipes.
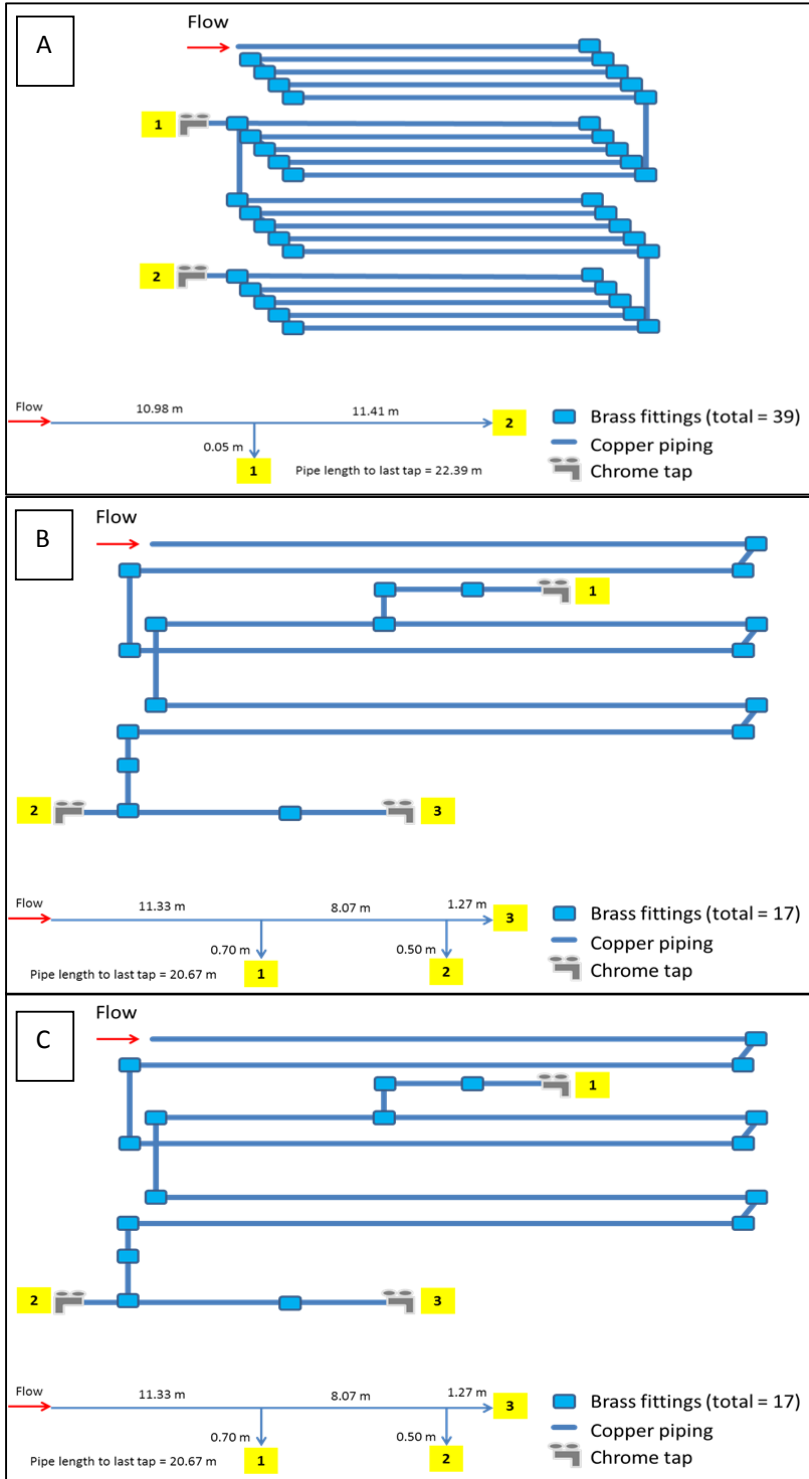
Figure 2.3 Graphical representations of Systems A, B and C

Figure 2.4 Photographs of Systems (a) A, (b) B and C

A minimum 24-h stagnation period to allow accumulation of lead contaminants and a smaller sample volume to reduce the dilution factor were considered in the sampling protocol. Samples were collected from taps in each system after 1, 3 and 7 d of stagnation. Initially, the first 400 mL sample was collected sequentially using 100 mL glass bottles. This allowed the detection of lead contamination within the system, but it was unable to locate the source of lead due to increased number of brass fittings near the taps. The method was revised to collect the first 200 mL sample using four 50 mL glass bottles. Each segmental sampling of 50 mL covers approximately 40 cm of the pipe based on the pipe diameter. The use of glass bottles instead of plastic bottles eliminated the need to transfer samples for acid digestion, solving the problem of underestimation of lead levels due to missed particulates which attached to the inner surface of the bottle [75].

For System A, two 100 mL bottles were used to collect the first 200 mL water from Tap 1 for the first 38 d. To identify the source of lead, the sampling method was changed to use four 50 mL bottles on Day 45. The number of samples collected for Tap A was eventually reduced to two (Tap 1, Sample 1: 0-50 mL and Tap 1, Sample 4: 150–200 mL) which showed consistently high levels of lead and brass fittings were confirmed to be the source of lead. A second tap (Tap 2) was installed in System A on Day 153.

Similarly, after identifying the source of lead, the number of samples is reduced to two (Tap 2, Sample 1: 0-50 mL and Tap 2, Sample 4: 150– 200 mL) on Day 210, 47 d after Tap 2 installation. For Systems B and C, three 50 mL samples were collected for each tap. Following the sample collection, the water in the plastic container has to be replaced with a fresh supply of water. Prior and after changing the water in the plastic container, each tap was flushed with 2-3 L of water to ensure the systems were filled with fresh water supply for the next sampling. Required chemicals were added to respective water container during the changeover. Sample solution in each glass bottle was tested for pH, residual free chlorine and monochloramine before 5% (v/v) concentrated nitric acid was added. The bottles were then placed on a hot plate and heated to 85 ºC for at least 2 h prior to total copper, lead and zinc measurement. The flow rate of the samples complied with PUB's allowable flow rate for constant flow regulations whereby a basin tap should not exceed 6 L/min [76]. Table 2.2 shows the average flow rate during sampling of each tap for all three systems.

Table 2.2 Average flow rates of all taps in Systems A, B and C

	Tap 1 (L/min)	Tap 2 (L/min)	Tap 3 (L/min)
System A	2.62	2.37	-
System B	3.42	2.77	2.79
System C	2.78	2.41	2.29

2.3   Analytical methods

FE-SEM and energy dispersive X-ray spectroscopy (EDX) (JOEL 5600LV) were used to investigate morphology and chemical composition of solid samples. XRD (Siemens D5005) was performed to identify the mineral species. XRD data was collected using Cu Kα radiation (30 kV, 20 mA) with a diffracted beam monochromator. Scans were taken over a range of 20-90° 2θ

at 0.2 s/0.01°. Reference patterns were obtained from PDF-4 (Powder Diffraction File) released from the ICDD (International Center for Diffraction Data) in 2011. A Kratos Axis Ultra X-ray photoelectron spectrometer (XPS) was employed to distinguish between Pb(II) and Pb(IV) in the surface layers of solid phases. Samples were analyzed under high vacuum ($< 5 \times 10^{-7}$ torr) using monochromatic Al Kα X-rays. A scan area of 700×300 μm was employed. Wide scans (1100 to -5 eV) were made at 100 ms/1 eV while narrow scans (range < 20 eV) were made with 200 ms/0.1 eV. All binding energies were corrected using the C 1s line at 284.8 eV. The specific surface area of synthesized PbO_2 was measured by the seven-point N_2-BET using a NOVA 4200e surface area analyzer.

Free chlorine and monochloramine residual concentrations were measured using the DPD-FAS method in accordance to Standard Method 4500-Cl F [77]. For Section 2.2.1, soluble Pb(II) concentration was measured using the anodic stripping voltammetry (ASV) method with a 797 VA computrace (Metrohm) after acidifying the sample with 0.1 M acetate buffer to about pH 4.0. Total copper, lead and zinc (soluble + particulate) were measured by adding 5% (v/v) nitric acid to collected samples and digesting the mixture at 85ºC for at least 2 h. Soluble copper and lead were quantified by filtering the samples with 0.45-μm pore size nylon filter followed by acidifying the filtrate with dilute nitric acid to below pH 2 for at least 24 h. Copper, lead and zinc concentrations were measured using inductively coupled plasma mass spectrometer optical emission spectrometry (ICP-OES) in accordance with Standard Method 3125-B [77]. Chloride, sulfate and orthophosphate concentrations were measured using a DIONEX DX-120 ion chromatograph according to Standard Method 4110 [77]. The solution pH value was measured using a pH meter (Horiba F-51) equipped with an Ag/AgCl probe following the 3-point calibration.

Chapter 3

Role of orthophosphate as a corrosion inhibitor in chloraminated solutions containing tetravalent lead corrosion product PbO$_2$

Addition of orthophosphate has been commonly employed to suppress lead levels in drinking water. Its detailed mechanism and time required for it to become effective, however, have not been fully elucidated. In this chapter, the mechanistic role of orthophosphate in lead release from PbO$_2$ in chloraminated drinking water and its influence on the transformation of lead corrosion products were investigated. The effects of solution pH, monochloramine concentration and orthophosphate dosage on soluble lead release were examined and the mineral composition and surface characteristics of the secondary solid phases formed in the experiments were determined. Intensive periodic sampling was conducted for the first 48 h to observe changes that were often overlooked in prior investigations. Detailed insights of the dissolution of PbO$_2$ and the transformation of lead corrosion products in orthophosphate-containing monochloramine solutions were provided.

3.1 Effects of solution pH value on soluble Pb(II) release

Figure 3.1 summarizes the results of monochloramine auto-decomposition and soluble Pb(II) release as a function of time for experiments conducted at pH 6.0, 7.0, 8.0 and 9.0 at a constant initial NH_2Cl concentration of 2 mg/L as Cl_2 and 4 mM C_T. Monochloramine decomposed faster as the pH value decreased, with little decay being observed at pH $\geq$ 8.0. The presence of PbO_2 and orthophosphate had little effect on the rate of monochloramine auto-decomposition (Figure 3.1a), which followed an approximate second-order kinetics (Eq 3.1 and 3.2) with respect to monochloramine concentration (Figure 3.2).

$$\frac{d[NH_2Cl]}{dt} = -k_{obs}[NH_2Cl]^2 \qquad (3.1)$$

$$\frac{1}{[NH_2Cl]} - \frac{1}{[NH_2Cl]_0} = k_{obs}t \qquad (3.2)$$

The observed rate constants (k_{obs}) at pH 6.0, 7.0, 8.0 and 9.0 were 704 ± 56, 147 ± 11, 44 ± 10, and 22 ± 3 $M^{-1}h^{-1}$, respectively, which were consistent with the values reported in the literature [78].

Soluble Pb(II) release was reduced drastically by the addition of orthophosphate for all pH values (Figure 3.1b). Particularly at pH 6.0, soluble Pb(II) concentration continued to increase and reached 692 µg/L after 7 d without orthophosphate. With the addition of 1 mg/L as P of orthophosphate, the concentration of soluble Pb(II) was reduced to about 15 µg/L after 48 h and remained relatively constant afterwards. It should be noted that in control experiments without both monochloramine and orthophosphate, soluble Pb(II) concentration slowly increased with time and reached 136 µg/L, 56 µg/L and 13 µg/L after 7 d at pH 6.0, 7.0 and 8.0, respectively (Figure 3.3). One interesting phenomenon with orthophosphate addition in the presence of monochloramine was the peaking of soluble Pb(II) concentrations observed within the first 24 h, which could readily exceed the action level of 15 µg/L (Figure 3.1b). This event was transient and could be easily missed without

careful monitoring. For all pH conditions with orthophosphate addition, soluble Pb(II) concentrations stabilized within 48 h. This re-immobilization of soluble Pb(II) should be due to the precipitation of Pb-phosphate minerals [8].

In a study by Xie, et al., Pb(IV) species including PbO_2, Pb^{4+}, PbO_3^{2-} and PbO_4^{4-} are calculated to be the dominant lead species in the presence of free chlorine based on thermodynamic considerations [21]. The equilibrium dissolved lead concentration they measured in chlorinated solutions by ICP-MS was assumed to be the sum of all dissolved Pb(IV) species. To the best of our knowledge, however, no existing analytical technique can be used to quantify the concentration of Pb(IV) aqueous species, implying that they may be very short-lived and at extremely low concentrations if they do exist. In the present study, we measured soluble Pb(II) using ASV which is Pb(II) ion specific. This ascertains the reduction of PbO_2 in chloramined solutions.
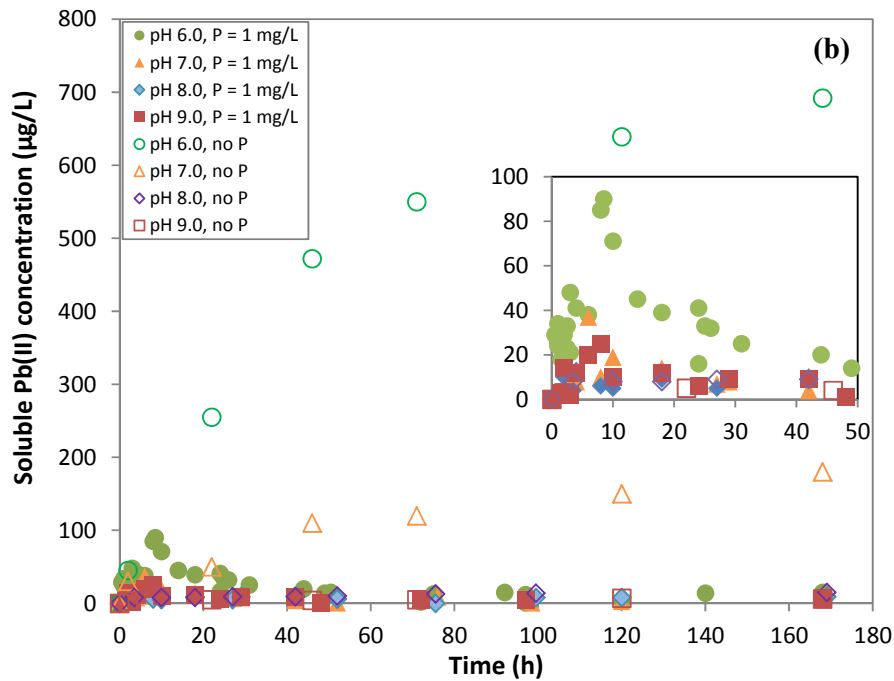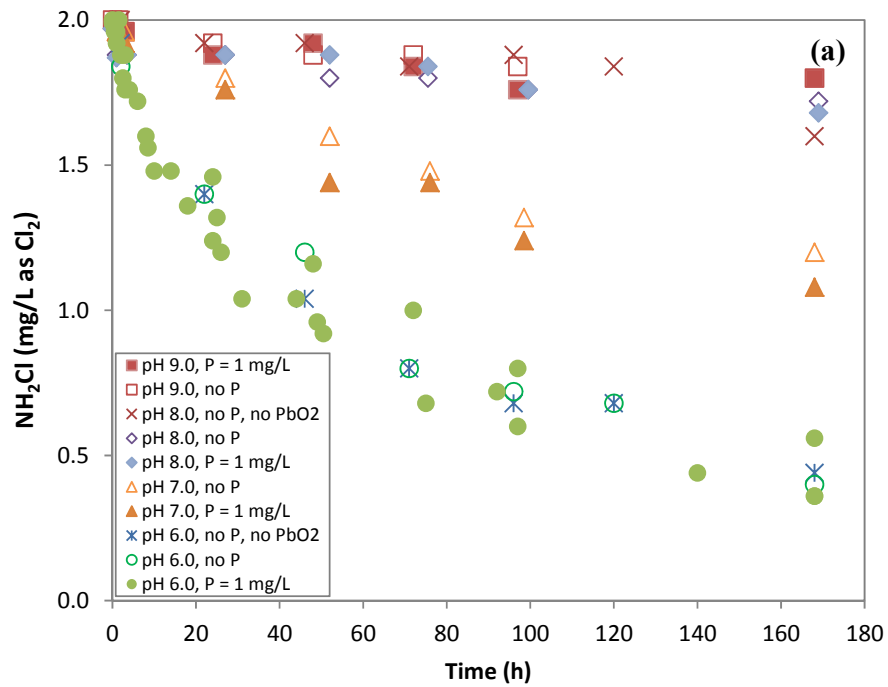
Figure 3.1 (a) NH$_2$Cl residual and (b) Soluble Pb(II) concentration as a function of time at different solution pH. Experiment conditions: $C_T = 4$mM, initial NH$_2$Cl = 2 mg/L as Cl$_2$. The inset shows a close-up graph during the first 50 h. Data for pH 6.0, no P and pH 7.0, no P are excluded in the inset.
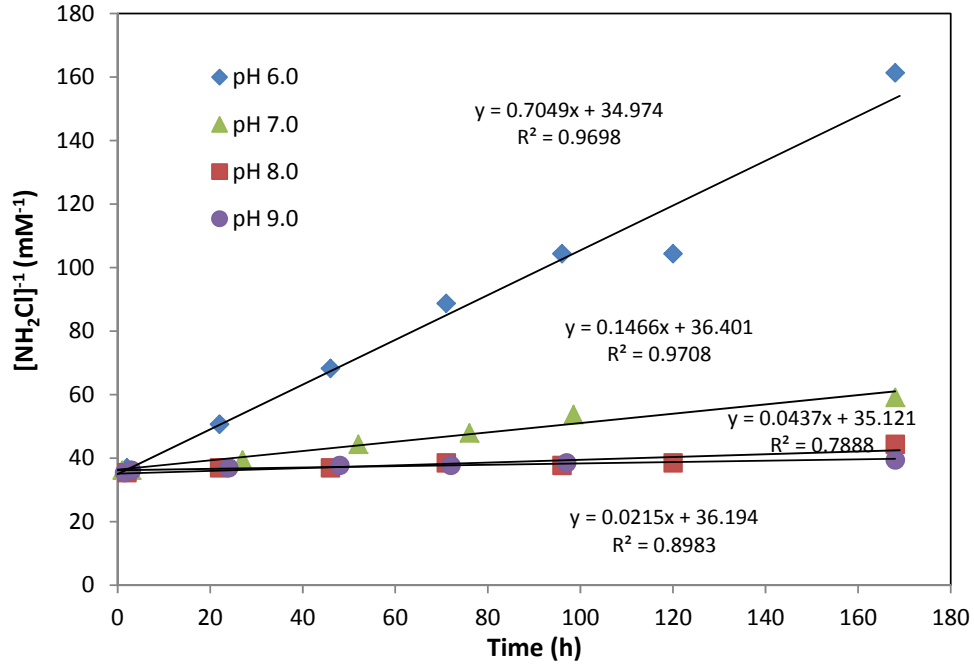
Figure 3.2 The second-order plot of monochloramine concentration as a function of time used to calculate k_{obs} for results obtained at pH 6.0, 7.0, 8.0 and 9.0 in the absence of PbO_2 and orthophosphate.
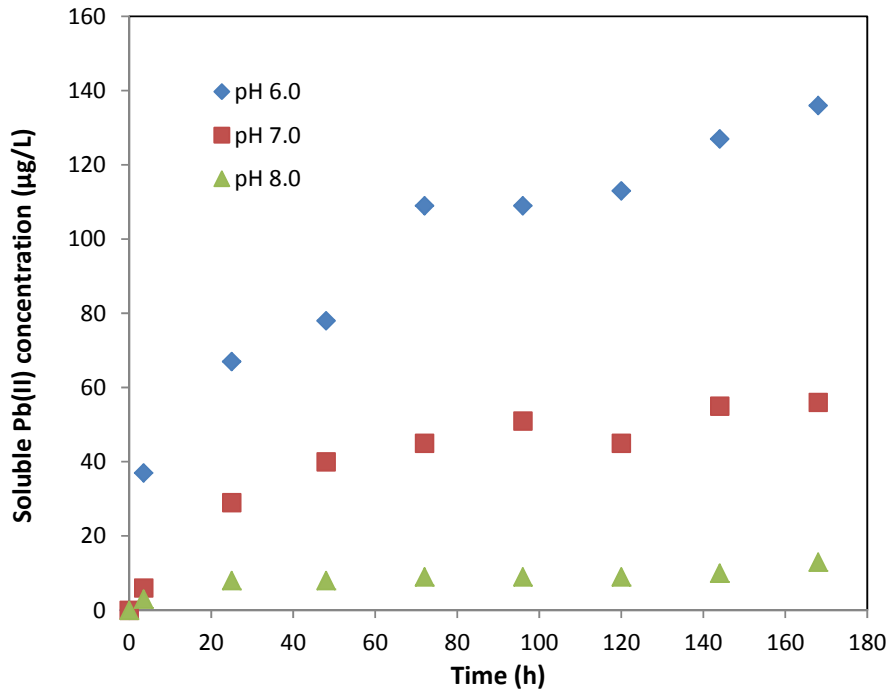
Figure 3.3 Soluble Pb(II) concentration as a function of time in the absence of both orthophosphate and monochloramine. Experiment conditions: $C_T = 4$ mM.

26

3.2 Effects of orthophosphate concentration on soluble Pb(II) release

Figure 3.4 shows the influence of orthophosphate concentration (0–5 mg/L as P) on monochloramine auto-decomposition and soluble Pb(II) release as a function of time at pH 6.0 and 8.0. The rate of monochloramine decomposition at pH 6.0 was not affected by orthophosphate addition, but at pH 8.0 the rate was accelerated with the addition of 5 mg/L as P of orthophosphate (Figure 3.4a). Monochloramine auto-decomposition is due to the formation of $NHCl_2$ either from the reaction of monochloramine with HOCl formed from the hydrolysis of NH_2Cl or from monochloramine disproportionation which is proton and general-acid catalyzed, with the latter playing a more important role [73]. As pH increases, proton catalysis becomes less important while general-acid catalysis becomes more dominant. Both carbonate and orthophosphate can accelerate the rate of monochloramine decomposition via the general-acid catalysis pathway. However, the catalysis induced by 5 mg/L as P (0.16 mM) of orthophosphate is negligible compared to that of carbonate at $C_T = 4$ mM. Hence, there should be other unknown mechanisms that contributed to the faster monochloramine decomposition observed at pH 8.0.

Soluble Pb(II) release at pH 8.0 remained under the action level of 15 µg/L throughout the course of the experiment due to the slow decomposition of monochloramine (Figure 3.4b) [17]. At pH 6.0, a peak in soluble Pb(II) concentration was observed during the first 24 h when orthophosphate was added, with lower orthophosphate concentration leading to higher soluble Pb(II) peak concentration and the later occurrences of the peak values. For example, with 1 mg/L as P of orthophosphate, the soluble Pb(II) concentration reached a maximum of 90 µg/L at 8.5 h while with 0.5 mg/L as P of orthophosphate, the maximum soluble Pb(II) concentration was 121 µg/L occurring at 18 h. For the condition with 5 mg/L as P of orthophosphate, the soluble Pb(II) concentration reached the maximum of 14 µg/L at 8 h before dropping below 10 µg/L for the remainder of the experiment. The

27

dependences of the maximum soluble Pb(II) level and the peak timing on orthophosphate concentration could be explained by the fact that the required degree of supersaturation for Pb-phosphate mineral precipitation was achieved earlier with a higher orthophosphate concentration, which hastened the precipitation process.
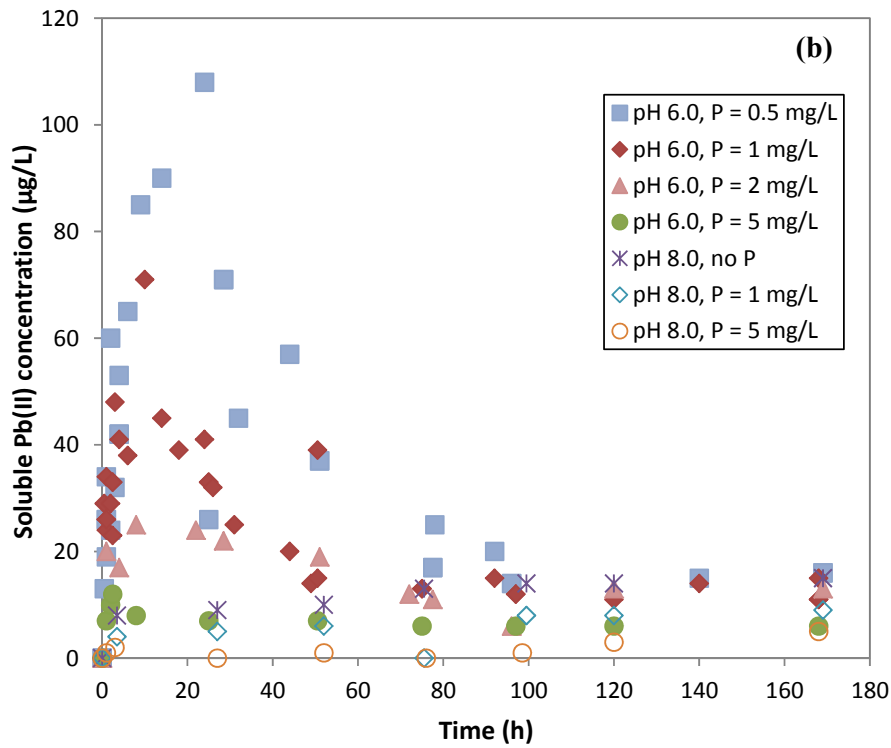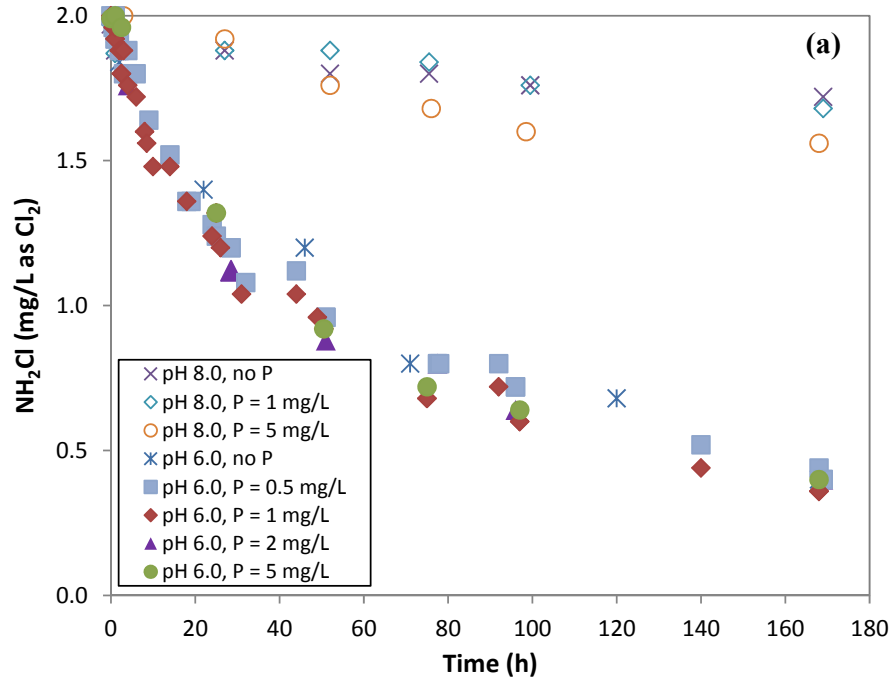
Figure 3.4 (a) NH$_2$Cl residual and (b) Soluble Pb(II) concentration as a function of time with different orthophosphate concentrations. Experiment conditions: C$_T$ = 4mM, initial NH$_2$Cl = 2 mg/L as Cl$_2$.

3.3 Effects of initial monochloramine concentration on soluble Pb(II) release

To illustrate the influence of initial monochloramine concentration on soluble Pb(II) release from PbO_2 with and without orthophosphate addition, experiments were conducted at pH 6.0 where monochloramine decomposition was the fastest. The rate of monochloramine decomposition increased with the increasing initial monochloramine concentration (Figure 3.5a) as predicted by the second-order kinetics [78]. The peak soluble Pb(II) concentration increased with the increasing initial monochloramine concentration (Figures 3.5b and 3.5c). Prior to the peak, the soluble Pb(II) concentration released from PbO_2 was positively correlated to the amount of monochloramine decomposed (Figure 3.6). At an initial monochloramine concentration of 5 mg/L as Cl_2, the highest soluble Pb(II) concentration measured at 0.5 and 1 mg/L as P of orthophosphate were 157 and 110 µg/L, respectively. Soluble Pb(II) concentration stabilized after 48 h but the levels after 7 d were above 20 µg/L for 0.5 mg/L as P and around 15 µg/L for 1 mg/L as P, indicating that 0.5 mg/L as P of orthophosphate was insufficient to control soluble Pb(II) release below the action level for both short (24 h) and long terms (7 d) at pH 6.0. In drinking water distribution systems, such acidic conditions can be found in low-alkalinity chloraminated waters when nitrification occurs [79].
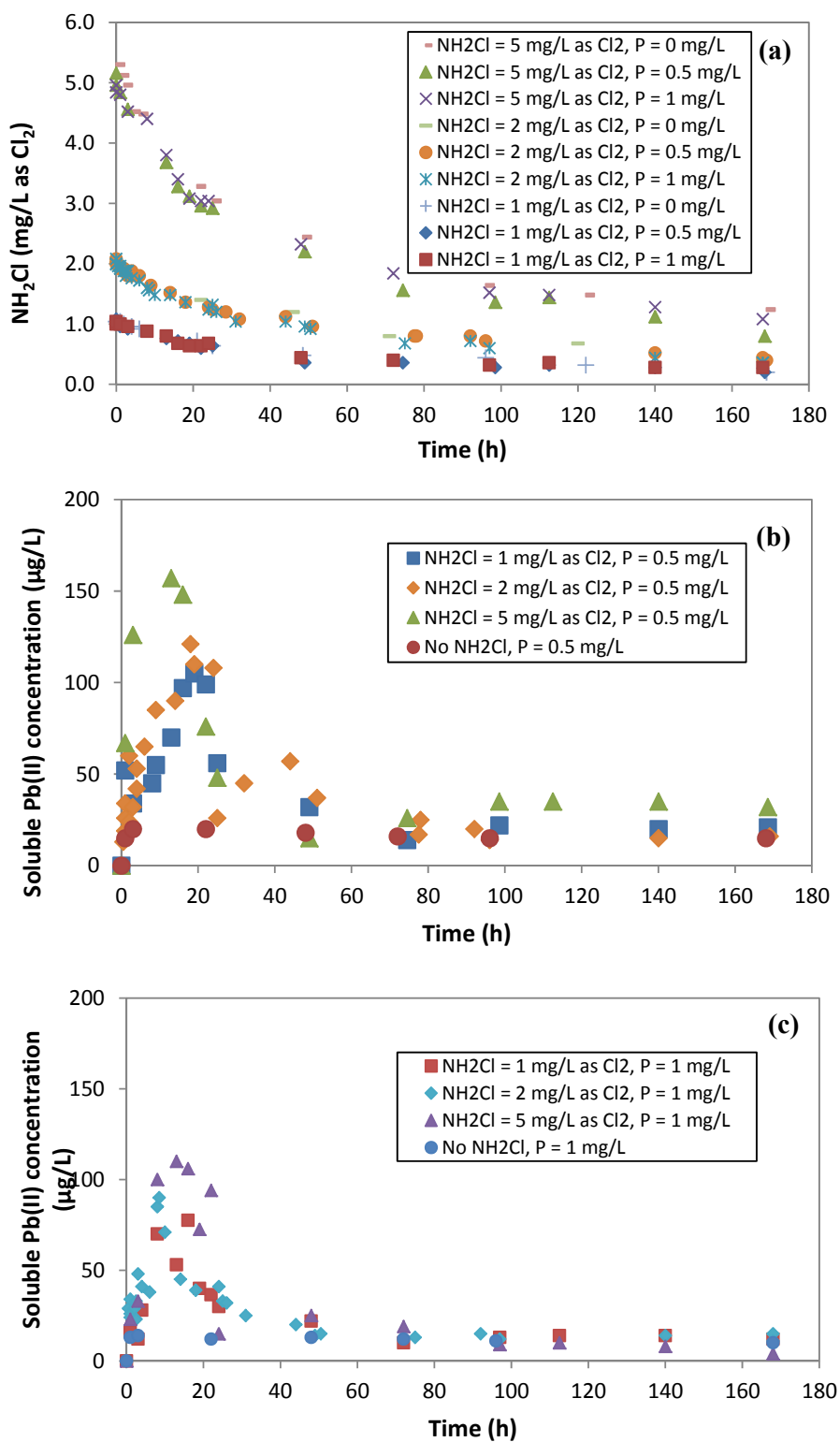
Figure 3.5 (a) NH$_2$Cl residual, (b) soluble Pb(II) concentration at P = 0.5 mg/L and (c) soluble Pb(II) concentration at P = 1 mg/L as a function of time with different initial monochloramine concentrations. Experiment conditions: Solution pH 6.0, C$_T$ = 4mM.
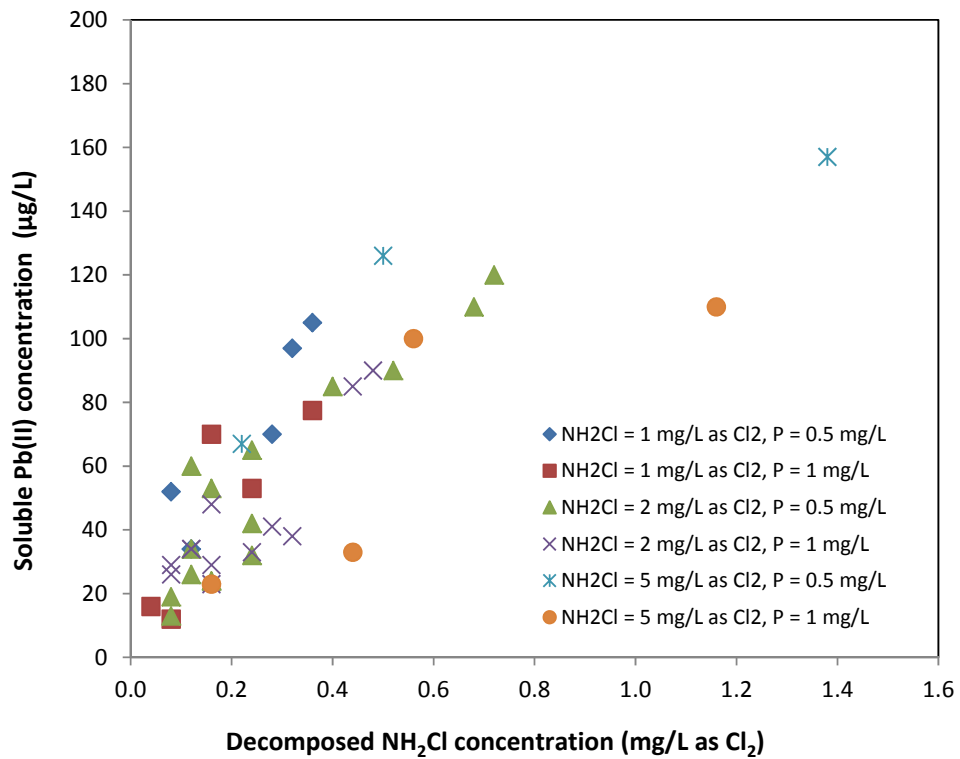
Figure 3.6 Soluble Pb(II) concentration vs. decomposed NH$_2$Cl concentration prior to the maximum point of the peak. pH = 6.0, C$_T$ = 4 mM.

3.4   Characterization of lead phosphate minerals

3.4.1 SEM-EDX

SEM-EDX was employed to examine the morphological and elemental composition changes of lead solid phases. Figure 3.7 shows the SEM images of solid phases collected at different reaction periods for the experiment conducted at pH 6.0 and 1 mg/L as P of orthophosphate. Before the experiment, aggregates of nanosized PbO_2 were observed (Figure 3.7a). Sparse rod crystals were found after 8 h (Figure 3.7d) and more such rods were produced after 7 d (Figure 3.7f). The rods grew larger in size over time, indicating that crystal growth was taking place. Similar trends were observed at other orthophosphate dosages at pH 6.0 and 7.0. At pH 8.0 and 9.0, however, such rod crystals were absent (data not shown).

In the absence of orthophosphate, low pH value conditions (< pH 6.5) favored the formation of cerussite while high pH value ones (> pH 8.0) favored that of hydrocerussite [10]. In the presence of orthophosphate, hydroxypyromorphite and secondary lead phosphate are more likely to form in typical drinking water with a pH value ranging from 7.0 to 9.0 [61]. If chloride exists, chloropyromorphite will form instead of hydroxypyromorphite at the same pH range. The distinct rod structure observed in the SEM images could belong to either cerussite or chloropyromorphite. After careful examination of SEM images found in the literature, it was noted that cerussite had a quadrilateral (4-sided) rod structure [50] while chloropyromorphite had a hexagonal (6-sided) one [64]. Elemental mapping (Figure 3.8) showed very little carbon element but abundant Pb, O, Cl and P elements on the solids collected after 7 d. P element was found to concentrate at the rod crystals and disperse at the surrounding PbO_2 solids, indicating the presence of phosphorus in the mineral lattice of the rod crystals and possible adsorption of orthophosphate ions on the PbO_2 surfaces. The adsorbed orthophosphate may provide some degree of protection for PbO_2 from reductive dissolution by preventing the direct contact between PbO_2 and reducing agents in the solution. This may explain why the addition of orthophosphate could still suppress soluble Pb(II) release from PbO_2 without the formation of rod crystals at pH

8.0 and 9.0. The formation of chloropyromorphite should be triggered by a sufficiently high ion activity product (IAP > K_{sp}) resulting from the soluble Pb(II) released from the reductive dissolution of PbO_2 within the first 24 h. Chloropyromorphite precipitation is known to be rapid and equilibrium could be achieved in a few h [60], but it should require a certain degree of supersaturation to be initiated [58]. Hence, soluble Pb(II) concentration must exceed a certain threshold for chloropyromorphite to precipitate. This could explain why chloropyromorphite was not formed at pH 8.0 and pH 9.0 where soluble Pb(II) concentration generally remained below 20 µg/L during the course of the experiments, which may not be sufficient to initiate chloropyromorphite precipitation.
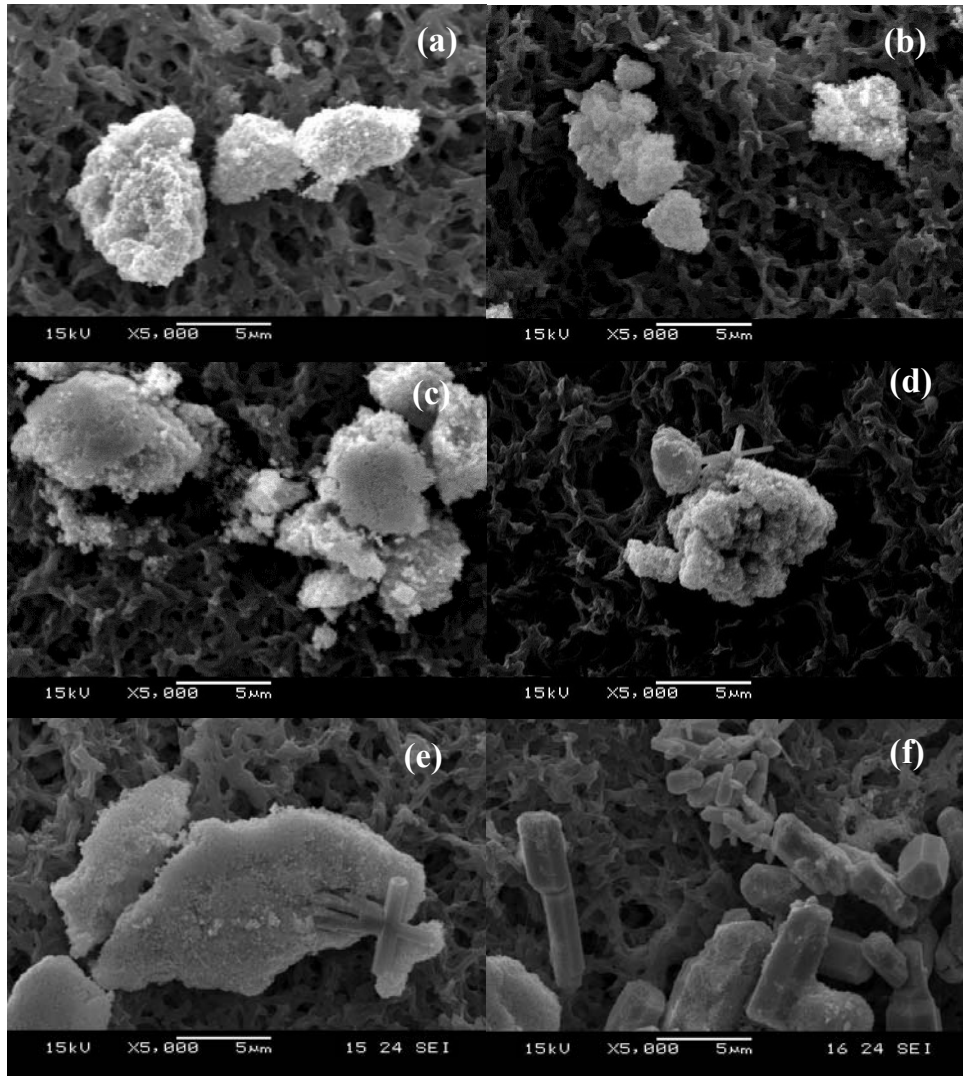
Figure 3.7 SEM images of solid samples collected at (a) 0 h, (b) 4 h, (c) 6 h, (d) 8 h, (e) 13 h and (f) 7 d. Experiment conditions: pH 6.0, C_T = 4mM, NH_2Cl = 2 mg/L as Cl_2, orthophosphate = 1 mg/L as P.
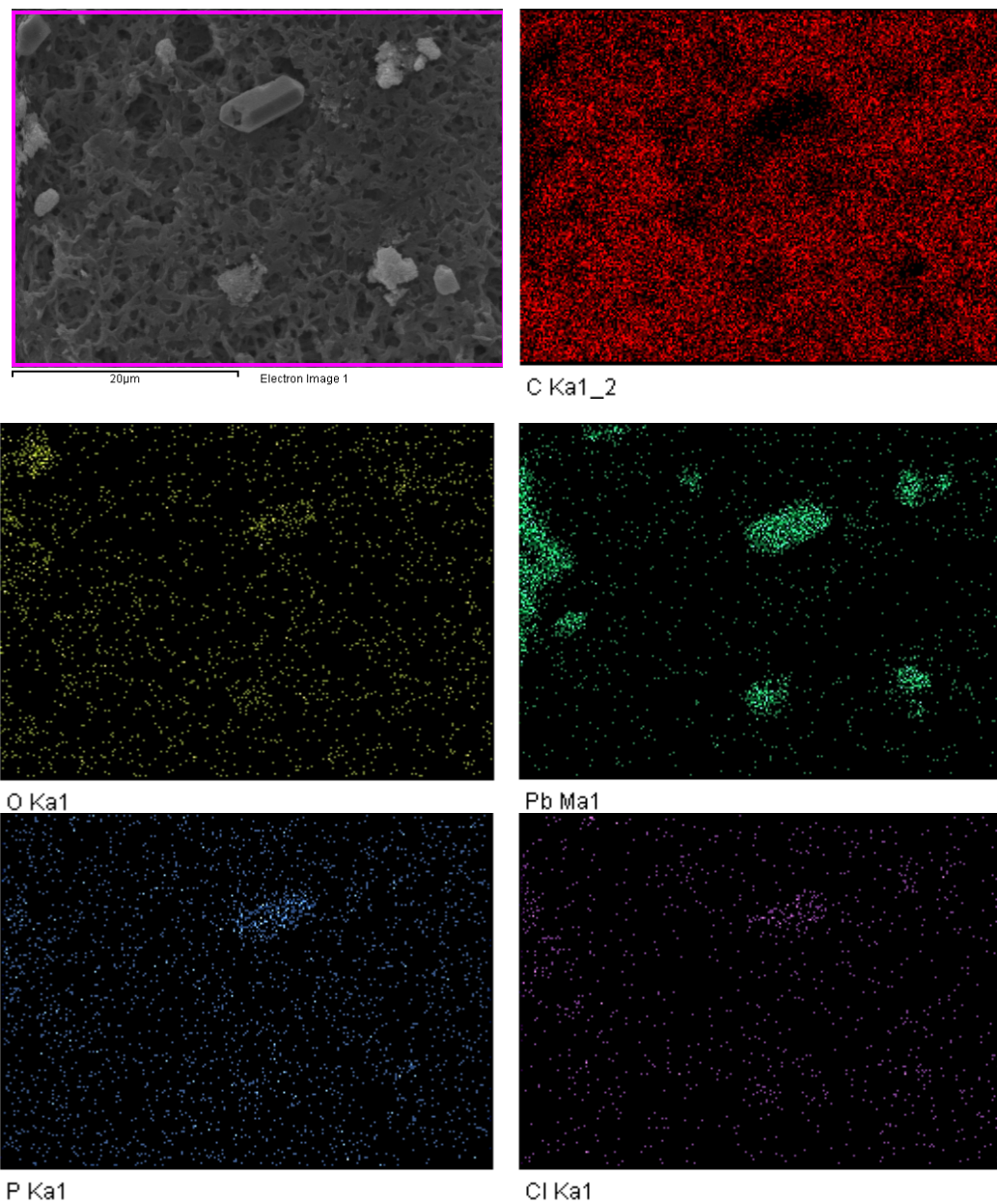
Figure 3.8 Elemental mapping (SEM-EDX) of solid particles collected after 7 d with experimental conditions: pH 6.0, C_T = 4mM, NH_2Cl = 2 mg/L as Cl_2, orthophosphate = 1 mg/L as P. Colored dots shown in the mapping indicate presence of specific elements.

3.4.2 XPS and XRD

To ascertain the formation of chloropyromorphite, solids were collected from repeated experiments and examined by XPS and XRD for the following condition: PbO_2 = 20 mg/L, pH 6.0, $[NH_2Cl]$ = 2 mg/L as Cl_2, orthophosphate = 1 mg/L as P. Under this condition, soluble Pb(II) concentration peaked at about 90 μg/L within the first 24 h and remained below the action level of 15 μg/L after 48 h (Figure 3.1b). Hexagonal rod crystals were formed and their quantity increased over time.

XPS allowed us to identify if there was any change in oxidation states of Pb in the exposed surfaces (top 1-10 nm) of the collected solids. Figure 3.9 shows the Pb 4f and O 1s core level spectra of the solids collected before and after the experiment. Before the experiment, the Pb 4f spectrum of β-PbO_2 consisted of a spin-orbit doublet each displaying an asymmetric peakshape with peak binding energies for Pb $4f_{7/2}$ and Pb $4f_{5/2}$ at 137.2 and 142 eV, respectively. The asymmetric peakshape can be fit with two Gaussian-Lorentzian components separated by 0.7 eV for both Pb $4f_{7/2}$ and Pb $4f_{5/2}$. The peak binding energies of the components were 136.9, 137.6, 141.8 and 142.5 eV. The lower components were narrower (Full width half maximum (FWHM) = 0.75 – 0.82 eV) compared to the higher components (FWHM = 1.625 – 1.681 eV). The O 1s signal was a singlet with a weak shoulder at higher binding energies and a peak at 529 eV. The peakshape can be fit with two Gaussian-Lorentzian components with peaks at 528.9 and 529.9 eV. These characteristics were in good agreement with previous reports on β-PbO_2 [20, 80, 81]. For solids collected after the experiment, Pb 4f spectrum showed 2 peaks overlapping at the lower binding energies. Both Pb $4f_{7/2}$ and Pb $4f_{5/2}$ peakshapes can be fit with 3 Gaussian-Lorentzian components in which two of them (136.8 and 137.6 eV) were similar to those observed before the experiment, while the third one (138.7 eV) could be attributed to chloropyromorphite. Similarly, a third component (530.9 eV) was well-fitted in the O 1s spectrum. Eighmy et al. [82] reported peak binding energies at 138.9, 143.7 and 530.9 eV for Pb $4f_{7/2}$, Pb $4f_{5/2}$ and O 1s respectively for chloropyromorphite.
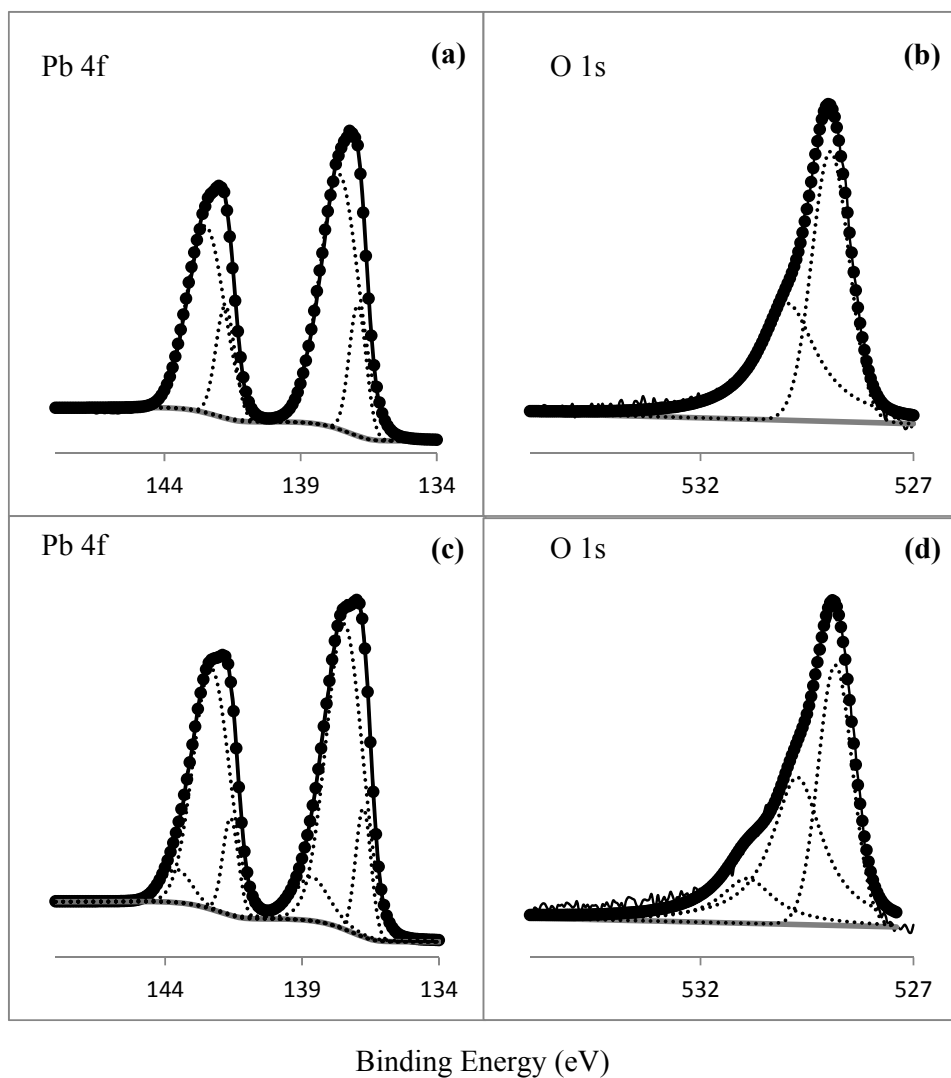
Figure 3.9 Pb 4f and O 1s core level spectrum of solid particles collected before (a and b) and after 7 d (c and d). Experimental conditions: pH = 6.0, C_T = 4mM, NH_2Cl = 2 mg/L as Cl_2, orthophosphate = 1 mg/L as P.

XRD analysis of the solids (Figure 3.10) collected after the experiments, in which β-PbO$_2$ remained the dominant species with new peaks observed near $2\theta = 27$, 30 and 44 degrees. These new peaks were compared against the ICDD (International Center for Diffraction Data) database [83] for possible lead minerals such as lead oxides, lead carbonates and lead phosphates. It was found that hydroxypyromorphite and chloropyromorphite possess prominent peaks in these observed peak regions. Close examination of the spectrum showed that there were 2 peaks between 29.5 and 30.5 degrees (Figure 3.11), which were characteristic of chloropyromorphite. Hydroxypyromorphite has only one peak in the same range. Based on the various characterization techniques, chloropyromorphite was precipitated with orthophosphate addition and played the major role in regulating soluble Pb(II) concentration although the minor precipitation of hydroxypyromorphite could not be completely ruled out.
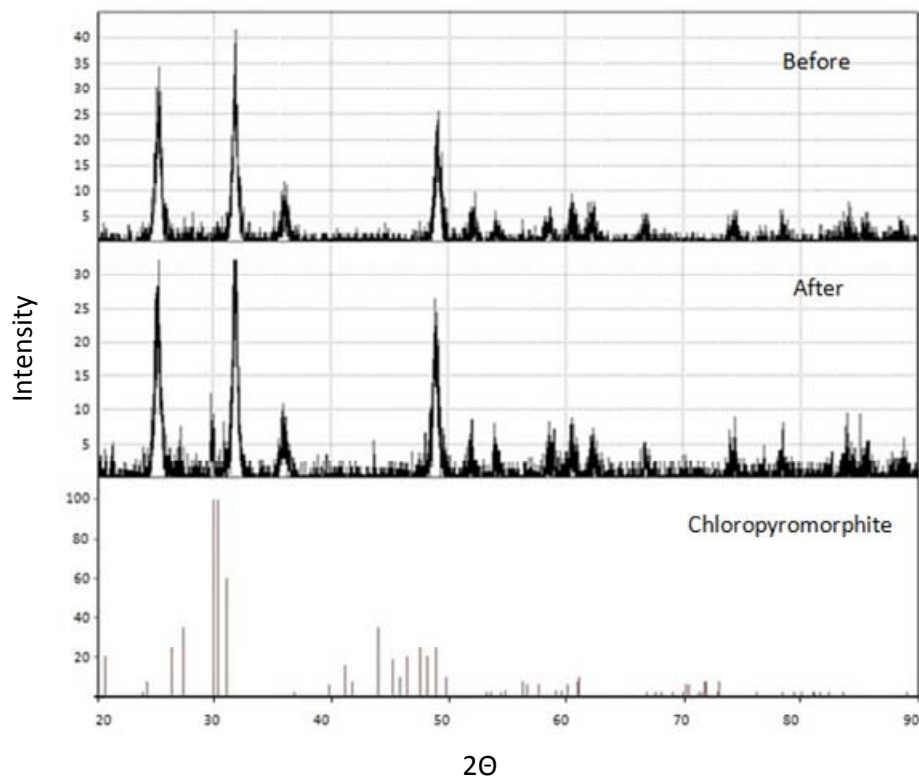
Figure 3.10 X-ray diffraction (XRD) patterns of solid particles collected before and after 7 d. Experimental conditions: pH = 6.0, C_T = 4mM, NH_2Cl = 2 mg/L as Cl_2, orthophosphate = 1 mg/L as P. Reference standard for chloropyromorphite obtained from PDF card: 00-019-0701.
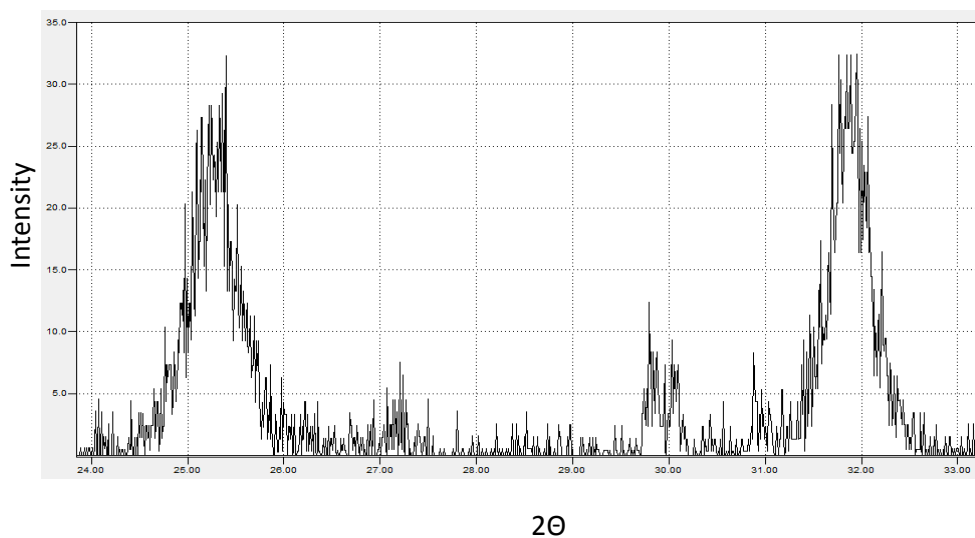
Figure 3.11 Magnified XRD patterns of solid particles collected after 7 d with experimental conditions: pH = 6.0, C_T = 4mM, NH_2Cl = 2 mg/L as Cl_2, orthophosphate = 1 mg/L as P.

3.5   Solubility considerations

The ion activity product and supersaturation ratio (Ω) could be calculated using Eqs (3.1) and (3.2) to determine whether the precipitation of chloropyromorphite would take place [59].

$$IAP = \{Pb^{2+}\}^5 \{PO_4^{3-}\}^3 \{Cl^-\} \qquad\qquad (3.1)$$

$$\Omega = \left(\frac{IAP}{K_{sp}}\right)^{\frac{1}{\eta}} \qquad\qquad (3.2)$$

where η is the total number of ions in the formula unit of a mineral. The normalization of degree of supersaturation ($\frac{IAP}{K_{sp}}$) with $1/\eta$ allows the saturation ratio to become independent of the total number of ions present in the mineral. The concentrations of Cl^-, total phosphate (P_T) and total soluble Pb(II) were measured in our experiments conducted at pH 6.0 and initial NH_2Cl concentration of 2 mg/L as Cl_2 (Table 3.1). These values, together with solution pH values and C_T, were input to Visual MINTEQ 3.0 [84] to obtain the ion activity product and supersaturation ratio with respect to chloropyromorphite. The thermodynamic data and input parameters were provided in Tables 3.2 and 3.3.

Table 3.1 Determination of ion activity product (IAP) and supersaturation ratio (Ω) as a function of time
Conditions: Initial pH 6.0, $C_T = 4$ mM, $NH_2Cl = 2$ mg/L as Cl_2

Time (h)	pH	Total soluble Pb(II) (μg/L)	Cl⁻ (mg/L)	#P_T (μg/L)	P_T (mg/L as P)	IAP	*Ω
Orthophosphate = 1 mg/L as P							
2	6.0	29	117	10.6	3.39E-03	1.12E-84	1.13
8	6.1	85	120	10.8	3.45E-03	8.32E-82	2.36
22	6.2	40	111	10.5	3.36E-03	4.05E-83	1.68
72	6.2	15	109	10.1	3.23E-03	2.12E-85	0.94
168	6.4	13	121	10.3	3.29E-03	1.06E-84	1.12
Orthophosphate = 2 mg/L as P							
2	6.1	21	111	1950	0.62	1.12E-78	5.42
8	6.1	25	108	1940	0.62	6.21E-78	6.35
22	6.1	24	105	1970	0.63	5.79E-78	6.30
72	6.2	12	109	1850	0.59	3.06E-79	4.54
168	6.3	13	106	1870	0.60	1.11E-78	5.24
Orthophosphate = 5 mg/L as P							
2	6.1	10	114	7660	2.45	3.22E-78	5.90
8	6.1	12	114	7630	2.44	7.94E-78	6.52
22	6.1	7	114	7550	2.41	6.55E-79	4.94
72	6.3	6	114	7460	2.38	1.56E-78	5.44
168	6.3	6	114	7880	2.52	3.12E-78	5.88

\# - Total phosphate, P_T = measured value using ion chromatography. The MDL for P_T and Cl⁻ were 1 μg/L as P and 1 μg/L, respectively.

* - Supersaturation ratio, $\Omega = \left(\dfrac{IAP}{K_{sp}} \right)^{\frac{1}{\eta}}$ where η = total number of ions in the formula unit of a mineral. Calculations were done using Visual MINTEQ 3.0 and thermodynamic data listed in Table 3.2.

Table 3.2 Equilibrium constants used for reactions in lead phosphate-carbonate-chloride aqueous system

Reaction	log K[#]
Solid phases	
$PbCO_3 = Pb^{2+} + CO_3^{2-}$	-13.2
$Pb_5(PO_4)_3Cl = 5Pb^{2+} + 3PO_4^{3-} + Cl^-$	-84.43
$PbCl_2 = Pb^{2+} + 2Cl^-$	-4.78
$Pb_3(CO_3)_2(OH)_2 + 2H^+ = 3Pb^{2+} + 2CO_3^{2-} + 2H_2O$	-18.76
$Pb_5(PO_4)_3OH + H^+ = 5Pb^{2+} + 3PO_4^{3-} + H_2O$	-62.79
$PbClOH + H^+ = Pb^{2+} + Cl^- + H_2O$	0.623
$PbO \text{ (litharge)} + 2H^+ = Pb^{2+} + H_2O$	12.69
$PbO \text{ (massocot)} + 2H^+ = Pb^{2+} + H_2O$	12.89
$Pb(OH)_2 + 2H^+ = Pb^{2+} + H_2O$	8.15
$Pb_{10}(OH)_6O(CO_3)_6 + 8H^+ = 10Pb^{2+} + 6CO_3^{2-} + 7H_2O$	-8.76
$Pb_2(OH)_3Cl + 3H^+ = 2Pb^{2+} + Cl^- + 3H_2O$	8.793
$Pb_2O(OH)_2 + 4H^+ = 2Pb^{2+} + 3H_2O$	26.19
$Pb_2OCO_3 + 2H^+ = 2Pb^{2+} + CO_3^{2-} + H_2O$	-0.5578
$Pb_3(PO_4)_2 = 3Pb^{2+} + 2PO_4^{3-}$	-43.54
$Pb_3O_2CO_3 + 4H^+ = 3Pb^{2+} + CO_3^{2-} + 2H_2O$	11.02
$PbHPO_4 = Pb^{2+} + H^+ + PO_4^{3-}$	-23.805
$Pb_2Cl_2CO_3 = 2Pb^{2+} + 2Cl^- + CO_3^{2-}$	-19.81
Aqueous species	
$H_2CO_3^* = 2H^+ + CO_3^{2-}$	16.681
$H_2PO_4^- = 2H^+ + PO_4^{3-}$	19.576
$H_3PO_4 = 3H^+ + PO_4^{3-}$	21.721
$HCO_3^- = H^+ + CO_3^{2-}$	10.329
$HPO_4^{2-} = H^+ + PO_4^{3-}$	12.375
$Pb(CO_3)_2^{2-} = Pb^{2+} + 2CO_3^{2-}$	9.94
$Pb(OH)_2 + 2H^+ = Pb^{2+} + 2H_2O$	-17.094
$Pb(OH)_3^- + 3H^+ = Pb^{2+} + 3H_2O$	-28.091
$Pb_2OH_3^+ + H^+ = 2Pb^{2+} + H_2O$	-6.397
$Pb_3(OH)_4^{2+} + 4H^+ = 3Pb^{2+} + H_2O$	-23.888
$Pb_4(OH)_4^{4+} + 4H^+ = 4Pb^{2+} + 4H_2O$	-20.888
$PbCl^+ = Pb^{2+} + Cl^-$	1.56
$PbCl_2 = Pb^{2+} + 2Cl^-$	1.9
$PbCl_3^- = Pb^{2+} + 3Cl^-$	1.8
$PbCl_4^{2-} = Pb^{2+} + 4Cl^-$	1.38
$PbCO_3 = Pb^{2+} + CO_3^{2-}$	6.53
$PbH_2PO_4^+ = Pb^{2+} + 2H^+ + PO_4^{3-}$	21.073
$PbHCO_3^+ = Pb^{2+} + H^+ + CO_3^{2-}$	13.23
$PbHPO_4 = Pb^{2+} + H^+ + PO_4^{3-}$	15.475
$PbOH^+ + H^+ = Pb^{2+} + H_2O$	-7.597

[#] All values of log K were taken from Visual MINTEQ 3.0

Table 3.3 Parameters used in Visual MINTEQ 3.0 calculations

Input Parameters	Value
alkalinity	$HCO_3^- = 244$ mg/L
pH	Fixed at sample pH = 6.0
Components	$Cl^- = 120000$ µg/L
	P (PO_4) = 3.45 µg/L
	$Pb^{2+} = 85$ µg/L

Sources of chloride concentration include pH adjustment using dilute HCl, monochloramine decomposition and preparation. For instance, the addition of monochloramine in our experiments can introduce about 30 mg/L Cl^- at 2mg/L NH_2Cl as Cl_2. In drinking water, chloride concentration may increase due to various treatment processes, such as use of ferric chloride as a coagulant, anion exchange and desalinated water as a water source. The highest chloride concentration (~ 110 mg/L) used in this study is well below the 250 mg/L USEPA National Drinking Water Standard for chloride.

The measured P_T indicated that over 50% of the added orthophosphate was removed from the aqueous phase within the first 2 h of experiments, which could be due to its adsorption onto PbO_2 surfaces. Since SEM images showed that chloropyromorphite primarily grew on PbO_2 surfaces, it was likely that PbO_2 might serve as heterogeneous seeds which reduced the surface energy for chloropyromorphite precipitation to take place. Orthophosphate can form complexes such as $PbHPO_4^0$ and $PbH_2PO_4^+$ with Pb^{2+}, hence reducing the availability of free Pb(II) ions for precipitation [85]. More such complexes are expected to form with increasing orthophosphate concentrations. However, at an orthophosphate concentration of 5 mg/L as P, calculations suggest that the lead-phosphate complexes only contributed 0.2% of total soluble lead.

Calculated supersaturation ratios over the course of the experiments ranged from 0.94 to 2.36, 4.54 to 6.35, and 5.44 to 6.52 for initial orthophosphate concentrations of 1, 2 and 5 mg/L as P, respectively. For all three conditions, precipitation of chloropyromorphite had taken place after 8 h based on SEM images. No precipitation could be observed by SEM analysis before 8 h for 1 mg/L as P (Figure 3.7) where the highest soluble Pb(II) concentration around 90 µg/L was observed. The supersaturation ratio of 2.36 obtained for this peak should correspond to the critical value where precipitation was initiated. The supersaturation ratio decreased over time as precipitation continued to take place in oversaturated solutions ($\Omega > 1$). This meta-saturated phenomenon has been reported in several other lead phosphate precipitation studies [5, 86, 87]. The K_{sp} value of chloropyromorphite (Eq(1.3)) was argued to be an underestimation as it was obtained under low pH value and high ionic strength conditions [60]. Systems that contain more than one lead solid phases should not give the predicted values for soluble Pb(II) concentration based on the lowest K_{sp} because it is a thermodynamic parameter and does not provide any kinetics information. Zhang and Ryan [63] reported that lead concentrations were more than 2 orders of magnitude higher than predicted in a study of chloropyromorphite formation from cerussite and hydroxyapatite. The supersaturation ratio was expected to be determined by system kinetics. Our results showed that soluble Pb(II) concentrations stabilized after 48 h and this may be due to the dynamic steady-state reached by the system in which the rate of soluble Pb(II) release from the reductive dissolution of PbO_2 equaled to the rate of soluble Pb(II) consumption due to the precipitation of chloropyromorphite. Figure 3.12 summarizes the proposed dissolution-precipitation mechanism for the peaking and subsequent stabilization of soluble Pb(II) concentration.
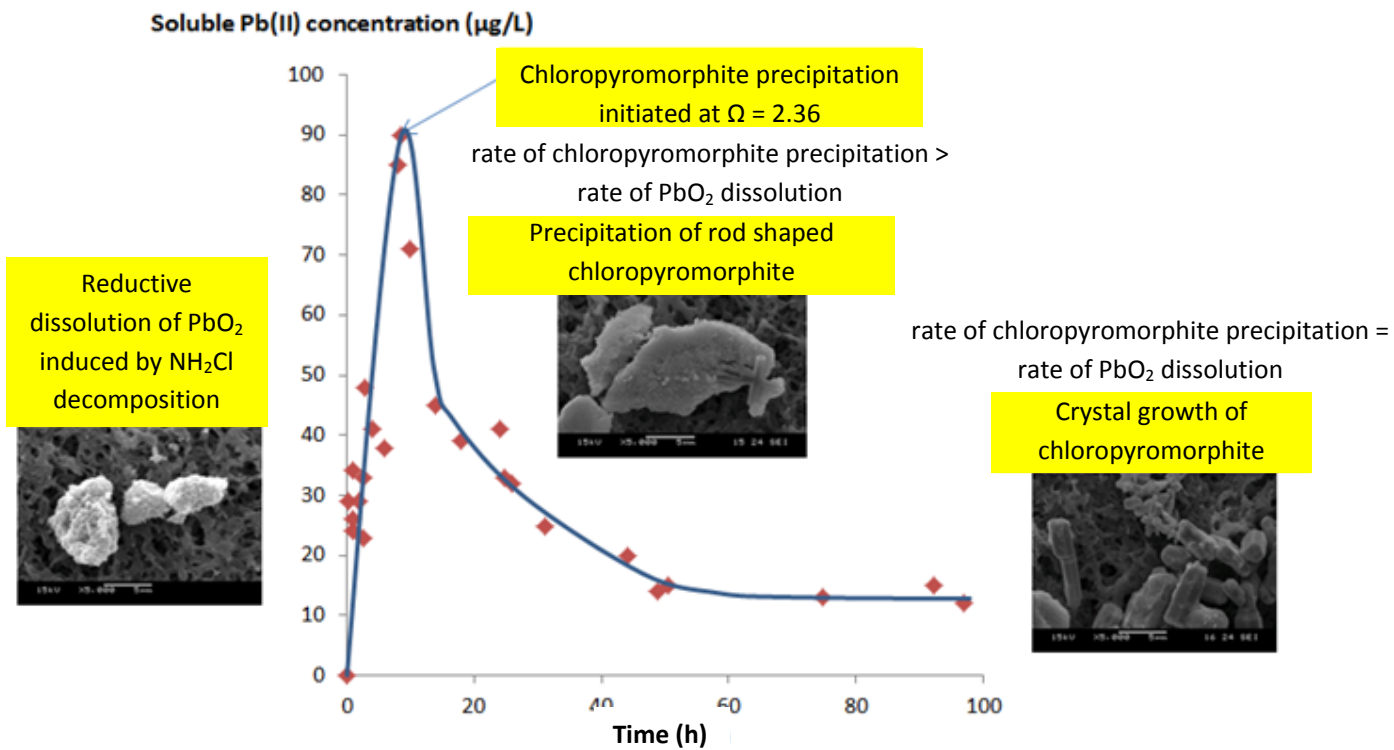
Figure 3.12 Proposed dissolution-precipitation mechanism to explain the lead concentration profile and transformation of lead solid phases. Data were obtained at C_T = 4 mM, NH_2Cl = 2 mg/L as Cl_2, P = 1 mg/L and pH = 6.0.

3.6   Summary

In this chapter, the mechanistic role of orthophosphate as a corrosion inhibitor in controlling lead release from tetravalent lead corrosion product PbO_2 in chloraminated solutions was investigated. This system represents distribution networks experiencing disinfectant changeover from free chlorine to monochloramine. In all experiments with orthophosphate addition of at least 1 mg/L as P, peaking of soluble Pb(II) concentration within the first 24 h was observed before lead concentrations decreased and stabilized at levels lower than 15 μg/L. The variation of soluble Pb(II) concentration could be attributed to the dynamics between the rate of PbO_2 reductive dissolution, primarily induced by monochloramine decomposition, and that of chloropyromorphite ($Pb_5(PO_4)_3Cl$) precipitation, which did not occur until a critical supersaturation ratio of about 2.36 was reached in the solution. This study provides insights to how orthophosphate addition reduces lead levels under drinking water conditions and highlights the potential risk of short-term elevated lead concentrations. Intensive monitoring following the disinfectant changeover may be required to determine the overall lead exposure when using orthophosphate as a corrosion inhibitor.

Chapter 4

Effects of various water parameters on galvanic corrosion between lead and copper in drinking water

In recent years, lead contamination in drinking water caused by galvanic corrosion in leaded solders, brass fittings and during partial replacement of lead pipes has raised concerns of the public. Many studies have been conducted using new or used pipes and fittings. However, some phenomena could not be explained due to the complex nature of these systems. In this chapter, a simpler and more direct methodology was adopted via the use of pure lead and copper wires to gain insight to galvanic corrosion in drinking water. The objective of this study is to investigate the effects of stagnation, complete mixing, pH, chloride, sulfate, free chlorine, monochloramine and orthophosphate on galvanic corrosion between lead and copper. Characterizations of formed corrosion products, copper and lead release profiles, wire mass differences and disinfectant residual were used to provide a better understanding of the mechanisms and processes involved in galvanic corrosion in drinking water.

4.1   Effects of stagnation, complete mixing and solution pH

Figure 4.1 and 4.2 illustrate the effects of stagnation and complete mixing on galvanic corrosion with various total effective lengths. In stagnant water, soluble copper release decreased (Figure 4.1a) and soluble lead release increased (Figure 4.1b) as the total effective length increased. In the copper/lead couple, oxygen can be reduced to OH^- on the copper cathode surface ($O_2 + 2H_2O + 4e^- \rightarrow 4OH^-$) resulting in the local increase of pH. On the other hand, the released lead ion due to the oxidation of lead anode ($Pb \rightarrow Pb^{2+} + 2e^-$) served as a Lewis acid, which decreased the local pH near lead wire surface via the formation of soluble complexes or insoluble precipitates that contain OH^- [88]. In stagnant conditions, the magnitude of localized pH

increase around copper is much smaller than the localized pH decrease around lead [43]. At a shorter total effective length, the proximity of the two metals allowed the localized acidic pH at the lead anode surface affecting the copper cathode surface and causing higher copper release. The release of copper gradually decreased as copper ions can serve as an electron acceptor and be reduced to elemental copper again at the cathode (Figure 4.1a). Soluble lead was the lowest at 168 μg/L after 7 d when lead was not connected with copper (Figure 1b), in which the release of lead was solely due to oxidative dissolution of lead wire by oxygen ($2Pb + O_2 + 2H_2O \rightarrow 2Pb^{2+} + 4OH^-$). When lead wire was connected to copper wire, the galvanic cell accelerated lead release and the amount of lead released increased with the increasing total effective length. The extent of soluble lead increase due to surface area became more significant as the lead surface area increased. This implies that lead release due to galvanic corrosion and oxidative dissolution were taking place simultaneously with galvanic corrosion occurring predominantly near the contact area and oxidative dissolution taking place along the length of the wire. Triantafyllidou and Edwards [41] and Reiber and Dufresne [89] also reported that the segment nearest to the lead-copper junction was the most affected by galvanic corrosion.
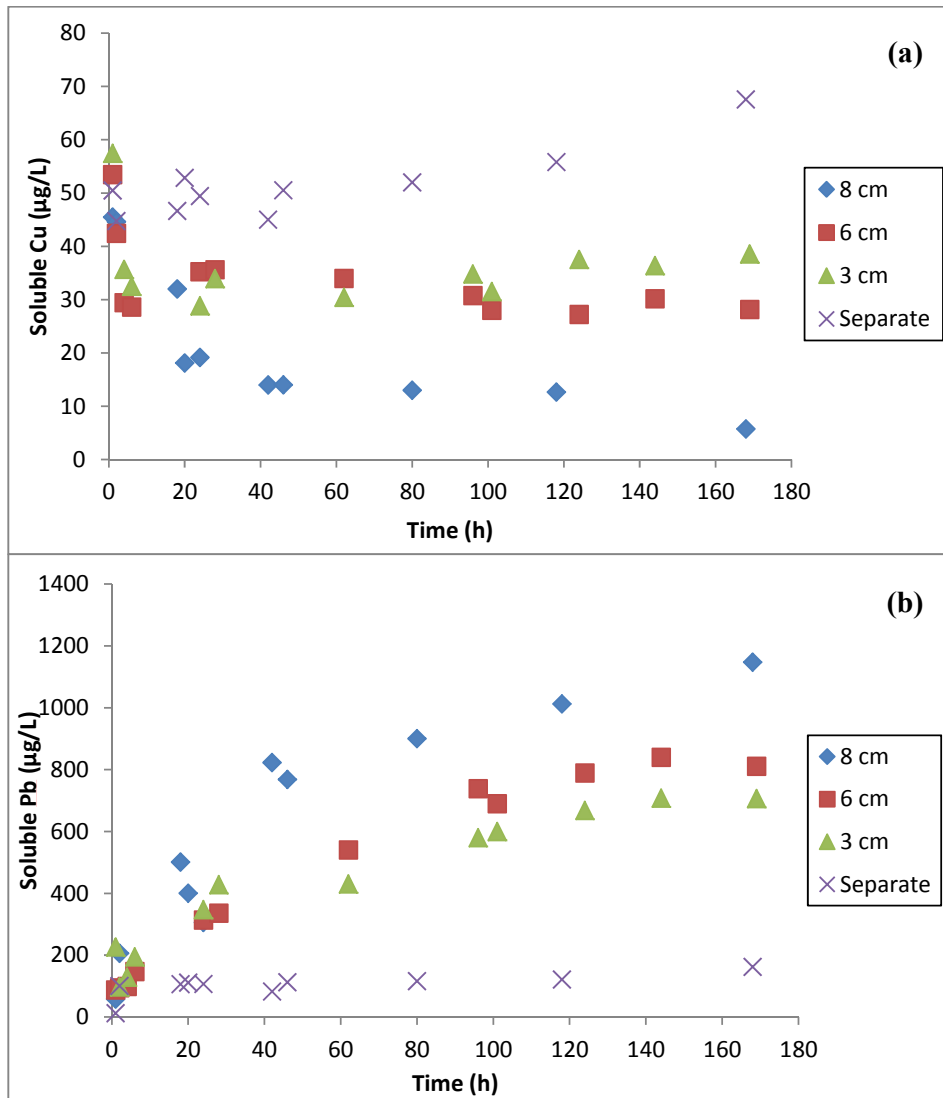
Figure 4.1 Soluble (a) copper and (b) lead concentrations as a function of time in stagnant water for 5 cm of Pb and Cu wires separated, and knotted into total effective lengths of 3 cm, 6 cm and 8 cm at pH 7.8.

Under completely-mixed conditions, localized acidic pH was eliminated. The various total effective lengths had no observable effects on copper release and the soluble copper decreased gradually over time and reached a steady level of about 25 µg/L at the end of 7 d (Figure 4.2a). Soluble lead release, however, was accelerated by mixing and its impact was more significant when a longer total effective length was exposed to water. The highest soluble lead concentration was 2200 µg/L for the longest total effective length of 8 cm (Figure 4.2b). After 7 d, soluble lead increased by 46%, 74% and 92% for total effective lengths of 3 cm, 6 cm and 8 cm, respectively when compared to those under stagnant conditions. More than 90% of the total lead existed as the soluble lead under stagnant conditions compared to 66% under completely-mixed conditions (Figure 4.3). The physical action of stirring may cause erosion corrosion [90] and can speed up both oxidation and reduction reactions at the anode and cathode respectively. Erosion corrosion on the copper surface may have been compensated by the increased reduction reactions. In real systems, mixing will be provided by the water flow which provides both mixing and removal of corrosion products. The main differences between mixing in experimental system and real system are that corrosion products and by-products, such as soluble copper and lead and surface scaling, will accumulate while oxidants such as dissolved oxygen will deplete in the batch experiments but not in real systems.
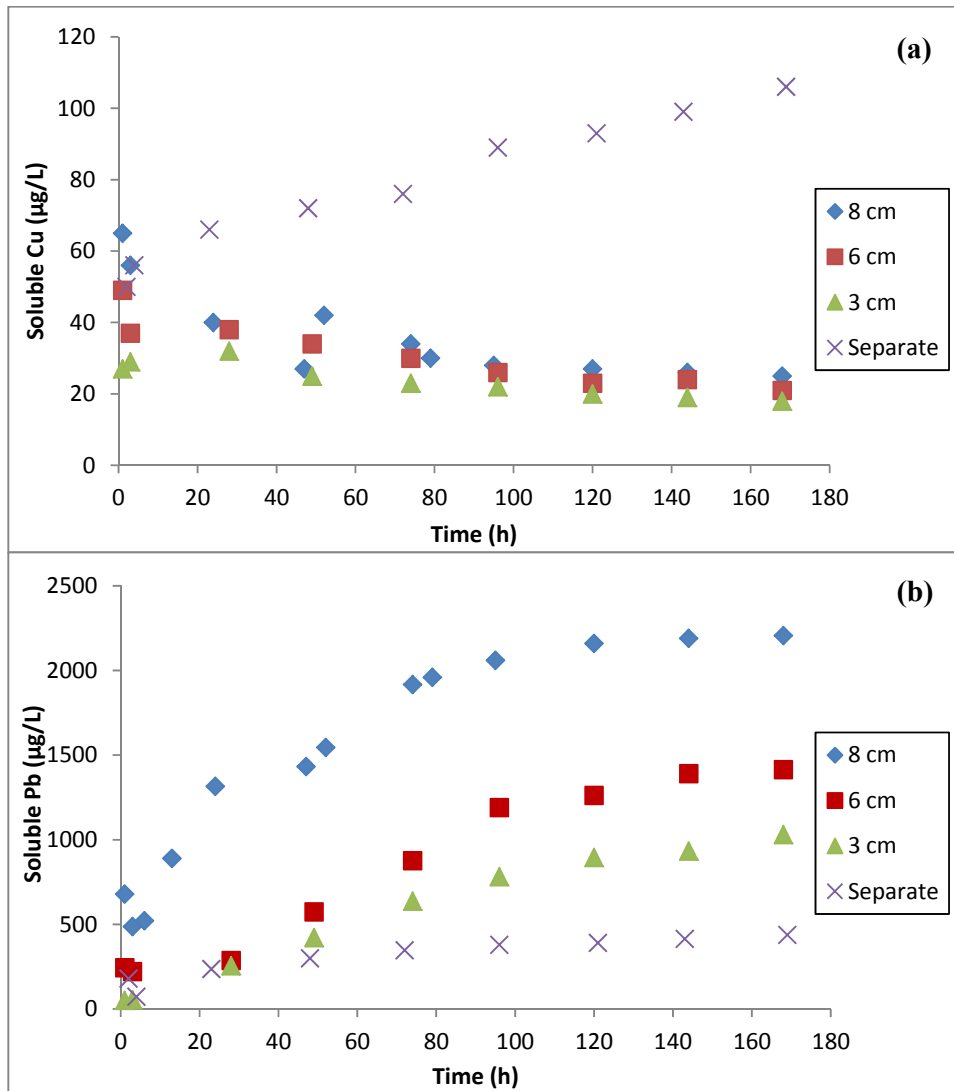
Figure 4.2 Soluble (a) copper and (b) lead concentrations as a function of time in completely-mixed water for 5 cm of Pb and Cu wires separated, and knotted into total effective lengths of 3 cm, 6 cm and 8 cm at pH 7.8.
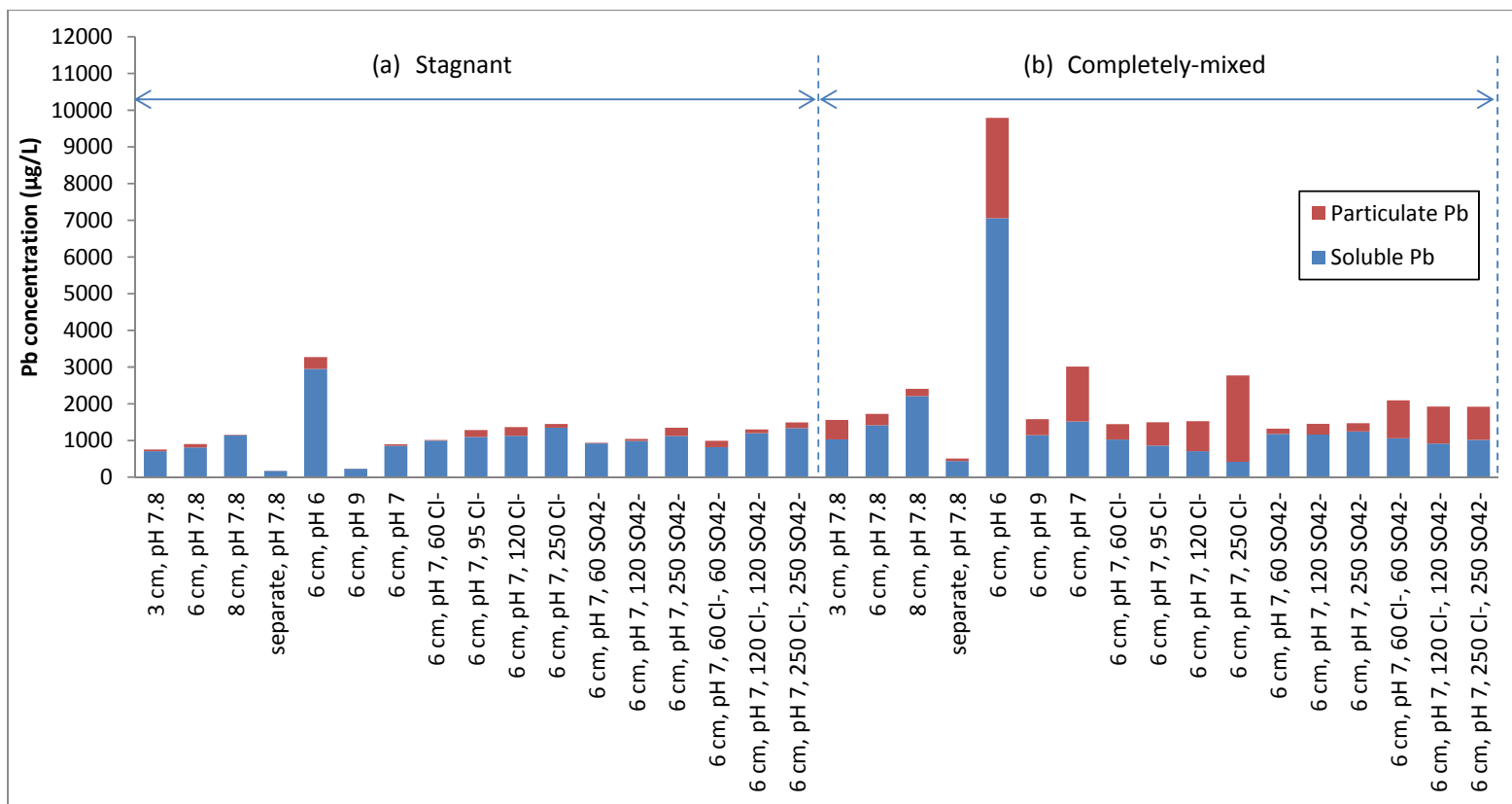
Figure 4.3 Summary of total lead release in (a) stagnant and (b) completely-mixed conditions after 7 d.

53

Figure 4.4 shows the effects of solution pH on soluble copper and lead release under stagnant and completely-mixed conditions. In stagnant water, lower pH increased both soluble copper and lead release whereas in completely-mixed water, lower pH only promoted soluble lead release. In completely-mixed water, soluble copper concentrations appeared to have reached steady state of about 50 μg/L after 48 h regardless of solution pH (Figure 4.4a). When copper was not connected to lead, copper was not protected resulting in a higher release (Figure 4.5). When copper was connected to lead, copper was protected and lead release was accelerated due to galvanic corrosion (Figure 4.4b). At pH 6.0, the release of soluble lead showed the following increasing trend: 1108 μg/L (without galvanic connection in stagnant water) → 2096 μg/L (without galvanic connection in completely-mixed water) → 2950 μg/L (with galvanic connection in stagnant water) → 7055 μg/L (with galvanic connection in completely-mixed water) after 7 d (Figure 4.6). Mixing may have a synergistic effect with galvanic corrosion, resulting in more lead release than the sum caused by each condition alone. Figure 4.7 shows the changes in solution pH as a function of time at different initial solution pH. Solution pH remained relatively stable for initial pH of 6.0 for both stagnant and completely-mixed conditions. Under stagnant conditions, solution pH decreased from 9.0 to 7.7 and 7.8 to 7.5; while under completely-mixed conditions, solution pH decreased from 9.0 to 7.2 and 7.8 to 7.0 after 7 d. The decrease in solution pH could be attributed to the formation of lead complex or lead solids containing carbonate or hydroxide ions. The experimental solutions were not buffered on purpose because addition of buffer will not only lose the relevance and applicability of this study for using raw tap water over synthetic water, but also any changes in solution pH will not be captured and the interaction between the buffer and galvanic corrosion will add to the complexity of this study.
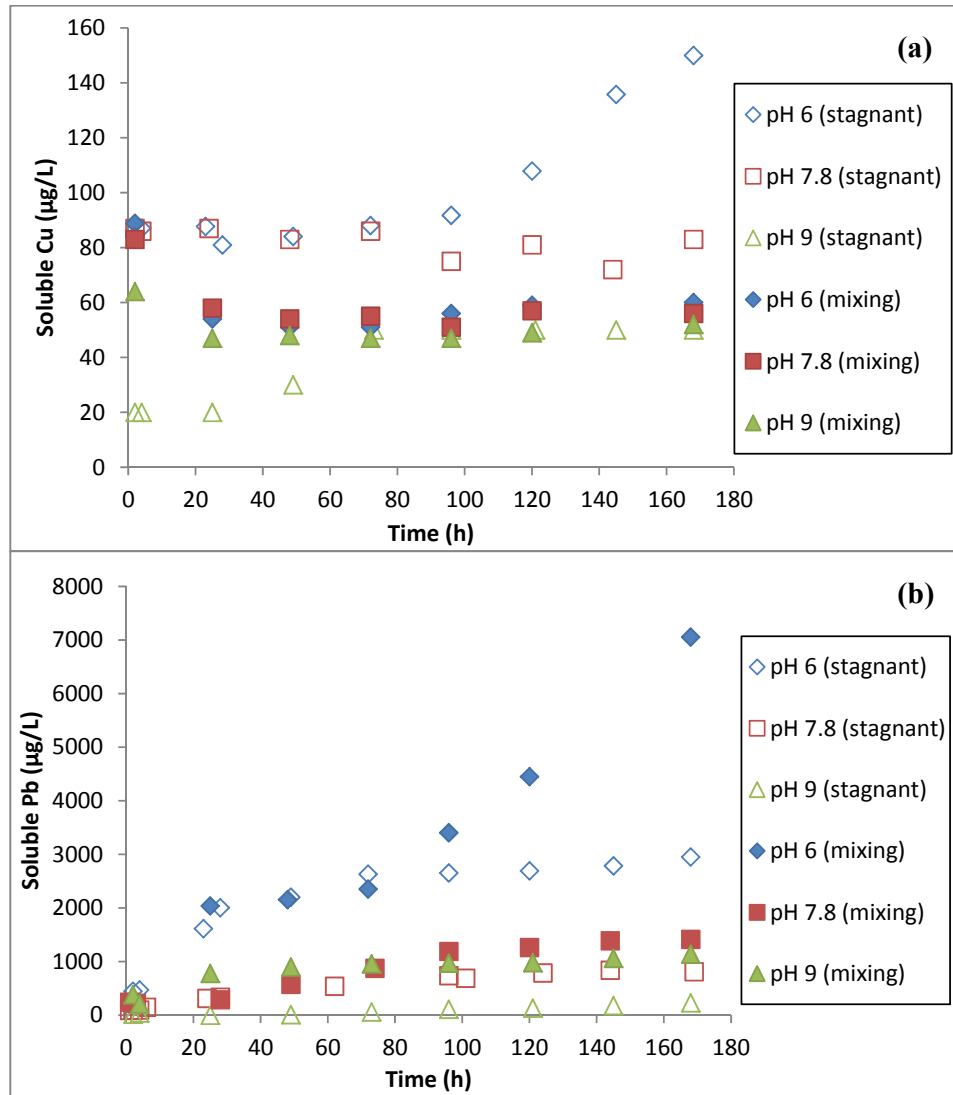
Figure 4.4 Soluble (a) copper and (b) lead concentrations as a function of time at different solution pH. Experimental conditions: total effective length = 6 cm.
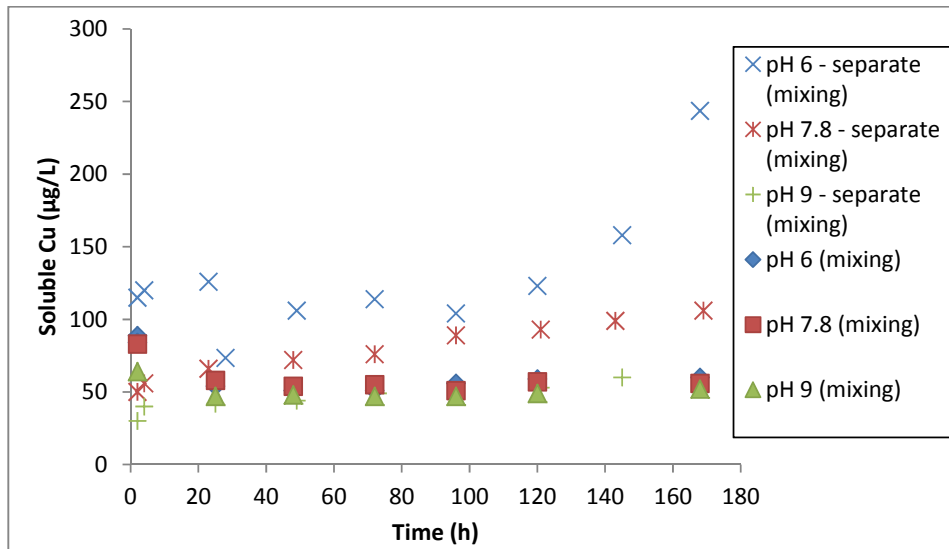
Figure 4.5 Soluble copper concentration as a function of time at different pH values in completely-mixed conditions. Experimental conditions: total effective length = 6 cm.
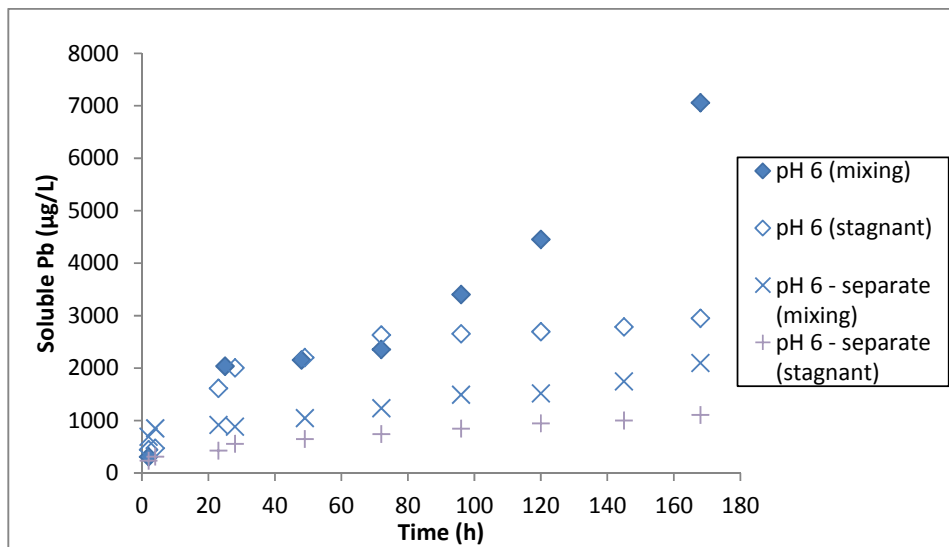
Figure 4.6 Soluble lead concentration as a function of time at pH 6.0. Experimental conditions: total effective length = 6 cm.
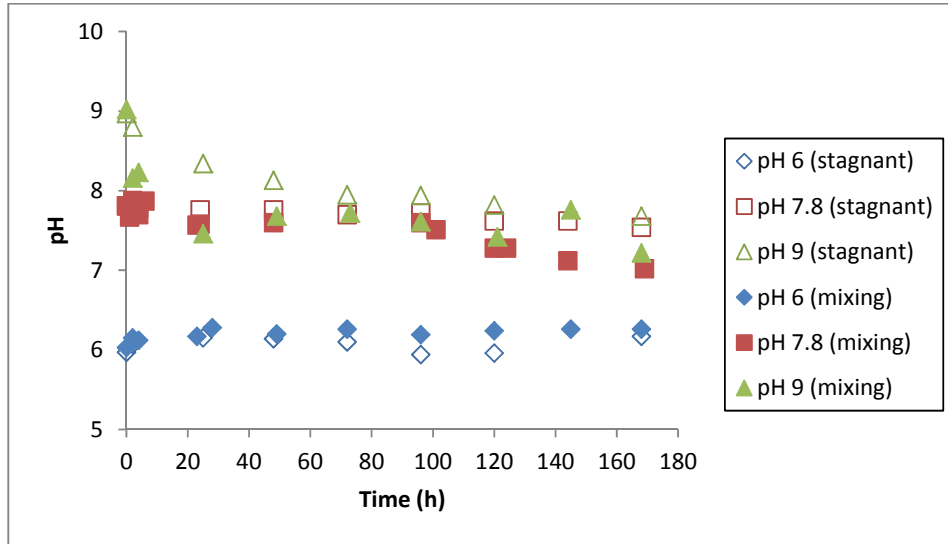
Figure 4.7 Solution pH as a function of time at different solution pH. Experimental conditions: total effective length = 6 cm.

4.2 Effects of chloride and sulfate dosages

4.2.1 Effects of chloride dosages

Figure 4.8 shows the effects of varying chloride dosages on soluble lead release in stagnant and completely-mixed conditions at pH 7.0. In stagnant water (Figure 4.8a), released soluble lead concentration increased with the increasing chloride dosage (or increasing CSMR). This observation is consistent with the works of Edwards and Triantafyllidou [28] and Nguyen et. al [40]. They proposed that the complexation of chloride and free lead ion forming $PbCl^+$ enhanced soluble lead release. Modeling results using Visual MINTEQ 3.0 [84] showed that $PbCl^+$ contributed 4% and 11% to soluble Pb species with free Pb^{2+} being the dominant species at 50% for both 60 mg/L and 250 mg/L chloride dosages respectively after 7 d. This suggests that lead complexation due to the addition of chloride can promote soluble lead release. A more rapid soluble lead release should also initiate earlier precipitation of lead minerals when their solubility products are exceeded. Precipitation of lead minerals removes soluble Pb(II) from the solution, driving the system to produce more soluble Pb(II) to maintain the equilibrium. Soluble copper remained at a steady concentration of about 50 µg/L throughout the experiment (data not shown).

57

In completely-mixed water, the trends of soluble lead release as a function of time differed with different chloride concentrations (Figure 4.8b). In tap water without additional addition of Cl⁻ (Cl⁻ = 35 mg/L), the soluble lead concentration gradually increased and reached a plateau of about 1600 µg/L in 100 h. With additional chloride added, the soluble lead concentration reached a maximum then decreased. Similar trend was observed by Liu, et. al [91] who investigated lead release using lead-tin coupon in jar tests. It was also observed that the maximum lead concentration was reached in a shorter time interval when a higher chloride dosage was employed. For example, the soluble lead concentration peaked at approximately 24 h, 36 h, 47 h and 70 h for spiked chloride dosages of 60 mg/L, 95 mg/L, 120 mg/L and 250 mg/L, respectively (Figure 4.8b). The high chloride concentration, coupled with mixing, caused the release of tremendous amounts of soluble lead into the solution resulting in the precipitation of a white mineral coating both on the copper and lead wires in 24 h and passivating the surface to prevent further galvanic corrosion. It should be noted that as chloride concentration increased, the amount of particulate lead became more significant, reaching as high as 85% of total lead (Figure 4.3). The results suggested that drinking water containing high concentrations of chloride may experience more lead contamination issues in the form of particulate lead which is more dynamic and harder to control. The release of soluble copper decreased with the increasing chloride dosage (Figure 4.9). Soluble copper reached a steady state below 25 µg/L for all chloride dosages employed indicating that the chloride concentration had no significant impact on the long-term soluble copper release. Figure 4.10 shows that solution pH increased slightly from 7.0 to 7.1 and 7.0 to 7.3 under stagnant and completely-mixed conditions respectively after 7 d.
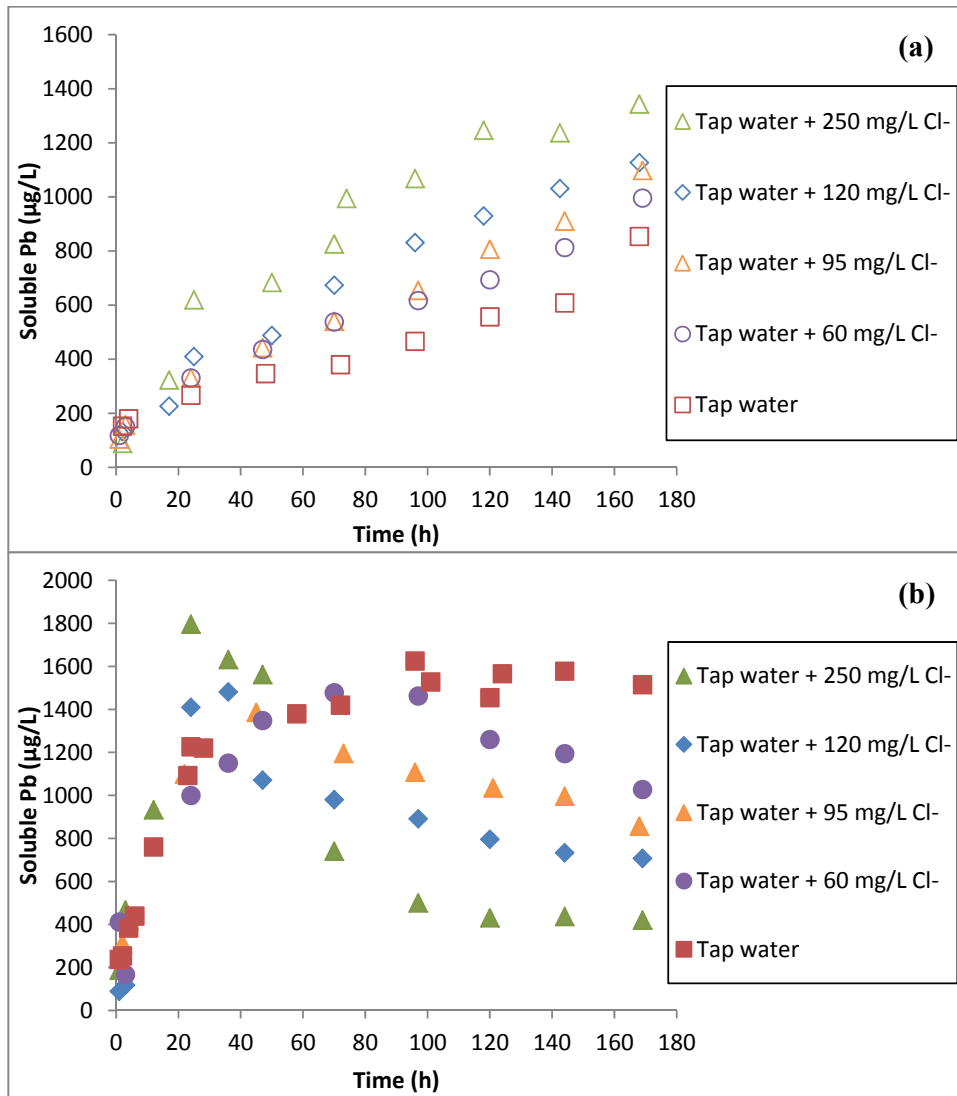
Figure 4.8 Soluble lead concentration in (a) stagnant and (b) completely-mixed conditions as a function of time with different chloride dosages. Tap water conditions: 35 mg/L Cl⁻ and 18 mg/L SO_4^{2-}. Experimental conditions: total effective length = 6 cm, pH = 7.0.
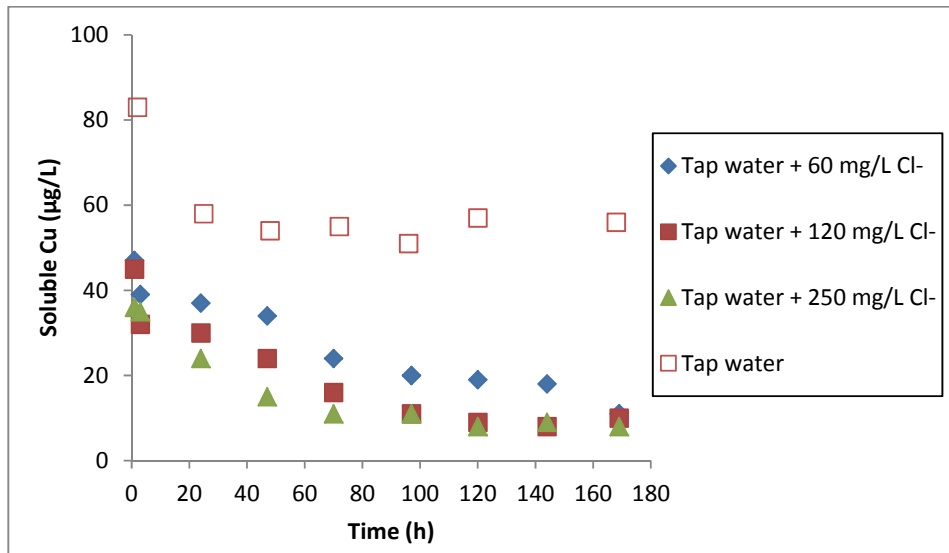
Figure 4.9 Soluble copper concentration as a function of time with different chloride dosages in completely-mixed conditions. Tap water conditions: 35 mg/L Cl$^-$ and 18 mg/L SO$_4^{2-}$. Total effective length = 6 cm, pH = 7.0.
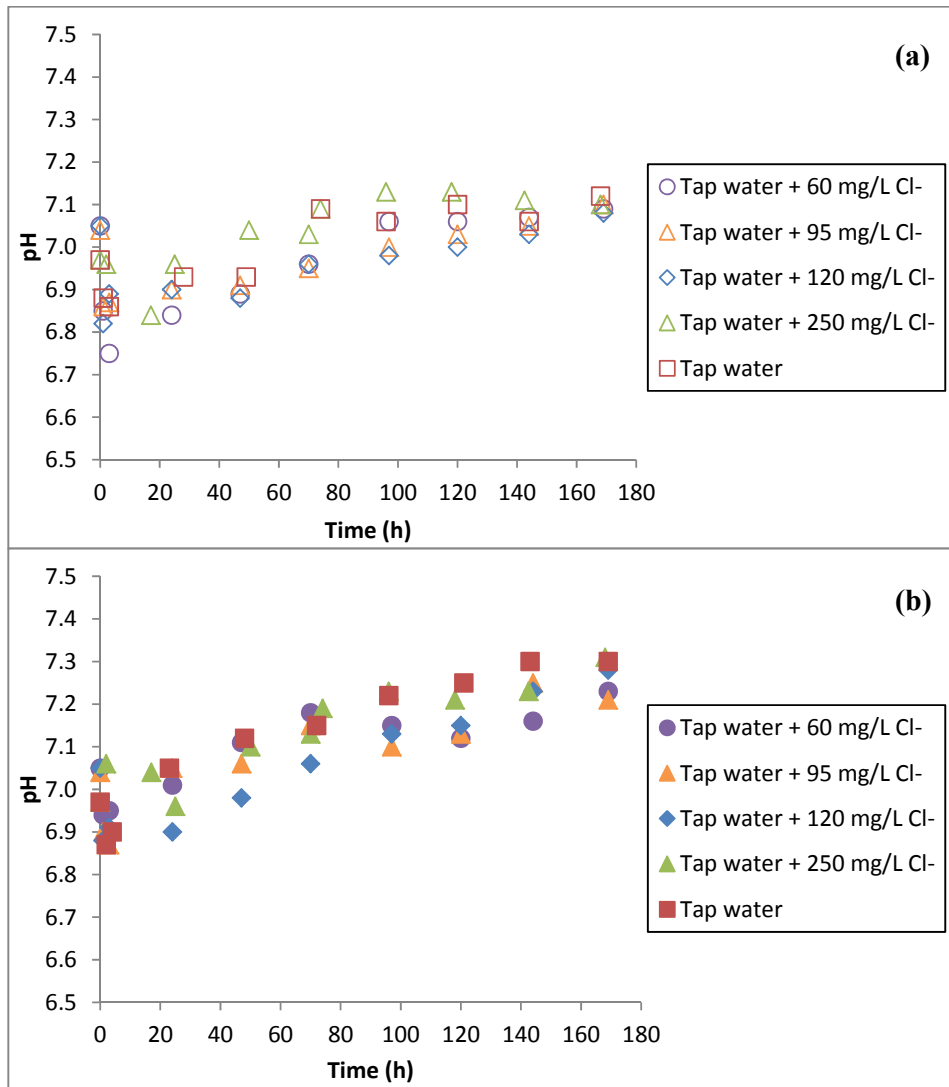
Figure 4.10 Solution pH in (a) stagnant and (b) completely-mixed conditions as a function of time with different chloride dosages. Tap water conditions: 35 mg/L Cl⁻ and 18 mg/L SO_4^{2-}. Experimental conditions: total effective length = 6 cm, pH = 7.0.

4.2.2 Effects of sulfate dosages

Figure 4.11 shows the effects of varying sulfate dosages on soluble lead release in stagnant and completely-mixed conditions at pH 7.0. In stagnant water (Figure 4.11a), increasing sulfate (or decreasing CSMR) dosages promotes soluble lead release. This finding is contradictory to the works by Edwards and Triantafyllidou [28] and Nguyen et. al [40] which showed that an increase in CSMR would promote lead release. Both studies used treated water shipped from the treatment plants without further addition of sulfate or chloride. Lead-tin solder and copper tubing with a dump-and-fill protocol were used in these studies, giving a stagnation period of 2-4 d prior to each sampling. The ratio of cathode-to-anode (copper-to-lead) surface area was also not controlled in their studies as the amount of lead on solder surface is not known. A large cathode-to-anode surface area concentrates galvanic attack in small areas and hastens depth of anode penetration [44]. Hence, it is possible that differences in surface area ratio could have caused inherent differences in galvanic corrosion. Precipitation of lead sulfate was proposed as a reason for the decrease in lead release in low CSMR waters [28]. In this study, pure copper and lead wires with known dimensions were used (cathode to lead surface area ratio is approximately constant for all conditions) for up to 7 d. According to modeling results using Visual MINTEQ 3.0 [84], precipitation of cerussite ($PbCO_3$), hydrocerussite ($Pb_3(CO_3)_2(OH)_2$), lead hydroxide ($Pb(OH)_2$) and larnakite ($PbO:PbSO_4$) may occur under our experimental conditions. Among the four minerals, hydrocerussite has the lowest solubility product (K_{sp}) of $10^{-18.8}$, followed by cerussite ($K_{sp} = 10^{-13.2}$), larnakite ($K_{sp} = 10^{-0.4}$) and lead hydroxide ($K_{sp} = 10^{8.15}$). The saturation index, $SI = \log\left(\dfrac{IAP}{K_{sp}}\right)$, calculated using Visual MINTEQ 3.0 where IAP is the ion activity product shows that the experimental solution after 7 d is the most saturated with respect to hydrocerussite ($SI = 2.45$), followed by cerussite (0.71), larnakite (0.54) and lead hydroxide (0.52). The calculations indicated that hydrocerussite would most likely to be formed. In addition, soluble Pb(II) can also form soluble $PbSO_4^0$ complex with sulfate ions. $PbSO_4^0$ contributed 10% and 25% to soluble Pb species for 60 mg/L and 250 mg/L sulfate dosages respectively,

indicating that lead sulfate complexation could have also promoted soluble Pb(II) release. In completely-mixed water (Figure 4.11b), the addition of sulfate resulted in a decrease in soluble lead after 72 h before reaching about 1100 µg/L after 7 d, in which soluble lead contributed 80-89% to total lead (Figure 4.3). Similarly, this could be due to the formation of scales that passivated the surface. Characterization of formed solids is presented later in Section 4.5.1. The presence of sulfate had negligible impact on copper release (data not shown). Similar to chloride addition, solution pH had a slight increase of 0.3 pH unit after 7 d (Figure 4.12).
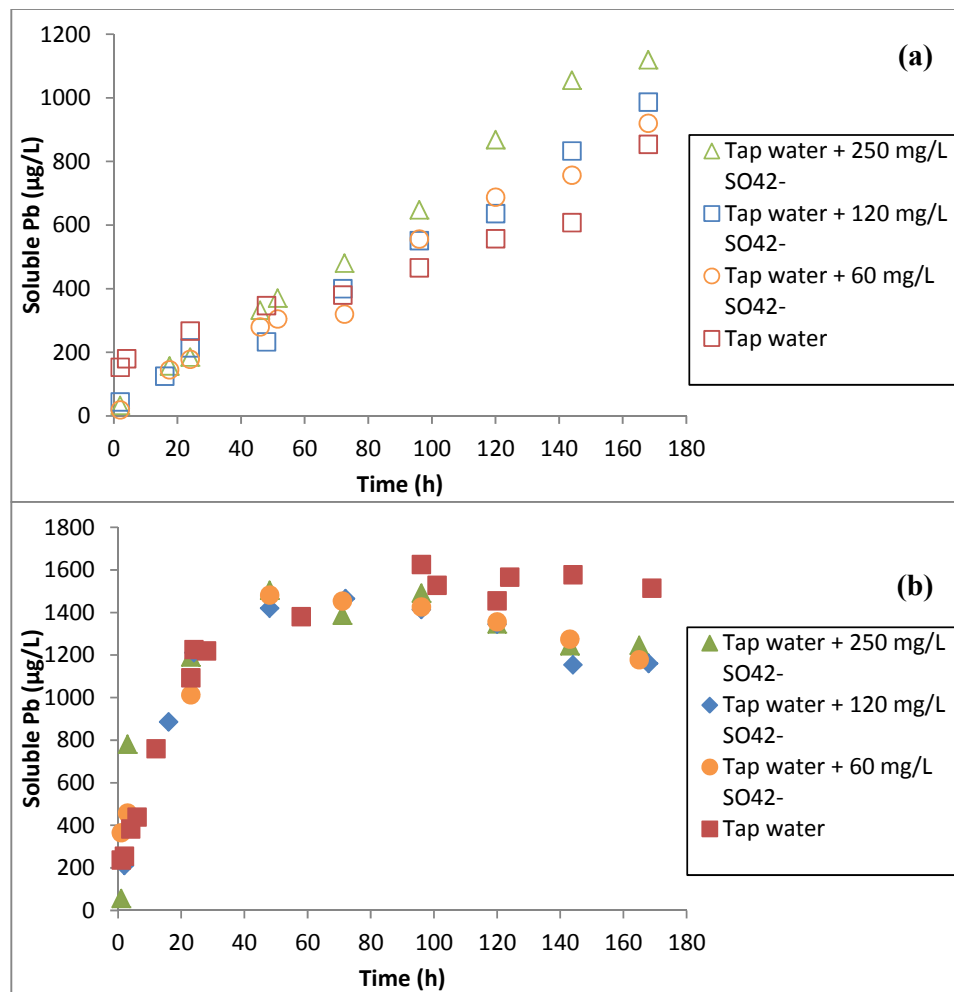
Figure 4.11 Soluble lead concentration in (a) stagnant and (b) completely-mixed conditions as a function of time with different sulfate dosages. Tap water conditions: 35 mg/L Cl^- and 18 mg/L SO_4^{2-}. Experimental conditions: total effective length = 6 cm, pH = 7.0.
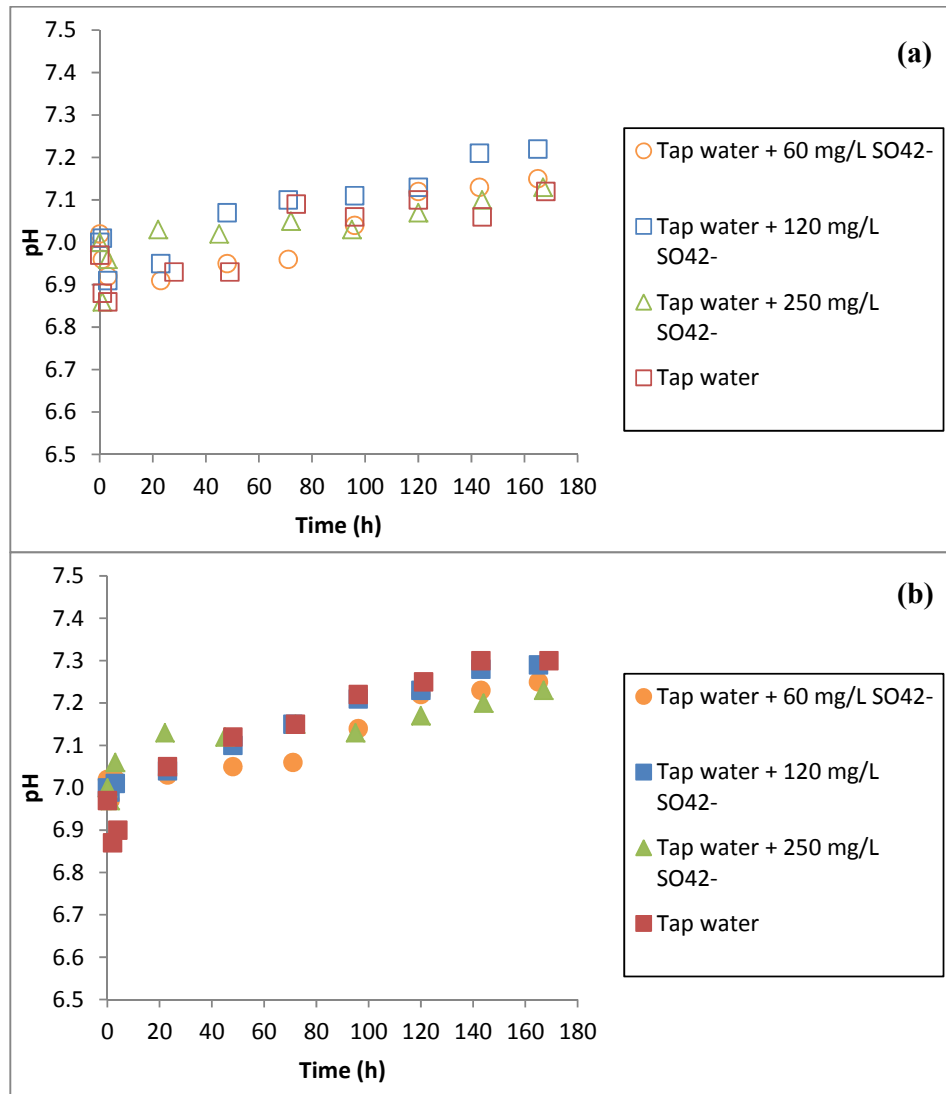
Figure 4.12 Solution pH in (a) stagnant and (b) completely-mixed conditions as a function of time with different sulfate dosages. Tap water conditions: 35 mg/L Cl⁻ and 18 mg/L SO_4^{2-} . Experimental conditions: total effective length = 6 cm, pH = 7.0.

4.2.3 Comparison between effects of chloride and sulfate dosages

The effect of chloride addition on soluble lead release was compared to that of sulfate addition at the same mass concentration of 250 mg/L in stagnant (Figures 4.8a and 4.11a) and completely-mixed conditions (Figures 4.8b and 4.11b) at pH 7.0. In stagnant water, chloride promoted more soluble lead release as compared to sulfate at the same mass concentration. However, it is important to note that the molar concentration of 250 mg/L of chloride (7.04 mM) is 1.67 times greater than that of 250 mg/L of sulfate (2.63 mM). A better comparison based on molar concentration would be between 95 mg/L chloride (2.68 mM) and 250 mg/L sulfate (2.63 mM) (Figure 4.13), in which soluble lead concentrations after 7 d were 1098 µg/L and 1120 µg/L, respectively. Hence, at the same mass concentrations, chloride was more corrosive than sulfate, causing more lead release. However, at the same molarity, chloride and sulfate caused approximately the same amount of lead release.

In completely-mixed water, the addition of both chloride and sulfate caused a peaking effect on lead release, while the process with sulfate addition was slower. After 7 d, soluble lead reached a steady state of about 420 µg/L with 250 mg/L chloride addition (Figure 4.8b) and appeared to be still decreasing at 1246 µg/L with the same addition of sulfate mass concentration (Figure 4.11b). The latter exhibited a similar trend obtained at a chloride addition of 95 mg/L (Figure 4.8b). In addition, 250 mg/L sulfate addition caused 1470 µg/L total lead release compared to 1496 µg/L total lead release with 95 mg/L chloride addition (Figure 4.3). This further supports the theory that chloride and sulfate at the same molar concentration can induce the similar amount of soluble lead release in drinking water. However, visual observations showed that there was more white scaling formed on the wires in solutions containing chloride than sulfate at the same molar concentration. Soluble Pb(II) complexation with chloride and sulfate promoted Pb(II) release in this study. The stability constant of $PbSO_4^0$ (log K = 2.69) is higher than that of $PbCl^+$ (log K = 1.56). This could explain the formation of lead minerals

of higher solubility such as $PbO:PbSO_4$ with sulfate addition compared to chloride addition, hence resulting in less particulate lead with sulfate addition than chloride addition at the same molar concentration. Molar concentration, which is typically used in chemical stoichiometry and kinetics, is seldom used to express drinking water parameters as compared to mass concentration. Our results suggest that molar concentration of chloride and sulfate should be considered when accessing galvanic corrosion.
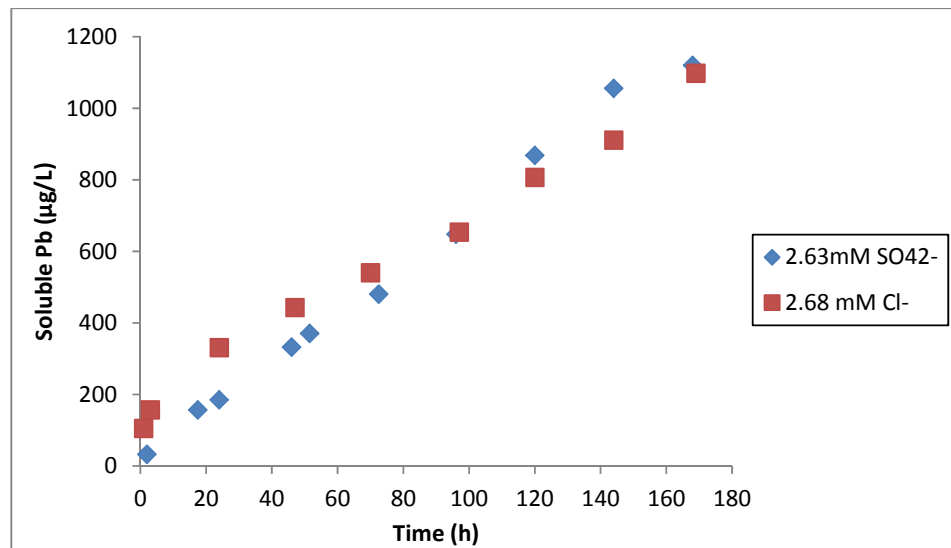
Figure 4.13 Soluble lead concentration as a function of time with about 2.65mM chloride and sulfate additions in stagnant conditions. Total effective length = 6 cm, pH = 7.0.

4.2.4 Effects of varying chloride and sulfate concentrations at a constant CSMR

Soluble lead release in the presence of varying chloride and sulfate concentrations at a constant CSMR of unity in stagnant and completely-mixed conditions at pH 7.0 is shown in Figure 4.14. In stagnant water, increasing chloride and sulfate concentrations at a constant CSMR of unity promoted soluble lead release. A recent study by Willison and Boyer [29] also reported a higher lead release at higher chloride and sulfate concentrations using Pb-Sn solder connected with copper tubing at a constant CSMR of 0.5 for a stagnation period of 3 to 4 d. Hence, CSMR may not be a good indicator for

corrosivity of water as it can be misleading especially in waters with high chloride and sulfate concentrations but a low CSMR. Varying chloride and sulfate concentrations at a constant CSMR did not have an observable effect on copper release (data not shown).

In completely-mixed water, soluble lead increased rapidly in the first 48 h before it started to decrease to a steady level of about 1100 µg/L. This trend was similar to that observed in experiments with the addition of sulfate (Figure 4.11b), but with a shorter time interval before soluble lead started to decrease. The presence of higher chloride and sulfate concentrations may have promoted lead release which subsequently resulted in a faster precipitation of the scales.
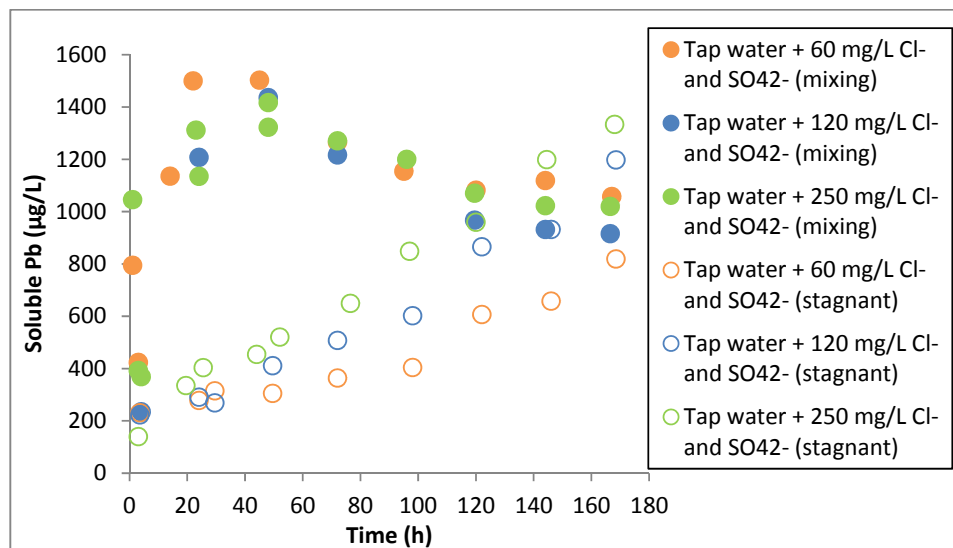
Figure 4.14 Soluble lead concentration as a function of time with different chloride and sulfate additions at a constant CSMR of 1 in stagnant and completely-mixed conditions. Tap water conditions: 35 mg/L Cl⁻ and 18 mg/L SO_4^{2-}. Experimental conditions: total effective length = 6 cm, pH = 7.0.

## 4.3 Effects of initial free chlorine and monochloramine concentration

4.3.1 Effects of initial free chlorine concentration

Figure 4.12 shows the effects of free chlorine concentration ($0.5 - 8.0$ mg/L as Cl_2) on the release of soluble copper and soluble lead as a function of time at pH 7.0 under stagnant conditions. The release of soluble copper decreased over time and the extent slightly decreased with the increasing free chlorine concentration (Figure 4.15a). Soluble lead released, on the other hand, increased over time for all free chlorine concentrations employed and the extent was promoted by a higher free chlorine concentration (Figure 4.15b). When copper wire is connected to lead wire, copper is protected while lead is sacrificed [14]. It was also noted that the release of soluble copper could be caused by the localized acidic pH at the anode (lead) in stagnant water condition since the released lead ion (Pb^{2+}) can act as a Lewis acid which decreases pH by removing OH^- ions from the water via the formation of soluble complexes and insoluble precipitates containing OH^- [88]. After 7 d, soluble copper concentration was approximately the same at about 82 μg/L with 0.5, 1 and 2 mg/L as Cl_2, and the lowest at 67 μg/L with 8 mg/L as Cl_2. Soluble lead was the highest at 1763 μg/L with an initial free chlorine concentration of 8.0 mg/L as Cl_2 and the lowest at 476 μg/L with 0.5 mg/L as Cl_2. The presence of free chlorine, which induced a high oxidation potential in the experimental solution, accelerated the release of lead in the galvanic couple in the 7-d tests. As the free chlorine concentration increased, galvanic corrosion seemed to be accelerated, causing a faster lead oxidation and copper reduction and resulting in a higher lead release and lower copper release. Reiber [46] observed an increase in galvanic currents between lead-tin solder and copper joint in the presence of free chlorine, implying that the rate of electron transfer increased in the presence of free chlorine. The addition of free chlorine introduced more ions such as chloride, hypochlorite and sodium ions into the solution. This increase in ionic concentration can have two effects on the system. First, it increases the conductivity of the solution, allowing for more rapid electron transfer. Second, it alters the reactions involved in galvanic corrosion within the system. For example, it is

thermodynamically possible that electron donors such as chloride ions (Cl⁻) can be oxidized at the anode to form hypochlorite ions (OCl⁻) and electron acceptors such as hypochlorous acid (HOCl) can be reduced at the cathode to chlorine gas (Cl_2) (Eq 4.1-4.6) [36].

$$O_2 + 4H^+ + 4e^- \rightarrow 2H_2O \qquad E° = +1.23 \text{ V} \qquad (4.1)$$

$$O_2 + 2H_2O + 4e^- \rightarrow 4OH^- \qquad E° = +0.40 \text{ V} \qquad (4.2)$$

$$ClO^- + H_2O + 2e^- \rightarrow Cl^- + 2OH^- \qquad E° = +0.89 \text{ V} \qquad (4.3)$$

$$2HClO + 2H^+ + 2e^- \rightarrow Cl_2 + 2H_2O \qquad E° = +1.63 \text{ V} \qquad (4.4)$$

$$Cu^{2+} + 2e^- \rightarrow Cu \qquad E° = +0.34 \text{ V} \qquad (4.5)$$

$$Pb^{2+} + 2e^- \rightarrow Pb \qquad E° = -0.13 \text{ V} \qquad (4.6)$$

When chloride ions are oxidized at the anode with dissolved oxygen being reduced at the cathode, hypochlorite ions are formed at the anode. These hypochlorite ions are strong oxidizing agents and can oxidize Pb(0) at lead anode to soluble Pb(II), resulting in more soluble Pb(II) release. Similarly, when hypochlorous acid is preferentially reduced to Cl_2 at the copper cathode with Pb(0) being oxidized to Pb(II) at the lead anode, copper reduction at the copper cathode will be impeded. However, hypochlorous acid can react directly with both Pb(0) and Cu(0) and oxidize them to their soluble forms. When this occurs, it is likely that the flow of electrons in the galvanic couple will be disrupted. Arnold, Jr and Edwards [51] observed a potential reversal between lead and copper pipes in the presence of free chlorine with intermittent flow. Solution pH increased slightly from 7.0 to 7.3 after 7 d (Figure 4.16).
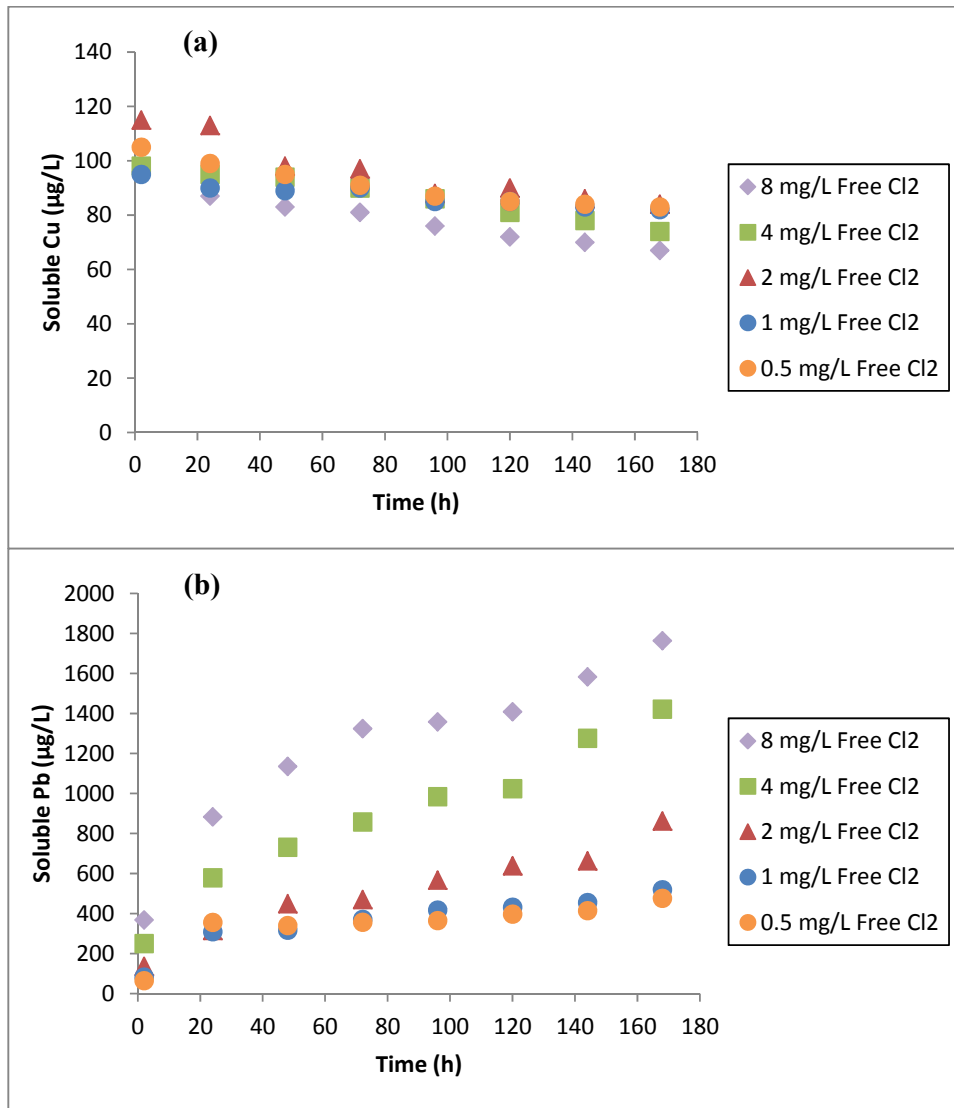
Figure 4.15 Soluble (a) copper and (b) lead concentrations as a function of time with different initial free chlorine concentrations under stagnant conditions. Experimental conditions: pH 7.0, initial free chlorine concentration = 0.5 – 8 mg/L as Cl_2.
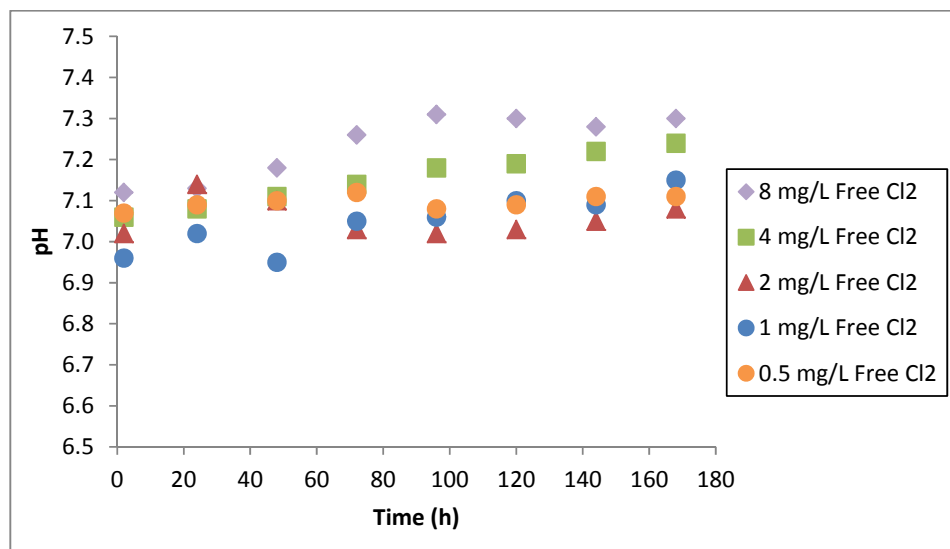
Figure 4.16 Solution pH as a function of time with different initial free chlorine concentrations under stagnant conditions. Experimental conditions: pH 7.0, initial free chlorine concentration = 0.5 – 8 mg/L as Cl_2.

The mass difference of the lead and copper wires before and after the experiment is shown in Figure 4.17. The mass of copper wires increased over time primarily due to the formation of a white precipitate observed on the copper wire surfaces. Although Cu^{2+} originally present in the solution (Table 2.1) may also be reduced to form copper solid, it was expected not to be significant considering its low concentration (17 μg/L). The white precipitate was suspected to be a lead mineral due to the high concentration of lead in the solution. Characterization of this mineral is presented later in Section 4.5.2. On the other hand, the mass of lead wires decreased over time due to accelerated oxidation of lead caused by galvanic corrosion and free chlorine. It was noted that no reddish brown precipitate (PbO_2) was observed throughout the 7-d experiments. In the presence of both Pb(0) metal and Pb(II) ions, oxidation of Pb(0) to Pb(II) by free chlorine is more thermodynamically favorable than that from Pb(II) to Pb(IV). It was observed that the mass loss of lead wire and the mass gained of copper wire increased with the increasing free chlorine concentration. Furthermore, the scaling was formed more readily on the copper wire (cathode) than on the lead wire (anode) due to the higher local pH at the cathode surface compared to that at the anode. Nguyen et. al [43] reported that the pH value at the lead-tin solder anode surface dropped

71

from 7.3 to 3.8 and that at the copper cathode surface increased from 7.3 to about 9.0. Figure 4.18 shows the decomposition of free chlorine as a function of time with different initial free chlorine concentration. Chlorine residual decreased at a faster rate with a higher initial free Cl_2 concentration.
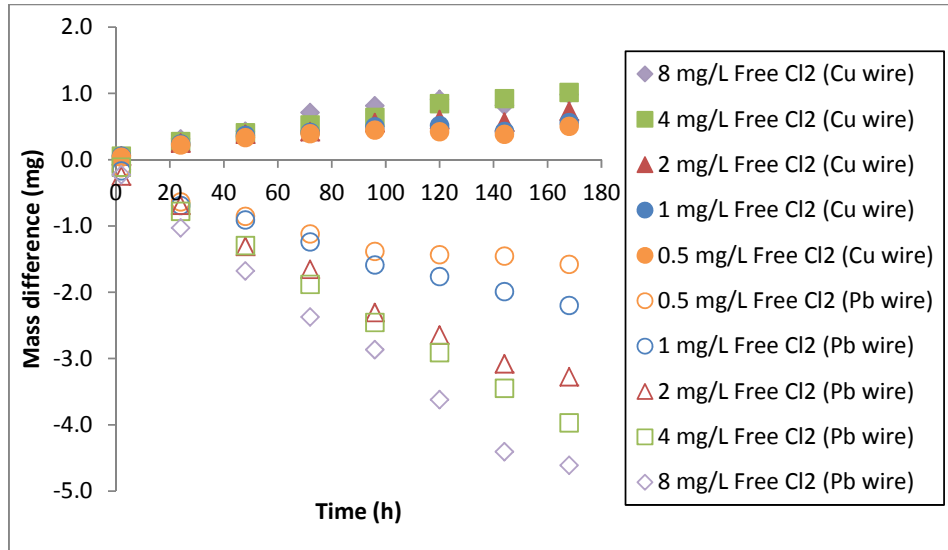
Figure 4.17 Mass difference as a function of time of lead and copper wires with different initial free chlorine concentrations under stagnant conditions. Experimental conditions: initial pH 7.0, initial free chlorine concentration = 0.5 - 8 mg/L as Cl_2.
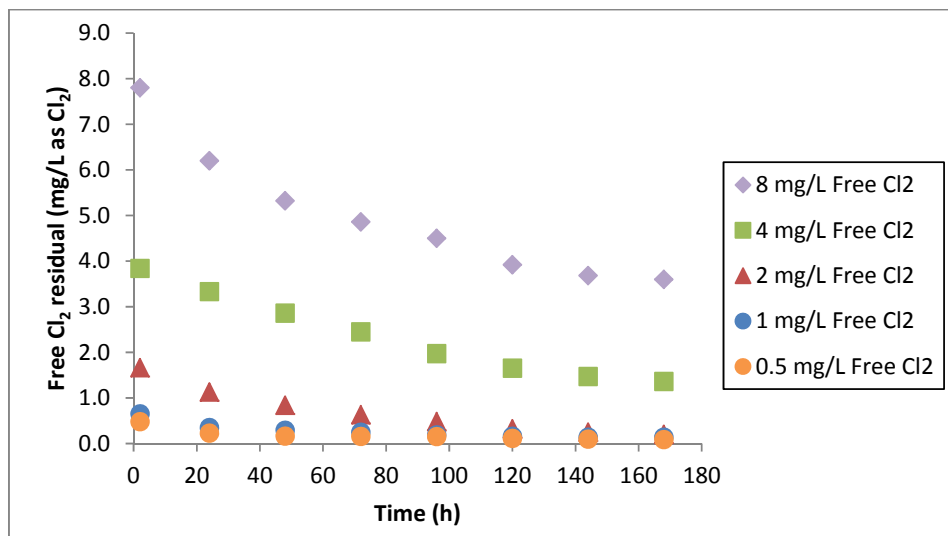
Figure 4.18 Free chlorine residual as a function of time with different initial free chlorine concentrations under stagnant conditions. Experimental conditions: initial pH 7.0, initial free chlorine concentration = 0.5 - 8 mg/L as Cl_2.

72

4.3.2 Effects of initial monochloramine concentration

Figure 4.19 shows the effects of monochloramine ($0.5 - 8$ mg/L as Cl_2) on soluble copper and soluble lead release as a function of time at pH 7.0 under stagnant conditions. Due to galvanic connection between lead and copper wires, soluble copper decreased gradually over the course of experiment (Figure 4.19a). Soluble copper concentration was the highest at an initial monochloramine concentration at 0.5 mg/L as Cl_2 and the lowest at 8 mg/L as Cl_2. The higher soluble copper at a lower initial monochloramine concentration observed may be due to a rapid direct oxidation of copper by monochloramine and a slower copper reduction due to slower galvanic corrosion at lower monochloramine concentration. Soluble lead increased at a faster rate as the initial monochloramine concentration was increased (Figure 4.19b). After 7 d, soluble lead increased from 660 to 1952 µg/L from an initial NH_2Cl concentration of 0.5 to 8.0 mg/L as Cl_2. The rate of galvanic corrosion increased with the increasing initial monochloramine concentration, resulting in faster lead oxidation and copper reduction. Monochloramine exhibited similar effects as free chlorine on galvanic corrosion in our experiment. Figure 4.20 shows that solution pH increased slightly from 7.0 to 7.2 after 7 d.

The mass difference of the lead and copper wires before and after the experiment is shown in Figure 4.21. The mass of copper wire increased gradually during the course of experiment. This increase was due to the formation of white precipitates observed on the copper wires. On the other hand, the mass of lead wires decreased over time due to accelerated oxidation of lead by galvanic corrosion and monochloramine. The mass decrease of lead wire and the mass increase of copper wire were the highest at an initial monochloramine concentration of 8 mg/L as Cl_2. This observation was consistent with the results shown in Figure 4.19 that a higher lead release corresponded to a higher mass decrease in lead wire and that the precipitation of lead solids on the copper wire surfaces caused the mass increase in copper wire. Figure 4.22 shows the monochloramine residual as a function of time. Monochloramine decreased at a faster rate at higher initial monochloramine concentration.
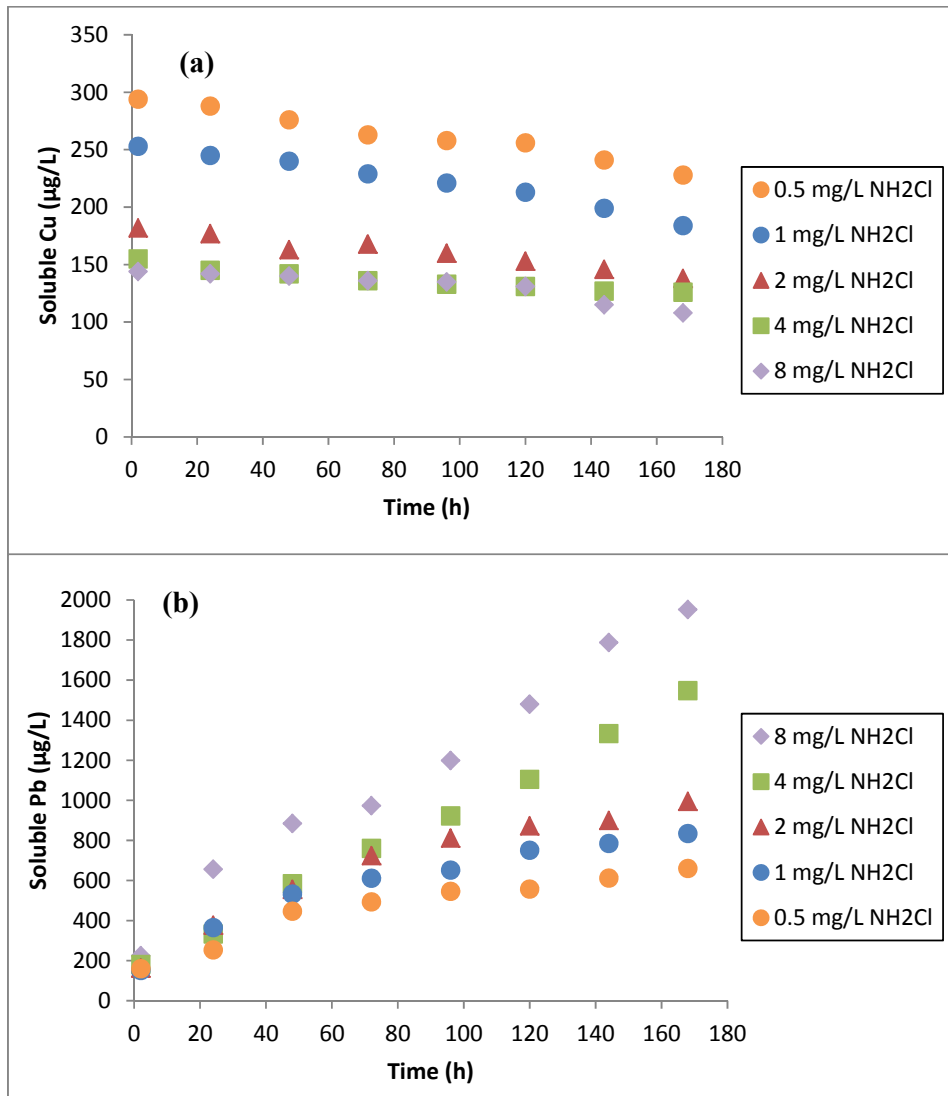
Figure 4.19 Soluble (a) copper and (b) lead concentrations as a function of time for galvanic corrosion for lead and copper with different initial monochloramine concentrations under stagnant conditions. Experimental conditions: pH 7.0, initial [NH$_2$Cl] = 0.5 - 8 mg/L as Cl$_2$.
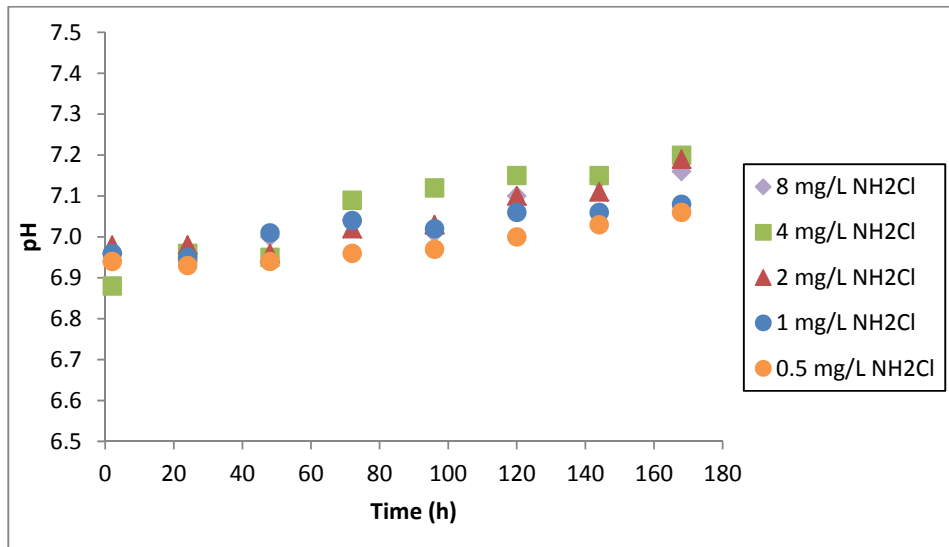
Figure 4.20 Solution pH as a function of time for galvanic corrosion for lead and copper with different initial monochloramine concentrations under stagnant conditions. Experimental conditions: pH 7.0, initial $[NH_2Cl] = 0.5 - 8$ mg/L as Cl_2.
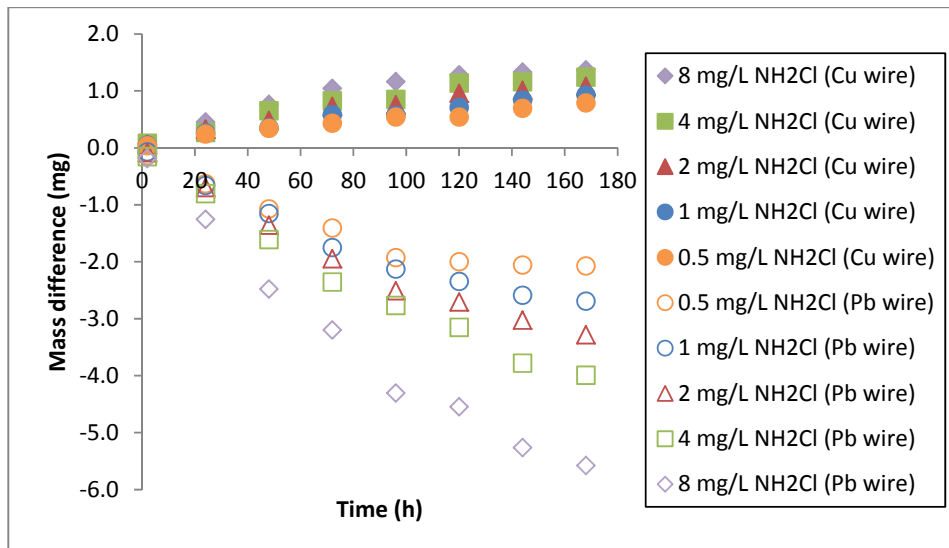
Figure 4.21 Mass difference as a function of time of lead and copper wires with different initial monochloramine concentrations under stagnant conditions. Experimental conditions: initial pH 7.0, initial $[NH_2Cl] = 0.5 - 8$ mg/L as Cl_2.
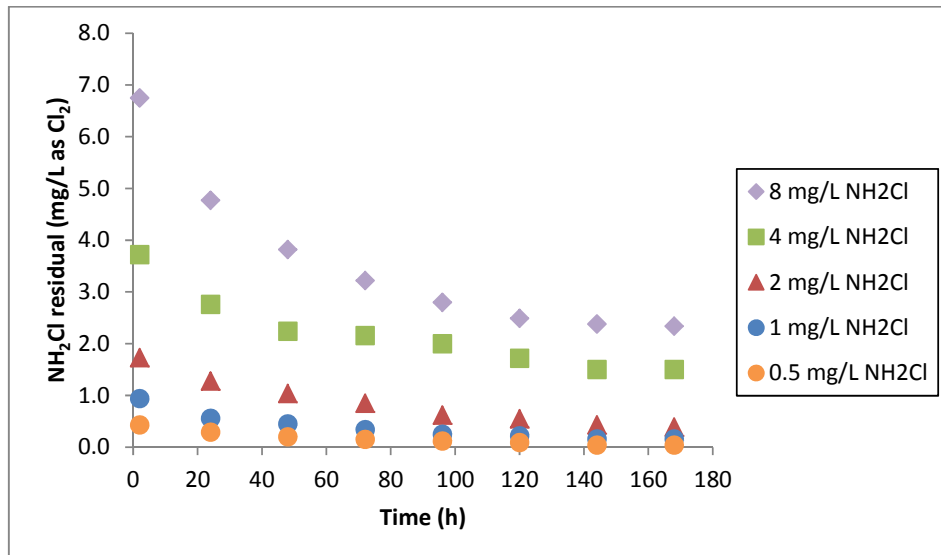
Figure 4.22 Monochloramine residual as a function of time with different initial monochloramine concentrations under stagnant conditions. Experimental conditions: initial pH 7.0, initial [NH$_2$Cl] = 0.5 - 8 mg/L as Cl$_2$.

4.3.3 Comparison between the effects of free chlorine and monochloramine

The effect of free chlorine on soluble copper and lead release was compared to that of monochloramine at the same initial concentrations of 4 and 8 mg/L as Cl_2 at pH 7.0 under stagnant conditions (Figure 4.15 and 4.19). After 7 d, the release of soluble lead in the presence of monochloramine was 9% and 11% higher than that in the presence of free chlorine at initial concentrations of 4 mg/L and 8 mg/L as Cl_2, respectively. Soluble copper release was higher in the presence of monochloramine than free chlorine, although the amount of copper release did not change significantly with the disinfectant concentration.

When there was no galvanic corrosion, free chlorine caused more lead and copper release than monochloramine. When both Pb(0) metal and Pb(II) ions are present, it is thermodynamically more favorable for free chlorine to oxidize Pb(0) to Pb(II) (E^o = -0.13 V) than from Pb(II) to Pb(IV) (E^o = +1.67 V). For the reaction period (7 d) employed in this study, we did not observe the formation of Pb(IV) solids or too little was formed to be detected in the SEM images. If a longer reaction period were allowed, Pb(IV) solids could be potentially formed [51]. Monochloramine caused a higher lead release than free chlorine at the same residual concentration when galvanic corrosion existed. This result is consistent with that reported by Dudi [88], who showed that in water systems involving brass devices, lead pipes and copper tubing, the galvanic current in the presence of monochloramine were about 6.3 times higher than in the presence of free chlorine after 100 h stagnation. Edwards and Dudi [14] demonstrated that free chlorine caused more lead release from pure lead pipes, but less lead release from brass devices as compared to monochloramine. In a more recent study by Arnold and Edwards [51], potential reversal of pipe surfaces was observed in the presence of free chlorine and it was proposed that copper would be sacrificed instead of lead due to the formation or Pb(IV) solids. Figure 4.23 summarizes the total lead release profile contributed by soluble lead and particulate lead in the presence

of free chlorine and monochloramine after 7 d. For galvanic conditions at pH 7.0, 33-54% of total lead was attributed to particulate lead in the presence of free chlorine and 41-52% in the presence of monochloramine. Fraction of particulate lead increased from pH 6.0 to pH 8.0.
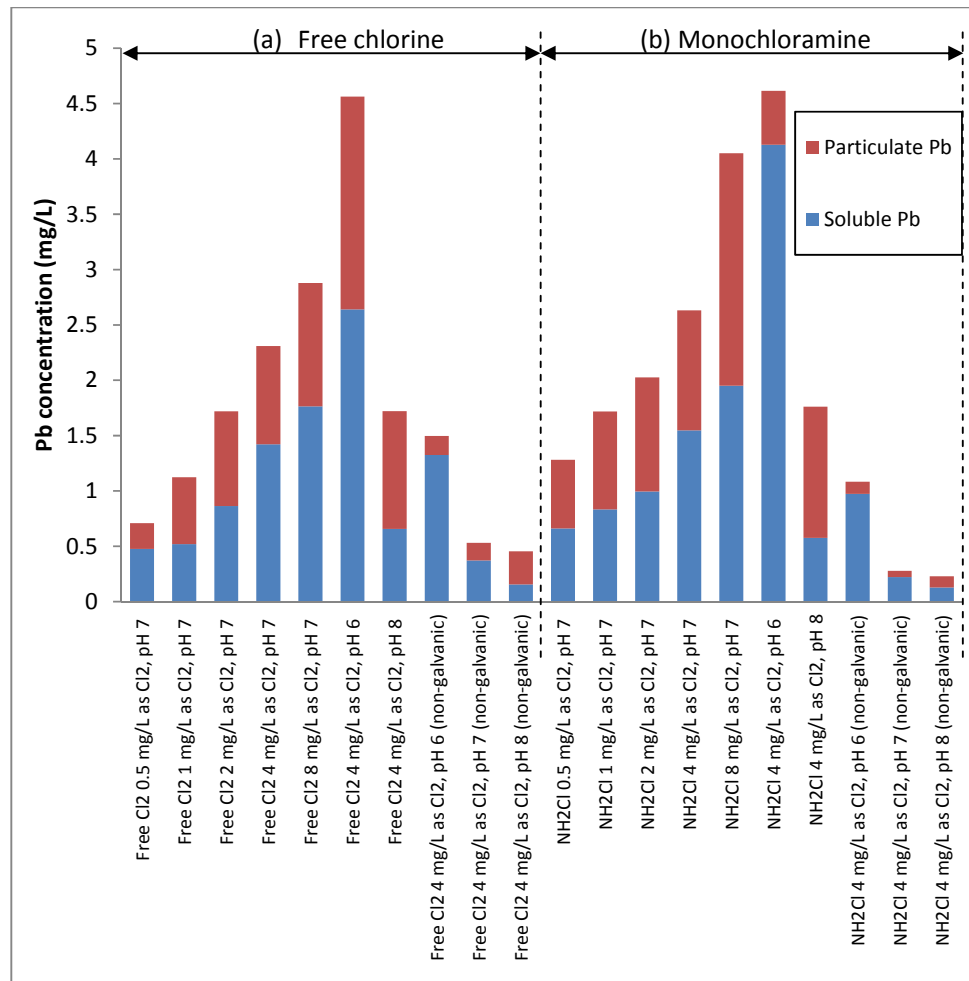
Figure 4.23 Summary of total lead release contributed by soluble lead and particulate lead in the presence of (a) free chlorine and (b) monochloramine after 7 d under stagnant conditions.

4.4 Effects of orthophosphate dosages as a corrosion inhibitor

Figure 4.24 shows the effects of orthophosphate dosages (1, 2 and 5 mg/L as P) on the release of total copper and total lead as a function of time at pH 7.0 under stagnant conditions. Total copper and lead were presented in this section as orthophosphate is known to form relatively insoluble precipitate readily which can be captured in total concentration measurement. The release of total copper decreased over time and different orthophosphate dosages had no observable effect on total copper release (Figure 4.24a). Total lead released increased over time for all orthophosphate dosages but the extent decreased with the increasing orthophosphate dosage (Figure 4.24b). After 7 d, total lead was the highest at 2412 µg/L with an orthophosphate dosage of 1 mg/L as P and the lowest at 1290 µg/L with 5 mg/L as P. For the same condition without orthophosphate addition, total lead only reached 900 µg/L after 7 d (Figure 4.3). Soluble Pb released was drastically reduced from 854 µg/L without orthophosphate addition to 26 µg/L and 7 µg/L with 1 mg/L as P and 5 mg/L as P orthophosphate addition, respectively (Figure 4.25). The presence of orthophosphate removed soluble Pb from solution by precipitation of relatively insoluble lead phosphate minerals such as pyromorphite and secondary lead phosphate [8, 62, 63]. The precipitation contributed significantly to total lead levels (98% as particulate Pb) in particulate forms. The precipitation was also not able to inhibit galvanic corrosion as the mass of lead wires decreased rapidly over the course of experiment (Figure 4.26). The lead phosphate precipitates can control soluble lead levels and when immobilized, they should not cause lead contamination issues. The mass of copper wire increased while that of lead wire decreased. The varying orthophosphate dosages had little effect on the mass difference of the wires. Figure 4.27 shows that solution pH increased from 7.0 to 7.8 and this increase in solution pH with orthophosphate addition was higher than in other conditions.
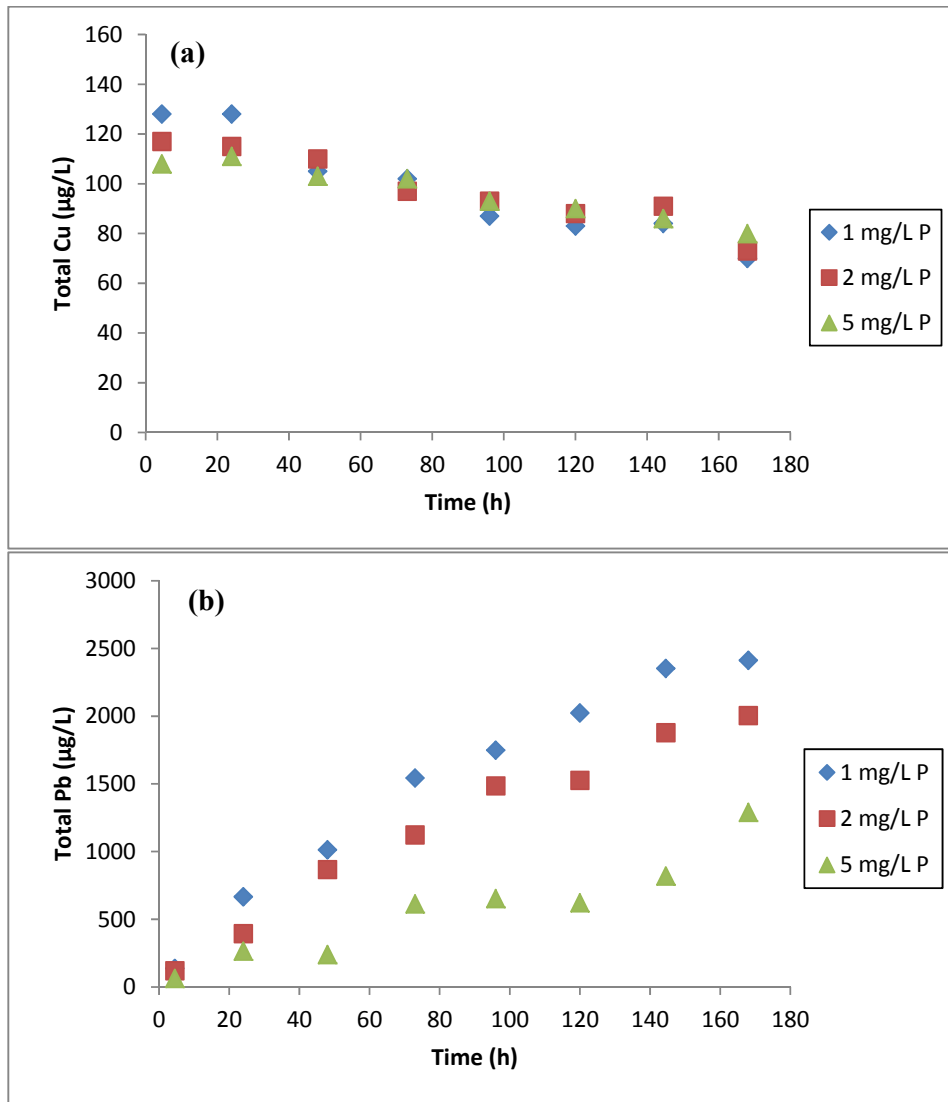
Figure 4.24 Total (a) copper and (b) lead concentrations as a function of time with different initial orthophosphate dosages under stagnant conditions. Experimental conditions: pH 7.0, orthophosphate = 1, 2 and 5 mg/L as P.

80
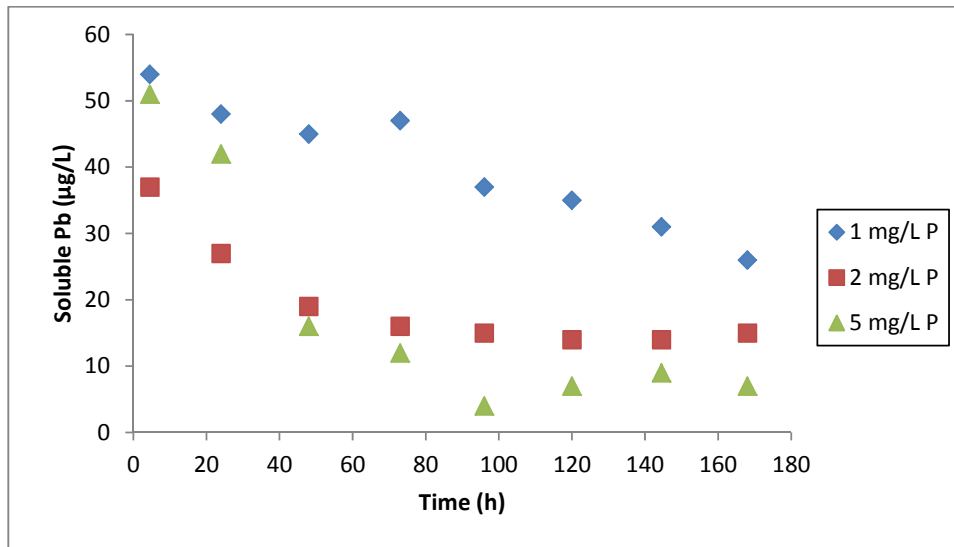
Figure 4.25 Soluble lead concentration as a function of time with different initial orthophosphate dosages. Experimental conditions: pH 7.0, orthophosphate = 1, 2 and 5 mg/L as P.
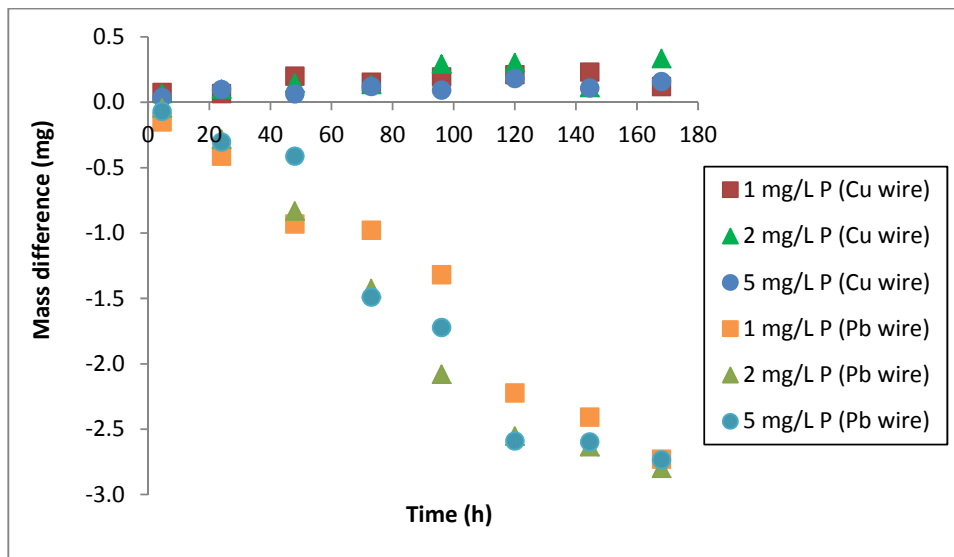
Figure 4.26 Mass difference as a function of time of lead and copper wires with different orthophosphate dosages. Experimental conditions: initial pH 7.0, orthophosphate = 1, 2 and 5 mg/L as P.
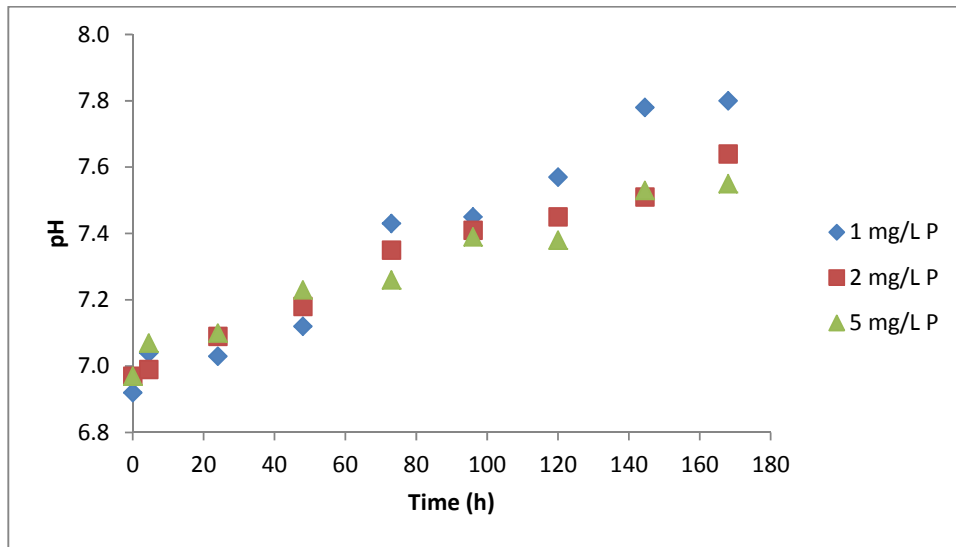
Figure 4.27 Solution pH as a function of time with different initial orthophosphate dosages. Experimental conditions: pH 7.0, orthophosphate = 1, 2 and 5 mg/L as P.

4.5   Characterization of solid phases

To identify the scales formed at the end of experiment, selected conditions were repeated multiple times (20-30 times) to collect sufficient amount of scales for analysis. SEM, SEM-EDX, XRD and acid digestion were employed for the scaling analysis.

4.5.1 Identification of scales collected from galvanic corrosion with chloride and sulfate addition

Scaling analysis was performed for completely-mixed conditions with chloride (250 mg/L) and sulfate additions (250 mg/L) in the absence of disinfectant and orthophosphate. For 250 mg/L chloride addition, SEM images (Figures 4.28a and 4.28b) showed plate-like solids covering both the lead and copper wire surfaces. SEM-EDX analysis (Table 4.1) showed significant levels of lead, carbon and oxygen in the scaling and XRD results (Figure 4.29a) confirmed the scales to be hydrocerussite ($Pb_3(CO_3)_2(OH)_2$). The plate-like structure of hydrocerussite has been reported previously [47, 48, 50, 92] and the precipitation of hydrocerussite was expected because its K_{sp} was exceeded the most based on modeling results using Visual MINTEQ 3.0 [84]. For 250 mg/L sulfate addition, SEM images showed that the scale on the lead wire had needle-like structures (Figure 4.28c) and that on the copper wire had plate-like structures (Figure 4.28d). SEM-EDX (Table 4.1) showed significant amounts of lead, carbon and oxygen in the scales and negligible amounts of sulfur, similar to that observed in the experiments with varying chloride dosages. This suggests that lead sulfate was not formed or present in very small amounts. XRD results (Figure 4.29b) indicated the presence of both cerussite ($PbCO_3$) and hydrocerussite. Thus, the needle-like and plate-like structures are likely to be cerussite and hydrocerussite, respectively. For 250 mg/L chloride and sulfate (CSMR = 1) addition, SEM images (Figures 4.28e and 4.28f) showed that the scales contained a mixture of plate-like and needle shaped solids. SEM-EDX analysis (Table 4.1) indicated that the scaling had similar chemical composition as those obtained with chloride or sulfate addition. XRD results (results not shown) showed that both cerussite and hydrocerussite were present in the scaling.
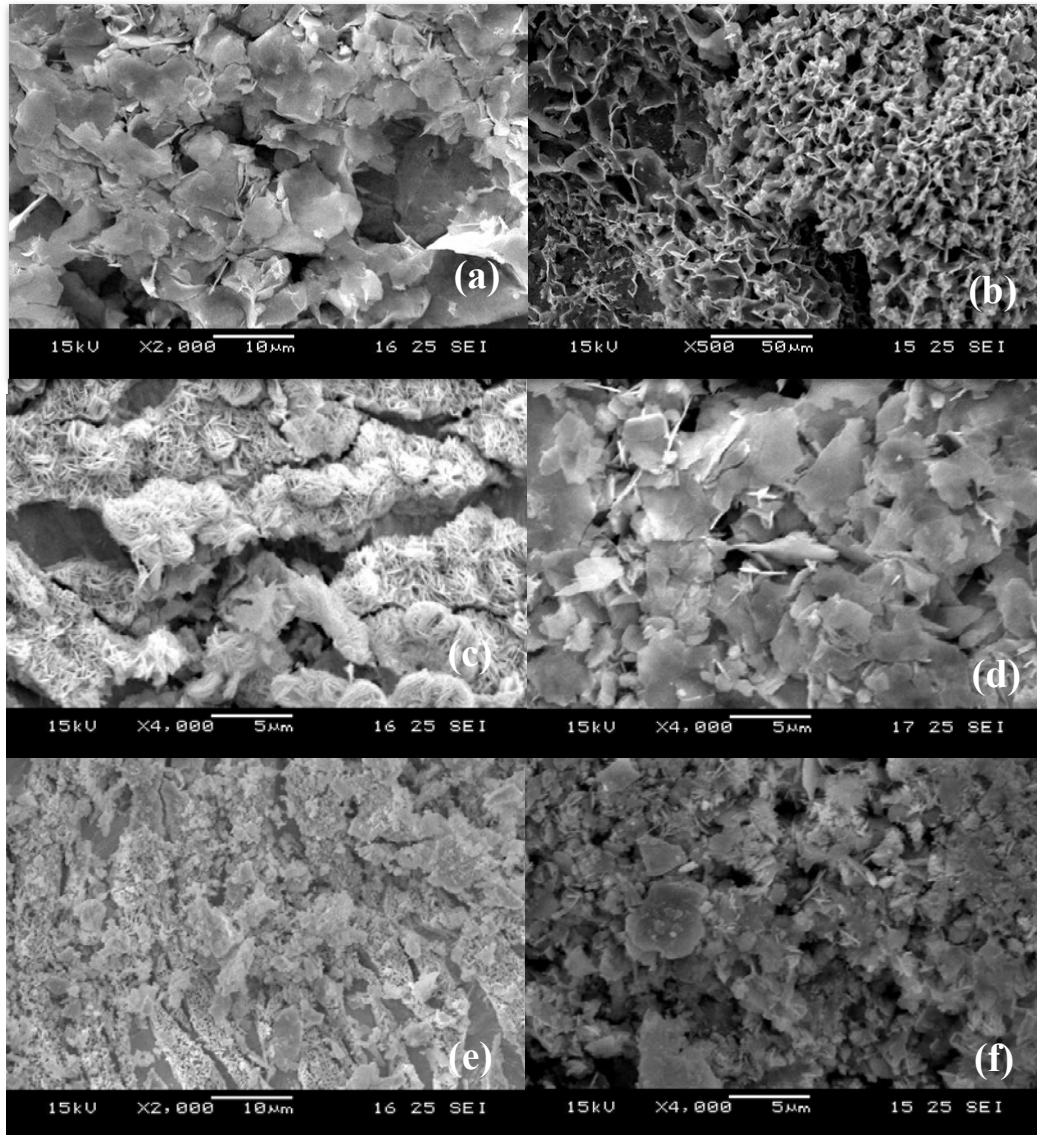
Figure 4.28 SEM images of scaling on lead wire (a, c and e) and copper wire (b, d and f) after 7 d in completely-mixed conditions with (a and b) chloride dosage of 250 mg/L, (c and d) sulfate dosage of 250 mg/L, and (e and f) chloride and sulfate dosage of 250 mg/L each. Experimental conditions: total effective length = 6 cm, pH = 7.0.

Table 4.1 SEM-EDX results of scales collected after 7 d in completely-mixed conditions in the absence of disinfectant and orthophosphate. Total effective length = 6 cm, pH = 7.0.

Conditions:	250 mg/L Cl$^-$		250 mg/L SO$_4^{2-}$		250 mg/L Cl$^-$ and 250 mg/LSO$_4^{2-}$	
Element	Weight%	Atomic%	Weight%	Atomic%	Weight%	Atomic%
C	13.83	49.35	21.87	52.53	18.57	55.60
O	12.61	33.75	21.27	38.35	13.91	31.22
S	0.01	0.01	0.73	0.66	0.16	0.18
Cl	1.09	1.32	0.59	0.48	1.56	1.58
Cu	1.25	0.85	0.57	0.26	0.01	0.01
Pb	71.20	14.72	54.7	7.62	65.79	11.42
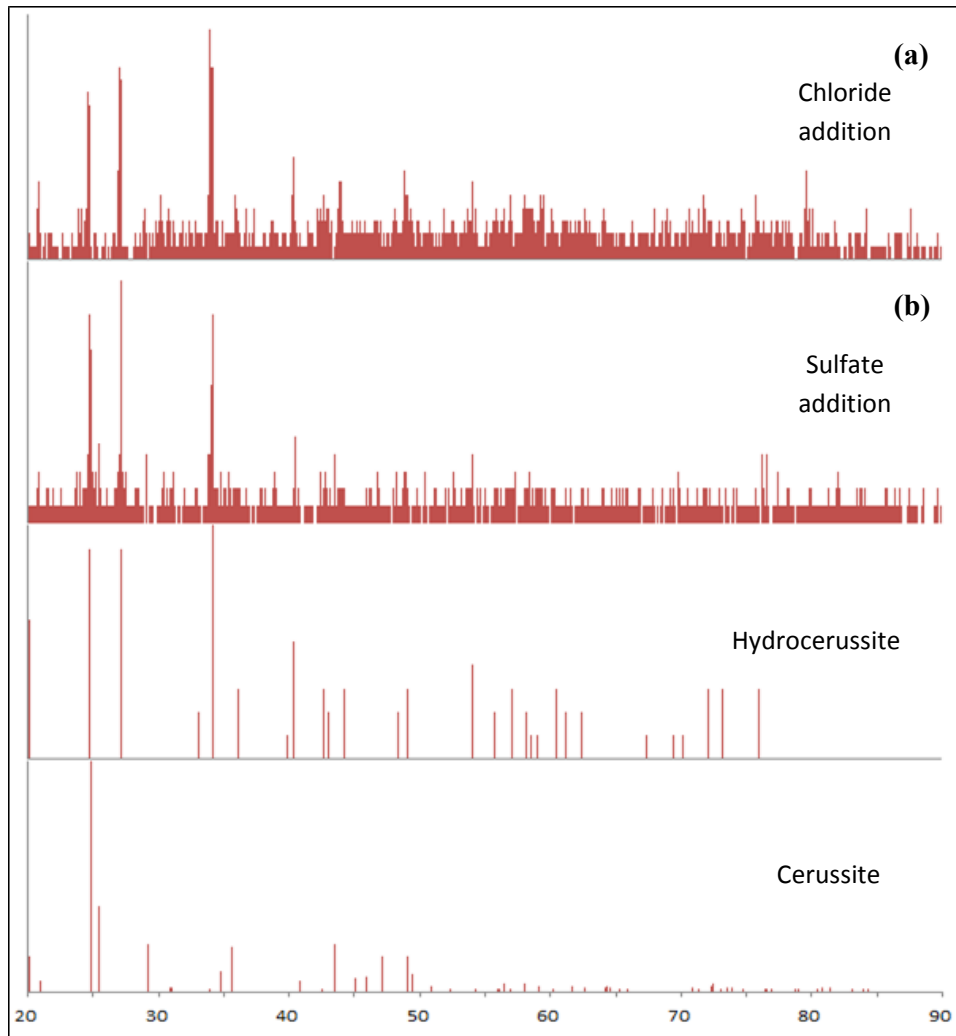
Figure 4.29 X-ray diffraction (XRD) patterns of scaling collected after 7 d in completely-mixed conditions at pH 7.0. (a) Chloride dosage of 250 mg/L, (b) sulfate dosage of 250 mg/L. Reference standard for hydrocerussite and cerussite obtained from PDF cards: 00-013-0131 and 00-047-1734 respectively.

4.5.2 Identification of scales collected from galvanic corrosion in the presence of free chlorine and monochloramine

Scaling analysis was performed for stagnant conditions with initial free chlorine and monochloramine concentrations of 4 mg/L as Cl_2. SEM images (Figure 4.30) showed the formation of both plate-like and rod shaped crystals on lead wire, but only plate-like crystals on copper wire in the presence of either free chlorine (4 mg/L as Cl_2) or monochloramine (4 mg/L as Cl_2) at pH 7.0. The rod shaped and plate-like crystals were suspected to be cerussite ($PbCO_3$) and hydrocerussite ($Pb_3(CO_3)_2(OH)_2$), respectively. The localized lower pH at the lead anode surface was expected to initiate cerussite formation. The scales were carefully removed from the wires using a pair of dry tweezers, weighed and treated with acid digestion in 10 mL ultra-pure water at 85 °C for 2 h. The samples were then analyzed for lead and copper as shown in Table 4.2. The results indicate that the scales formed on the wires are predominantly lead-containing minerals with an average of 57% of lead by mass while the proportion of copper was less than 1% by mass. XRD results show that the scaling in the presence of free chlorine and monochloramine is predominantly hydrocerussite with traces of cerussite (Figure 4.31). This result agrees with the initial deduction of the minerals observed in the SEM images.
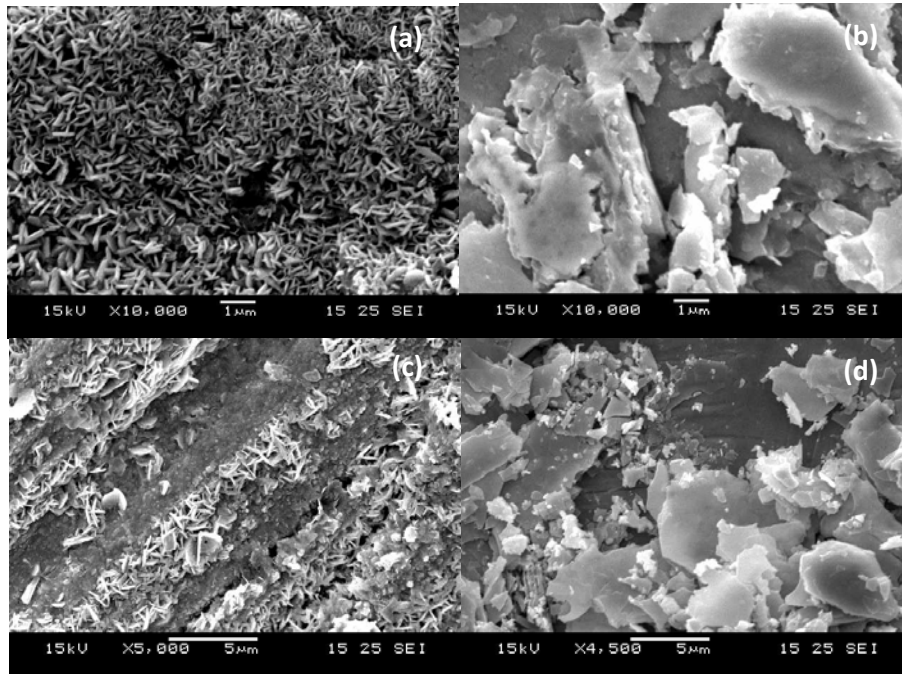
Figure 4.30 SEM images of scales on lead (a and c) and copper (b and d) wires with initial concentrations of free chlorine (a and b) and monochloramine (c and d) of 4 mg/L as Cl_2 after 7 d. Experimental conditions: initial pH 7.0, initial free chlorine concentration = 4 mg/L as Cl_2, initial $[NH_2Cl]$ = 4 mg/L as Cl_2.

Table 4.2 Mass percentage of Pb and Cu in scaling collected after 7 d.

Condition	Scaling mass (mg)	Total Pb (mg/L)	Total Cu (mg/L)	Mass % Pb	Mass % Cu
0.5 mg/L Free Cl_2	0.558	34.6	0.19	62.0	0.34
1 mg/L Free Cl_2	0.422	28.2	0.42	66.7	0.99
2 mg/L Free Cl_2	0.650	41.5	0.34	63.9	0.52
8 mg/L Free Cl_2	0.713	42.0	0.03	58.9	0.04
pH 6, 4 mg/L Free Cl_2	0.432	22.7	0.05	52.5	0.13
pH 7, 4 mg/L Free Cl_2	0.671	41.3	0.15	61.6	0.22
pH 8, 4 mg/L Free Cl_2	0.347	13.8	0.58	39.8	1.67
pH 6, 4 mg/L NH_2Cl	0.505	28.3	0.31	55.9	0.62
pH 7, 4 mg/L NH_2Cl	0.363	21.0	0.11	57.7	0.30
pH 8, 4 mg/L NH_2Cl	0.420	26.4	0.21	62.9	0.51
0.5 mg/L NH_2Cl	0.401	22.8	0.13	56.8	0.32
1 mg/L NH_2Cl	0.355	18.6	0.56	52.3	1.59
2 mg/L NH_2Cl	0.626	35.8	0.83	57.2	1.32
8 mg/L NH_2Cl	0.890	43.7	0.39	49.1	0.44
			Average	**56.9**	**0.64**
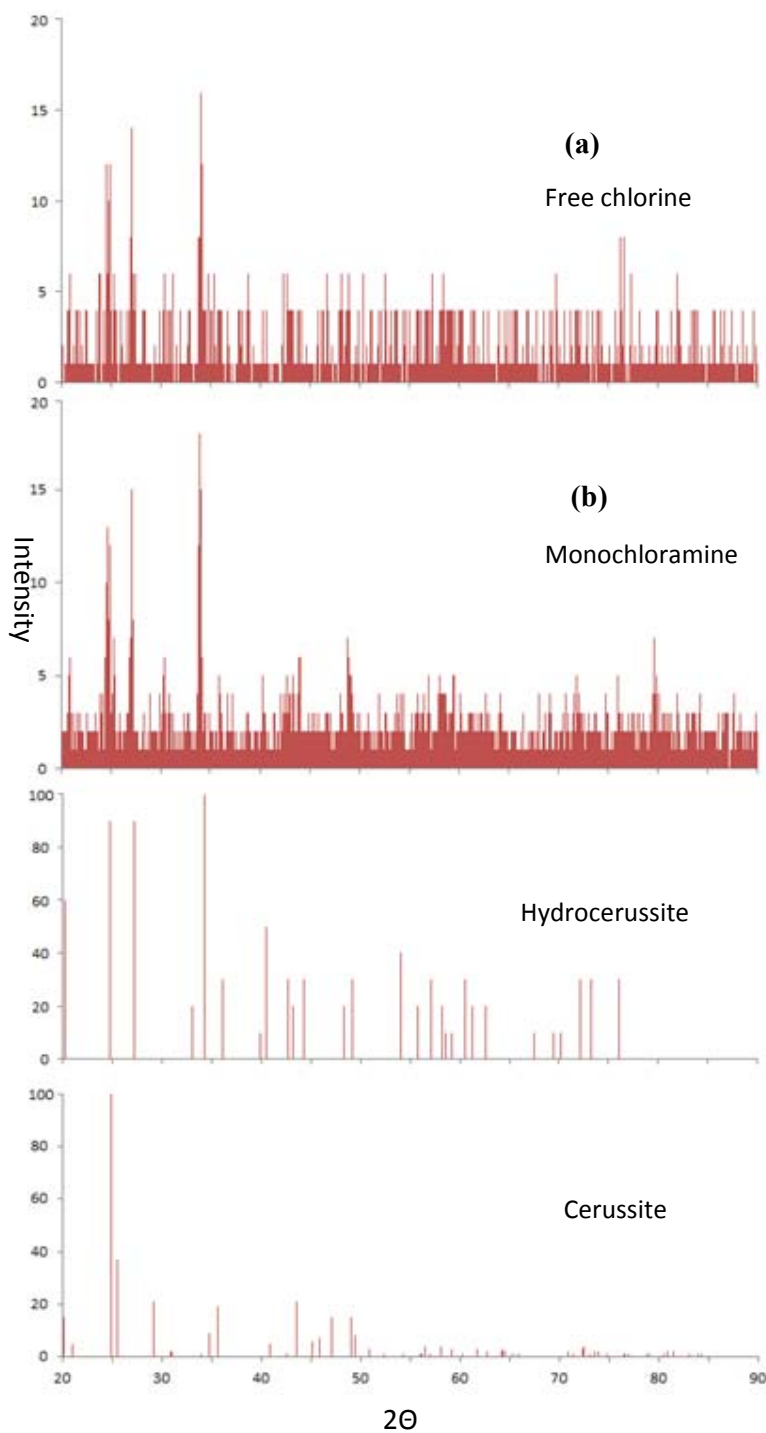
Figure 4.31 X-ray diffraction (XRD) patterns of scaling collected after 7 d with initial (a) free chlorine concentration of 4 mg/L as Cl_2 and (b) monochloramine concentration of 4 mg/L as Cl_2. Reference standard for hydrocerussite and cerussite obtained from PDF cards: 00-013-0131 and 00-047-1734 respectively. Experimental conditions: initial pH 7.0, initial free chlorine concentration = 4 mg/L as Cl_2, initial $[NH_2Cl]$ = 4 mg/L as Cl_2.

4.6   Summary

The effects of stagnation, complete mixing, pH, chloride, sulfate, free chlorine, monochloramine and orthophosphate on galvanic corrosion between lead and copper were investigated. Batch experiments using pure lead and copper wires were conducted.

In stagnant conditions, reducing pH and increasing either chloride or sulfate concentrations promoted soluble lead release with little precipitation observed. The effect of chloride concentration on soluble lead release was similar to that of sulfate at the same molar concentration and the chloride-to-sulfate mass ratio (CSMR) did not provide a good indication for soluble lead release. In completely-mixed conditions, higher total lead releases were observed than stagnant ones for the same solution composition. The mixing caused an initial rapid release of soluble lead followed by a gradual decrease. This lead peak coincided with the formation of a layer of white scaling on the wires. More precipitates were observed in the presence of chloride than sulfate under the same molar concentration. The precipitates were identified to be cerussite and hydrocerussite. These corrosion products inhibited galvanic corrosion and suppressed soluble lead levels. The findings suggest that distribution systems that have waters containing high levels of chloride may periodically experience lead contamination issues in the form of particulate lead when lead solids are formed and detached. This lead contamination scenario is more dynamic and harder to control.

When there was galvanic corrosion, soluble lead release increased while soluble copper release decreased as initial free chlorine or monochloramine concentration increased. The rate of disinfectant decay was slower in the presence of galvanic corrosion, which showed the potential to impede the oxidation of lead by free chlorine or monochloramine, resulting in less disinfectant demand. Free chlorine caused more lead release than monochloramine when there was no galvanic corrosion. When galvanic corrosion existed, however, monochloramine resulted in more lead release than free chlorine. Rod-shaped crystals (cerussite) were formed on the lead

surface and plate-like crystals (hydrocerussite) were found on the copper surface. Distribution systems using monochloramine is more susceptible to lead contamination due to galvanic corrosion than those using free chlorine.

When there was galvanic corrosion, total lead release increased with increasing orthophosphate concentrations while soluble lead release decreased. Particulate lead contributed over 96% to total lead concentrations. The lead phosphate precipitates can control soluble lead levels and when immobilized, they should not cause lead contamination issues.

Chapter 5

Lead release in simulated premise drinking water distribution systems

In recent years, exceedingly high lead levels have been found in drinking water in cities where no lead pipes were used. Sources of lead were traced to common plumbing materials such as "lead-free" brass fittings which by definition, may contain up to 8% lead by mass. In addition, current sampling protocol has been found to be inadequate to detect lead contamination in premise drinking water distribution systems. In Singapore, there are no lead service pipes since the ban of lead pipes in the 1980s and pre-flushing has been employed for sampling for lead and copper in the distribution system. In this chapter, three premise plumbing systems were built using locally available plumbing materials to determine if lead contamination in drinking water will occur in a "lead-free" distribution system using a modified sampling protocol. In each system, different scenarios were examined. The scenarios are orthophosphate addition, disinfectant switch from free chlorine to monochloramine and periodic flushing with free chlorine. Total lead, copper and zinc concentrations, and solution pH were measured and scaling composition was determined. The practicability and relevance of each scenario was discussed.

5.1   System A: orthophosphate addition

Figure 5.1 shows the total lead release in samples collected from System A over a period of 475 d (~16 mth). Total lead levels decreased gradually regardless of stagnation times (1, 3 and 7 d), but exceeded the WHO guideline levels of 10 µg/L during the first 5 mth. The highest lead concentration recorded was 83 µg/L on Day 31. On Day 45, the sampling procedure for collecting the first 200 mL was changed from using 2 x 100 mL bottles to 4 x 50 mL bottles as the former was unable to effectively locate the source of lead. This was due to an increased number of brass fittings near the tap. A sampling

volume of 100 mL is sufficient to detect lead contamination in drinking water in premise systems but an even smaller sampling volume may be used to provide a more accurate and precise location of the lead source. A second tap was installed on Day 153 and lead levels began to spike over the next 2 weeks. The scaling on the inner surface of the pipes and brass fittings could have been destabilized during the installation. The high lead levels may also be attributed to dissolution of surface lead of the brass fittings that were used to connect the copper pipes to the new tap. The high lead levels did not sustain for long period of time, returning to pre-installation levels (~10 µg/L) after one month. The decrease of lead with time after the installation of the second tap may be due to either the removal of destabilized scaling during the tap installation or the surface passivation of the newly installed brass fitting, inhibiting further lead release into the solution. Surface lead may also have been gradually depleted considering most of the lead found in brass exists as surface contaminants [31]. Residents moving into new buildings or renovating their homes are potentially at risk of lead contamination in their drinking water. Flushing the taps before consumption, especially if the water is left standing for long hours, will significantly minimize the exposure of lead in drinking water.

The addition of orthophosphate is commonly used as a lead control measure to suppress soluble lead levels in drinking water [55-57]. As predicted, total lead decreased with the addition of orthophosphate (1 mg/L as P) from Day 248 to 337. While the addition of orthophosphate can lead to the formation of relatively insoluble lead precipitate such as secondary lead phosphate $(Pb_3(PO_4)_2)$, hydroxypyromorphite $(Pb_5(PO_4)_3OH)$ and chloropyromorphite $(Pb_5(PO_4)_3)Cl)$ [8, 61-66], it can also precipitate with soluble copper and zinc to form copper phosphate $(Cu_3(PO_4)_2,$ $Cu_3(PO_4)_2.2H_2O)$ and zinc phosphate $(Zn_3(PO_4)_2,$ $Zn_3(PO_4)_2.4H_2O)$ respectively [93, 94]. The precipitation of insoluble phosphate minerals can control the soluble concentrations of various metals and inhibit their release by surface passivation. Occasional total lead spikes were observed throughout the duration and these spikes corresponded to samples collected after 1 d

stagnation.   Total copper levels exhibited peaks during orthophosphate addition and these peaks also corresponded to samples with 1 d stagnation (Figure 5.2). The scaling may become loose and detach from the surface when water is flushed through the system after the last sampling. 2 out of 4 segmental samplings showed total zinc levels were suppressed with the addition of orthophosphate (Figure 5.3). One segmental sampling (Tap 1: 0-50 mL) exhibited higher zinc levels, indicating source of dezincification to the brass fitting and the presence of orthophosphate accelerated dezincification, resulting in more zinc release.

    After orthophosphate addition had been ceased, total lead levels were seen to spike within a week (Figure 5.1). The presence of lead phosphate precipitate formed was not able to control lead release without continuous addition of orthophosphate into the system. Total copper concentration increased gradually for all samples (Figure 5.2), suggesting that the formation of copper phosphate minerals was not effective in controlling copper levels as well. This observation is consistent with the study by Zhang & Edwards [96] who reported that the inhibitive effect of dosing orthophosphate decreased substantially after 100 days. However, total zinc continued to decrease even after orthophosphate addition had stopped (Figure 5.3).
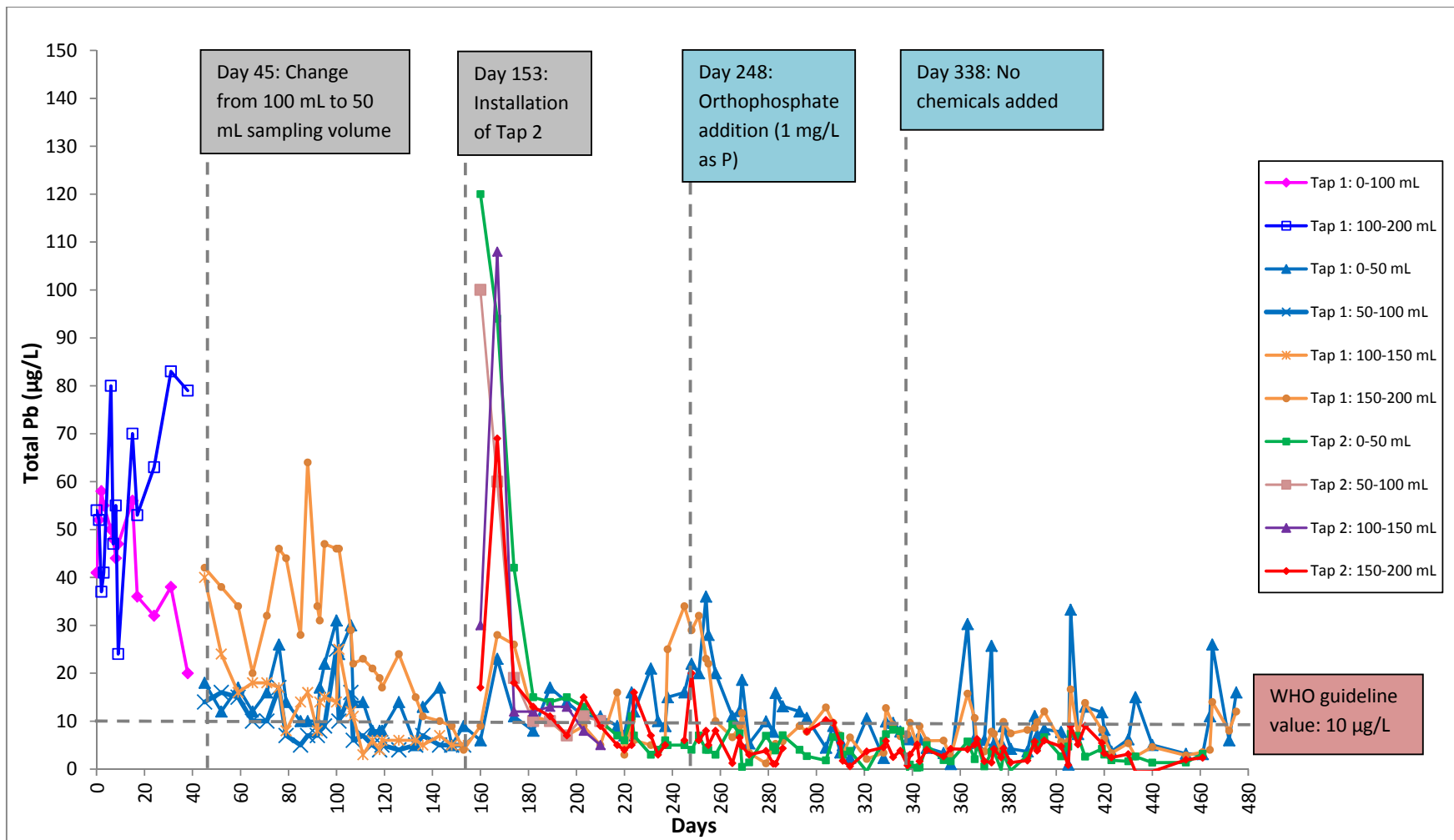
Figure 5.1 Total lead as a function of time in samples collected from System A
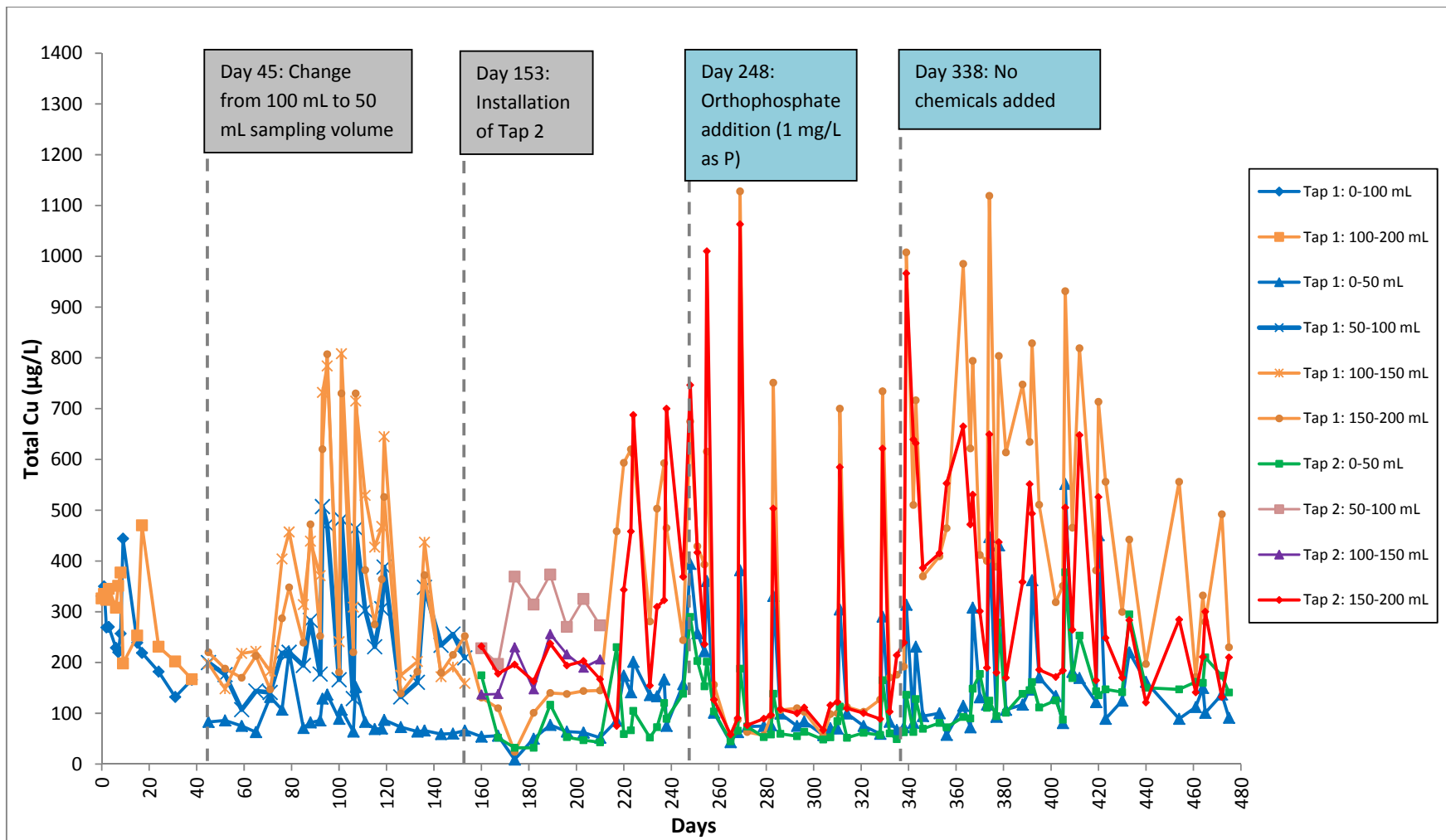
Figure 5.2 Total copper as a function of time in samples collected from System A
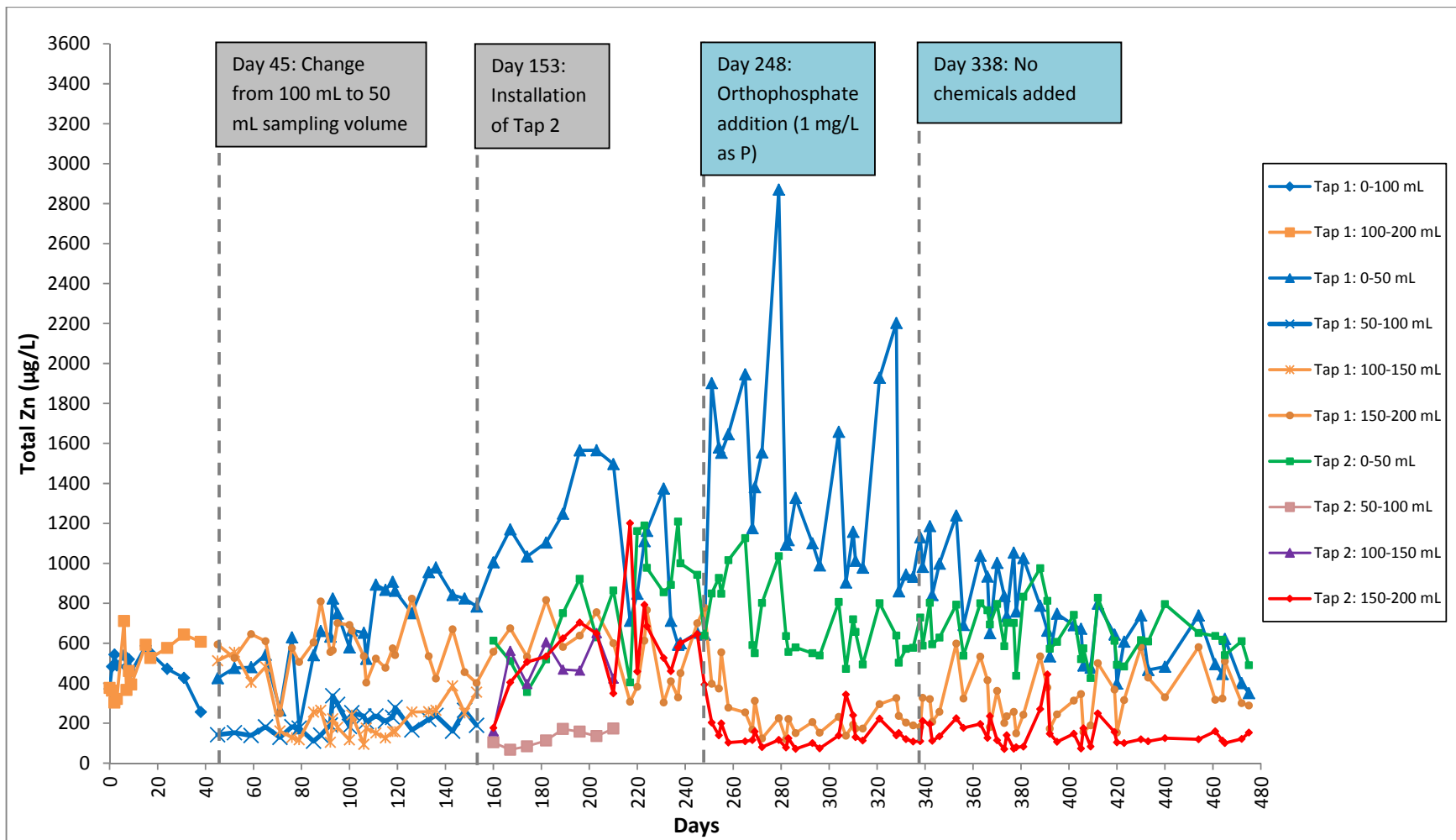
Figure 5.3 Total zinc as a function of time in samples collected from System A

The change in pH was obtained by taking the difference of the pH in tap water sample collected after desired stagnation time and the pH of the same water first introduced to the system after the last sampling. The pH values of samples collected were shown to increase at each phase of the experiment (Tables 5.1). During the conditioning phase, 82% of 136 samples collected showed an increase of at least 0.50 pH unit in pH values. Changes in pH could be caused by various chemical processes in the system. Lead, copper and zinc can react in the presence of oxygen to form an oxide layer. This basic oxide layer reacts with H^+ ions to release soluble metal ions and water (Eq 5.1). Oxidation of elemental metal by free chlorine and monochloramine also consumes H^+ ions (Eq 5.2 and 5.3), resulting in a rise in solution pH.

$$PbO + 2H^+ \rightarrow Pb^{2+} + H_2O \qquad\qquad (5.1)$$

$$Pb + 2HOCl + 2H^+ \rightarrow Pb^{2+} + 2H_2O + Cl_2 \qquad (5.2)$$

$$Pb + NH_2Cl + 2H^+ \rightarrow Pb^{2+} + NH_4^+ + Cl^- \qquad (5.3)$$
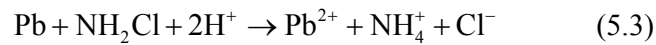
The extent of average pH increase raised further from 0.78 to 1.46 pH unit for samples in System A when orthophosphate was introduced into the system. However, this increase in pH returned to pre-orthophosphate level at 0.86 pH unit once the supply of orthophosphate had been stopped. 96 out of 100 samples collected had a pH increase between 1.21 and 1.92 pH unit when orthophosphate was added to system while 80 out of 132 samples had a pH increase between 0.60 and 1.56 pH unit when orthophosphate addition was stopped. The formation of phosphate minerals would deplete the soluble metal ions in the system and drive the system to produce additional soluble metal ions to replace the consumed ions. More H^+ will be consumed in the process, resulting in a rise in pH. The different stagnation times had little effect on pH changes in each phase.

Table 5.1 Change in pH values with respect to initial tap water pH in samples collected at different stages from System A

System A	Conditioning				Orthophosphate (1 mg/L as P)				No orthophosphate			
	1 d	3 d	7 d	Avg	1 d	3 d	7 d	Avg	1 d	3 d	7 d	Avg
Tap 1: 0-50 mL	0.45	0.91	0.76	0.69	1.62	1.62	1.40	1.57	1.03	1.06	0.74	0.97
Tap 1: 50-100 mL	0.21	0.60	1.07	0.71	-	-	-	-	-	-	-	-
Tap 1: 100-150 mL	0.17	0.63	0.76	0.59	-	-	-	-	-	-	-	-
Tap 1: 150–200 mL	0.49	0.77	0.75	0.71	1.51	1.42	1.33	1.42	1.05	0.84	0.44	0.79
Tap 2: 0-50 mL	0.77	0.58	1.13	0.96	1.33	1.45	1.44	1.44	0.79	0.84	0.64	0.79
Tap 2: 50-100 mL	-	-	0.92	0.92	-	-	-	-	-	-	-	-
Tap 2: 100-150 mL	-	-	0.80	0.80	-	-	-	-	-	-	-	-
Tap 2: 150–200 mL	0.82	0.90	0.89	0.88	1.50	1.42	1.32	1.41	1.09	0.97	0.63	0.91
Average				0.78				1.46				0.86

5.2   System B: disinfectant switch from free chlorine to monochloramine

Figure 5.4 shows the total lead release in samples collected from System B over a period of 300 d (10 mth). During the initial 72-d conditioning phase, samples were collected at random stagnation periods and the system was flushed after each sampling. Total lead in samples from Taps 1 and 2 exceeded the WHO guideline value of 10 μg/L with the highest reading recorded at 109 μg/L on Day 56. Total lead decreased rapidly when 2 mg/L as Cl_2 of free chlorine was introduced into the system. The presence of free chlorine also caused a decrease in total copper in all samples (Figure 5.5) but had no observable effect on total zinc except in one segmental sampling which had an increase in total zinc (Figure 5.6). The decrease in copper levels may be attributed to either precipitation of copper minerals or copper reduction by galvanic corrosion. In Section 4.3.1, the presence of free chlorine promoted copper protection and lead corrosion in the presence of galvanic connection. Considering our system was built using only copper pipes and brass fittings, total lead or total zinc should increase while total copper should decrease in the event of galvanic corrosion. The concentration of total copper can be used to determine if galvanic corrosion is occurring. Figure 5.6 shows that only one segmental sampling (Tap 2: 100-150 mL) had an increase in total zinc with a corresponding decrease in total copper when free chlorine was introduced to the system. Hence, galvanic corrosion is likely to be occurring at that segmental sampling.

Free chlorine (OCl^- and $HOCl$) is a strong oxidizing agent and can oxidize elemental lead, copper and zinc directly to their soluble forms. Soluble lead, copper and zinc ions can precipitate with carbonates and hydroxides in the solution. Given ample time and fresh supply of water to replenish the salts, the precipitates can form a layer of scaling, passivating the pipe surface and inhibiting further corrosion. Some of these precipitates such as carbonates and hydroxycarbonates can help control the soluble levels of copper, zinc and lead. Table 5.2 shows a list of lead, copper and zinc mineral species, with their respective log K_{sp} values, that can be potentially found in the system. The

formation of PbO_2, a lead compound of lower solubility than hydrocerussite and cerussite, would occur when $Pb(II)$ is oxidized to $Pb(IV)$ in the presence of free chlorine. Lytle and Schock [10] reported that PbO_2 did not form instantaneously, but form only after $Pb(II)$ solids such as cerussite and hydrocerussite had precipitated in their 400-d study using chlorination of lead ions. Other similar works by Liu and Korshin [47] and Zhang and Lin [50] also showed that PbO_2 can be formed by the chlorination of cerussite and hydrocerussite. PbO_2 can control soluble lead levels due to its extremely low solubility if the oxidation-reduction potential of the water can be maintained at a level favoring its formation.

When initial free chlorine concentration was increased to 4 mg/L as Cl_2, there was no significant change to the lead, copper and zinc level. The concentration of lead for all samples decreased when the initial free chlorine concentration was further increased from 4 mg/L to 8 mg/L as Cl_2. All the samples contained lead levels within the WHO guideline value of 10 μg/L [7]. The concentrations of total copper and zinc remained relatively unchanged. The increased free chlorine concentration may have further promoted precipitation of carbonate or hydroxide minerals, resulting in the rapid removal of soluble ions from the solution. It is also possible that the surface lead found on brass may have depleted by this stage of the experiment. It is to be noted that a free chlorine concentration of 8 mg/L as Cl_2 is not practised in real systems as the residual free chlorine would exceed the WHO guideline value of 5 mg/L as Cl_2 [7].

When free chlorine is replaced with monochloramine (2 mg/L as Cl_2) on Day 213, 2 segmental samplings (Tap 1: 50-100 mL and Tap 1: 100-150 mL) exhibited slight increase in total lead levels. Total copper concentration showed an increase for 2 weeks from Day 230 to 244. This could be due to a solid phase transformation of copper minerals from CuO to $Cu(OH)_2$ or $CuCO_3$ during the disinfectant changeover. Zhang et al. [95] reported that CuO and $CuCO_3$ or $Cu(OH)_2$ were formed in copper coupon immersed in monochloramine (4 mg/L as Cl_2) for 30 d based on XPS analysis while

Nguyen et al. [97] showed that $Cu(OH)_2$ was transformed to CuO in the presence of free chlorine (65 mg/L as Cl_2) after 8 d. No significant change was observed in total zinc for the samples collected. The addition of monochloramine could potentially trigger the release of soluble lead into the system, if a layer of lead (IV) oxide had been previously formed on the inner pipe surface. The total lead release (Figure 5.4), however, suggested that lead(IV) oxide was either not formed or present in negligible amount as the majority of the samples collected exhibited little to no change in total lead concentration. Possible reasons include the duration of chlorination which was 140 d as compared to years in real premise systems and the amount of lead release from brass may not be sufficient for PbO_2 to form. Although the findings suggest total lead release remains suppressed for the majority of the samples during the disinfectant switch from free chlorine to monochloramine, it is not conclusive to dismiss that disinfectant switch can result in more lead release due to the duration of this study. This study, however, demonstrates that disinfectant switch does not cause more lead release in new premise systems using copper pipes. This study can be improved by using aged premise copper pipes to represent systems in existing and old buildings.

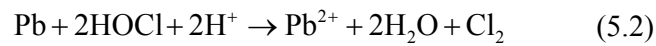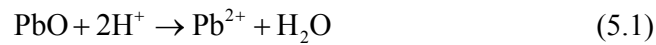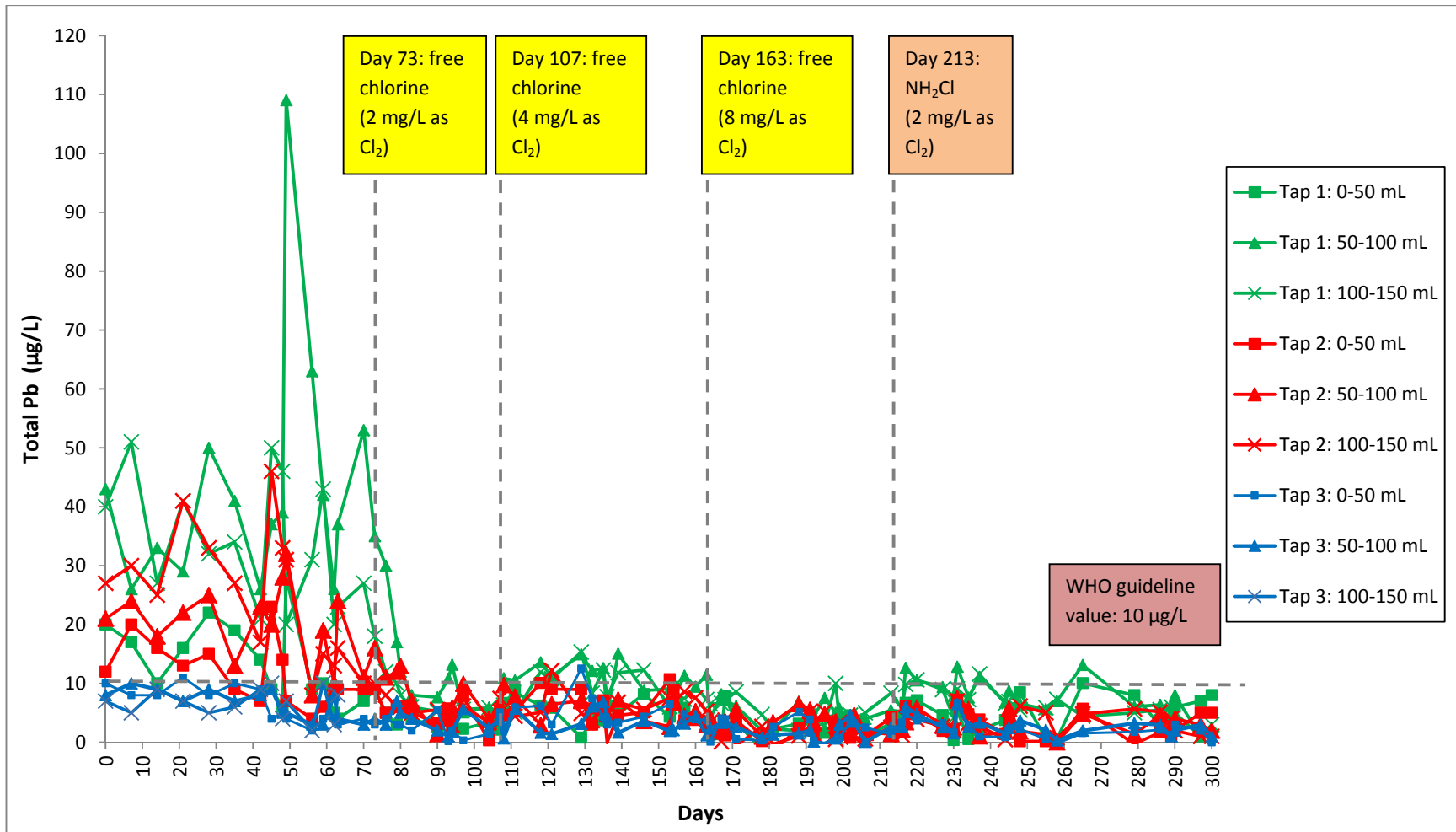**Figure 5.4** Total lead as a function of time in samples collected from System B

Figure 5.5 Total copper as a function of time in samples collected from System B

Figure 5.6 Total zinc as a function of time in samples collected from System B

Table 5.2 Lead, copper and zinc minerals and their respective log K_{sp} [84]

Species	log K_{sp}
$CuCl_2$	6.26
$Cu_2(OH)_3Cl$	7.39
$Cu(OH)_2$	9.29
$Cu_3(PO_4)_2$	-36.9
CuO	8.49
$CuCO_3$	-11.5
$Cu_2CO_3(OH)_2$	-5.49
$Cu_3(CO_3)_2(OH)_2$	-17.4
$Pb_5(PO_4)_3OH$	-62.8
PbO	12.9
$Pb(OH)_2$	8.15
$PbCO_3$	-13.2
$Pb_3(CO_3)_2(OH)_2$	-18.8
$Pb_3(PO4)_2$	-43.5
$PbHPO_4$	-23.8
$PbCl_2$	-4.78
$Pb_5(PO_4)_3Cl$	-84.4
ZnO	11.3
$Zn(OH)_2$	12.5
$ZnCl_2$	7.05
$ZnCO_3$	-10.8
$Zn_3(PO_4)_2 \cdot 4H_2O$	-35.4

Table 5.3 shows the increase in pH values of samples collected at each phase of the experiment. The pH values increased between 0.86 and 1.76 pH unit in 57 out of the 64 samples collected during the conditioning phase. When free chlorine was introduced into the System B, the average increase in pH decreased from 1.32 to 1.02 pH unit. The average increase in pH decreased further as the free chlorine concentration increased. The percentages of samples collected that showed a pH increase of at least 0.80 pH unit were 66%, 61% and 46% at free chlorine concentration of 2 mg/L, 4 mg/L and 8 mg/L as Cl_2 respectively. The higher free chlorine concentration should result in more soluble metal ions release while consuming more H^+ in the during the oxidation process. The extent of pH increase rose with increasing stagnation time in all segmental samplings except one (Tap 2: 100-150 mL) which also exhibited the lowest pH increase with either chlorine or monochloramine addition. Total zinc release (Figure 5.6) was the highest at that segmental sampling, indicating that dezincification may be linked to a lower pH increase. The average increase in pH decreased gradually as the system aged. The increase in pH could be negated by the precipitation of carbonate or hydroxide containing metal minerals which removed alkalinity from the solution.

Table 5.3 Change in pH values with respect to initial tap water pH in samples collected at different stages from System B

System B	Conditioning				Free chlorine (2 mg/L as Cl_2)				Free chlorine (4 mg/L as Cl_2)				Free chlorine (8 mg/L as Cl_2)				Monochloramine (2 mg/L as Cl_2)			
	1 d	3 d	7 d	Avg	1 d	3 d	7 d	Avg	1 d	3 d	7 d	Avg	1 d	3 d	7 d	Avg	1 d	3 d	7 d	Avg
Tap 1: 0-50 mL	1.23	1.40	1.18	1.30	1.09	1.25	1.20	1.20	0.96	1.17	1.25	1.16	1.06	1.05	1.17	1.07	0.83	1.09	1.07	1.03
Tap 1: 50-100 mL	1.10	1.48	1.40	1.37	0.63	0.89	1.03	0.87	0.32	0.65	0.79	0.64	0.76	0.68	0.52	0.68	0.56	0.60	0.61	0.59
Tap 1: 100-150 mL	0.77	0.94	1.20	0.96	0.46	0.64	0.94	0.66	0.30	0.49	0.91	0.57	0.68	0.53	0.55	0.57	0.49	0.55	0.50	0.52
Tap 2: 0-50 mL	1.30	1.58	1.64	1.53	1.11	1.39	1.61	1.38	1.03	1.33	1.70	1.39	1.07	1.30	1.38	1.18	0.86	1.08	1.08	1.04
Tap 2: 50-100 mL	1.01	1.50	1.69	1.42	0.61	1.07	1.20	1.00	0.36	0.94	1.20	0.93	0.79	0.90	1.06	0.87	0.59	0.77	0.88	0.79
Tap 2: 100-150 mL	1.08	1.47	1.47	1.37	0.45	0.72	0.57	0.64	0.50	0.48	0.53	0.50	0.70	0.55	0.50	0.58	0.52	0.52	0.43	0.48
Tap 3: 0-50 mL	1.31	1.45	1.29	1.37	1.11	1.56	1.52	1.46	1.01	1.34	1.65	1.38	1.19	1.32	1.22	1.26	0.88	1.19	1.30	1.18
Tap 3: 50-100 mL	0.98	1.28	1.56	1.28	0.65	0.92	1.31	0.94	0.32	0.83	1.45	0.93	0.79	0.78	1.22	0.84	0.58	0.77	0.87	0.78
Average				1.32				1.02				0.94				0.88				0.80

5.3 System C: monochloramine usage with periodic free chlorine flushing

Figures 5.7, 5.8 and 5.9 show the total lead, total copper and total zinc release in samples collected from System C over a period of 300 d (10 mth) respectively. Similar to System B, the majority of the samples had total lead levels exceeding the WHO guideline value of 10 µg/L with the highest reading recorded at 49 µg/L on Day 49 during the initial 72-d conditioning phase. When monochloramine (2 mg/L as Cl_2) was added to the system, total lead and total copper concentrations decreased rapidly for all samples. Total zinc levels also decreased for all samples, except in two segmental samplings (Tap 1: 50-100 mL and Tap 1: 100-150 mL). In Section 4.3.1, the presence of free chlorine accelerated galvanic corrosion, causing more lead release and reducing copper levels. As mentioned in Section 5.2, if galvanic corrosion were present, total lead or total zinc should increase while total copper should decrease, hence it is likely galvanic corrosion is occurring at those two segmental samplings. Like free chlorine, monochloramine is a strong oxidizing agent and it can oxidize elemental lead, copper and zinc to their soluble forms. However, monochloramine does not oxidize Pb(II) to PbO_2, but causes reductive dissolution of PbO_2 to release Pb^{2+} [17].

When the initial monochloramine concentration was increased to 4 mg/L as Cl_2 on Day 132, there were no significant changes in total lead, copper and zinc release. Total lead concentrations remained low, and well within the WHO guideline level. Like free chlorine, increased monochloramine concentrations could have promoted precipitation of Pb(II) minerals which removed soluble lead ions from the solution. Total copper levels for all samples remained unchanged while total zinc levels showed slight increase at the same two segmental samplings suspected to be affected by galvanic corrosion. This could be attributed to more chloride ions being introduced together with monochloramine that increased the propensity of water to cause dezincification, resulting in higher zinc release [39].

The chlorine flushing conducted on Day 213-230 and Day 244-258 did not have any observable effect on total lead release. The total lead release remained suppressed after the chlorine flushing. This indicates that PbO_2 may not be formed or may be present in negligible amounts during the chlorine flushing. Total copper release increased in 5 out of 9 segmental samplings during chlorine flushing. After flushing has concluded, total copper release decreased to their pre-flushing levels. The increase in total copper during flushing was likely due to a solid phase transformation of the copper minerals from CuO to $Cu(OH)_2$ or $CuCO_3$. No significant changes were observed in total zinc release. This finding suggests that new homes are relatively safe from lead contamination issues when monochloramine is used as the residual disinfectant.
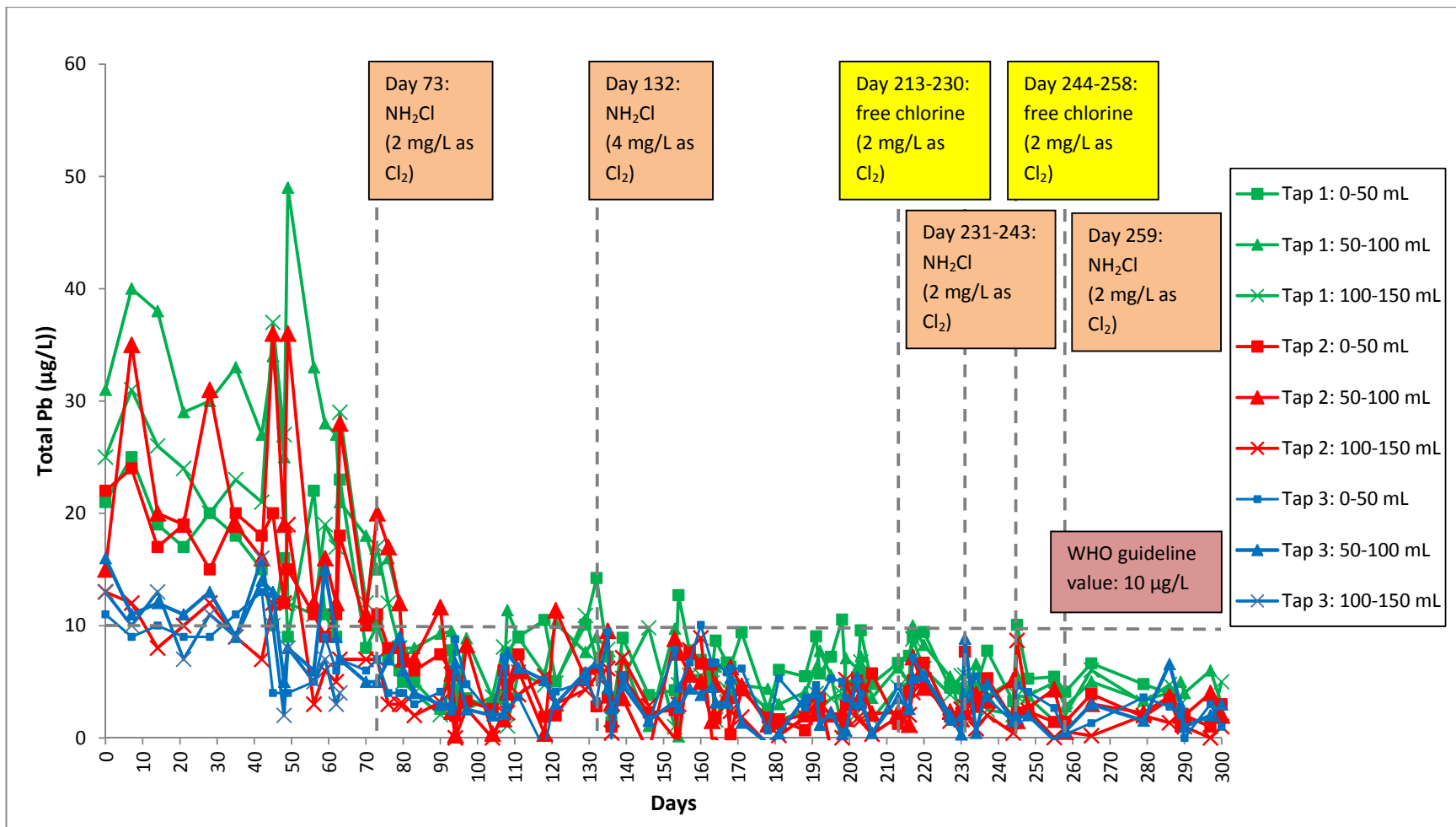
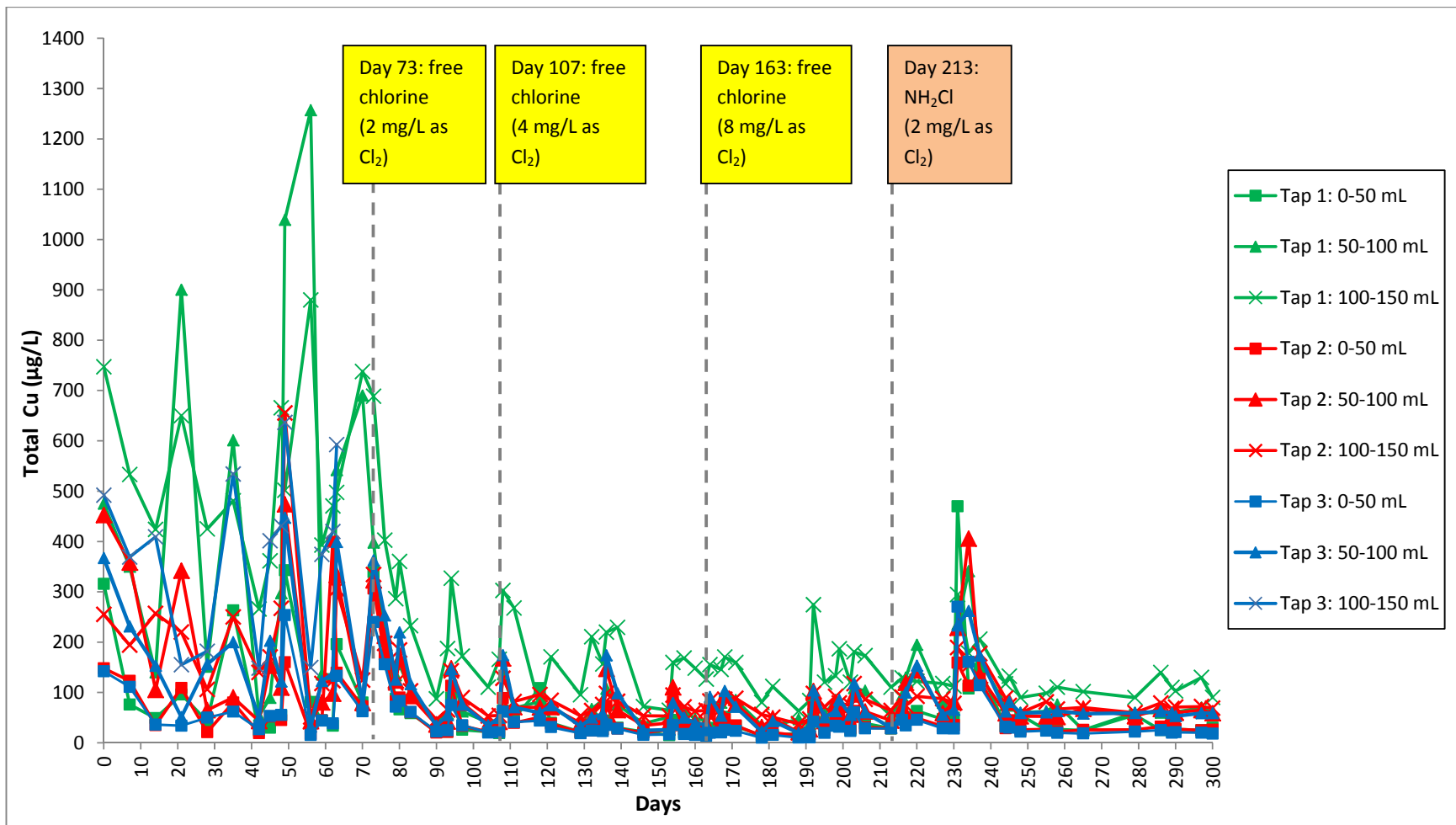**Figure 5.7** Total lead as a function of time in samples collected from System C
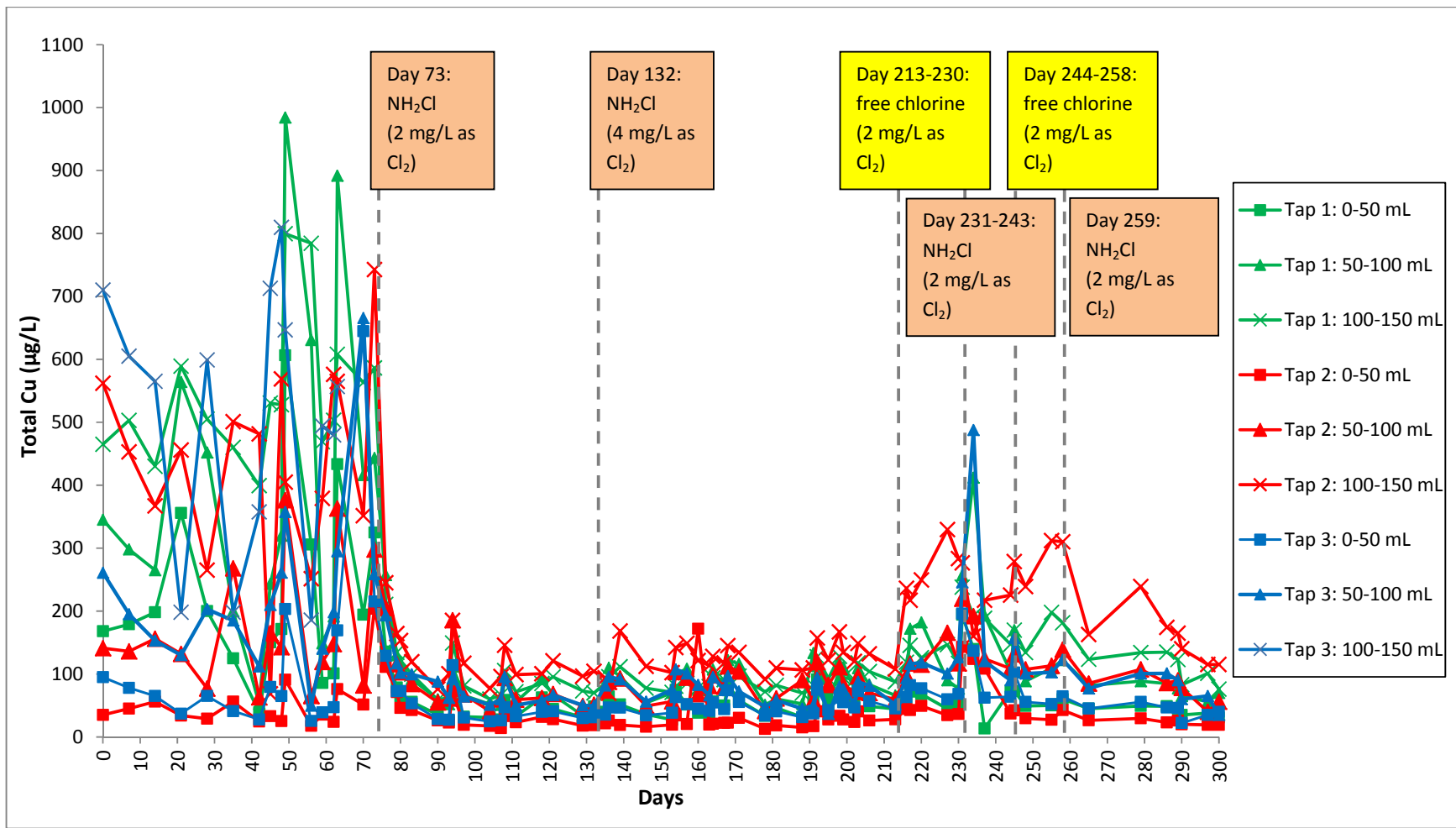
Figure 5.8 Total copper as a function of time in samples collected from System C
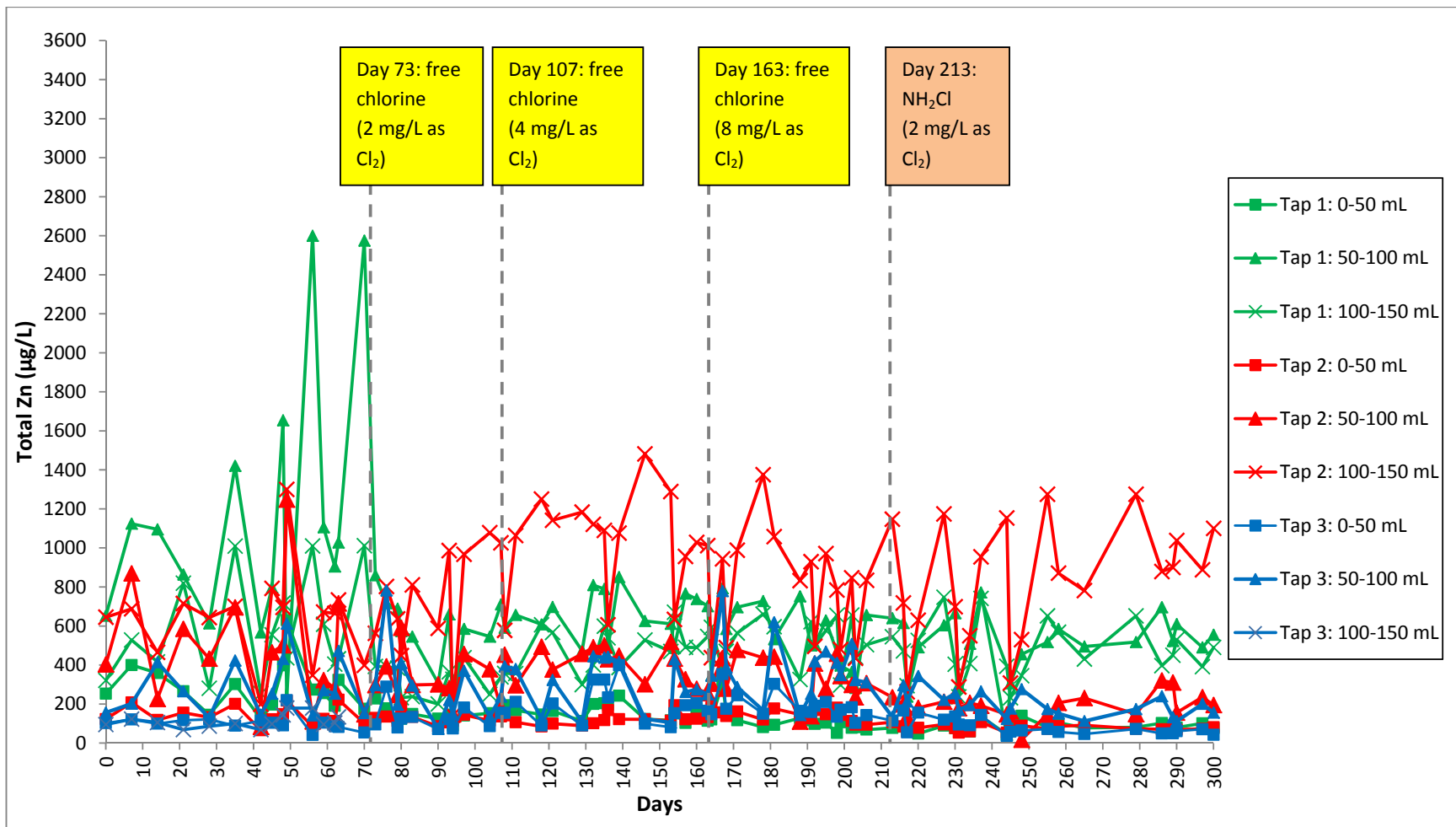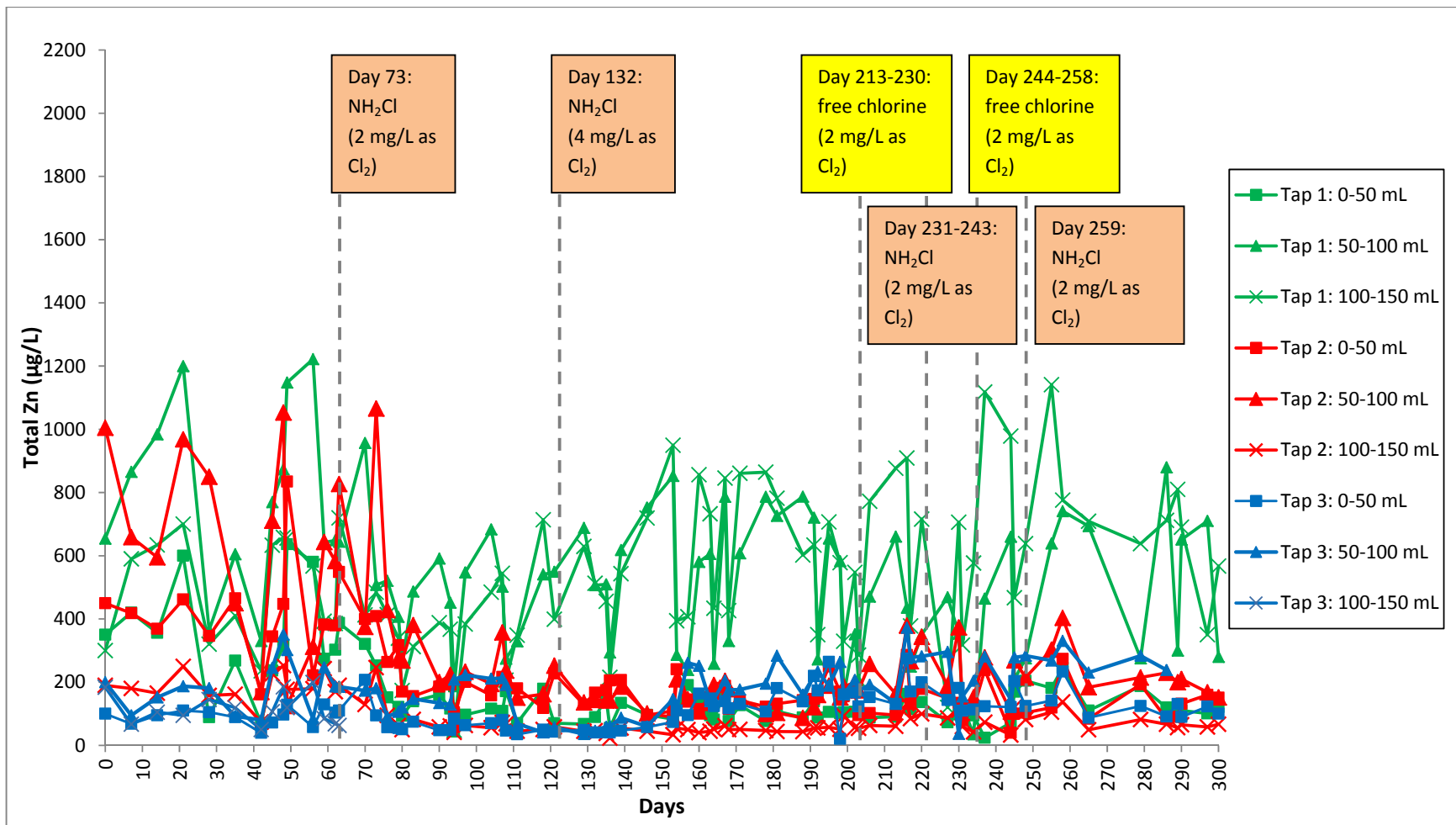
Figure 5.9 Total zinc as a function of time in samples collected from System C

Similar to Systems A and B, the pH values of all samples collected showed an increase at each phase of the experiment (Table 5.4). The pH values of all 64 samples collected increased at least 0.54 pH unit during the conditioning phase. The average increase in pH decreased slightly from 1.24 to 1.14 pH unit when monochloramine was introduced to the system. The average increase in pH decreased as the monochloramine concentration increased. When monochloramine concentration increased from 2 mg/L to 4 mg/L as Cl_2, the percentage of samples collected with an increase of at least 0.80 pH unit in pH values decreased from 92% to 78%. During free chlorine flushing, average pH increase was decreased further from 1.05 to 0.60 pH unit. 81% of 72 samples collected showed a pH increase between 0.25 and 0.94 pH unit during free chlorine flushing. Increasing stagnation times resulted in a higher pH increase in the majority of the samples. Similar to System B, the lowest pH increase was observed in the segmental sampling (Tap 1: 100-150 mL) with the highest total zinc release when disinfectant was added. Comparing pH changes in Systems B and C, the disinfectant switch from monochloramine to free chlorine suppressed the pH increase more than from free chlorine to monochloramine. More importantly, the effect of system age appeared to be the dominant factor in reducing pH changes, instead of the disinfectant used. This implies that the formation of corrosion scale plays an important role in stabilizing the system in terms of controlling pH fluctuation and metal releases.

114

Table 5.4 Change in pH values with respect to initial tap water pH in samples collected at different stages from System C

System C	Conditioning				Monochloramine (2 mg/L as Cl_2)				Monochloramine (4 mg/L as Cl_2)				Free chlorine flushing (2 mg/L as Cl_2)				Monochloramine post-flushing (2 mg/L as Cl_2)			
	1 d	3 d	7 d	Avg	1 d	3 d	7 d	Avg	1 d	3 d	7 d	Avg	1 d	3 d	7 d	Avg	1 d	3 d	7 d	Avg
Tap 1: 0-50 mL	1.28	1.51	1.39	1.42	1.06	1.30	1.40	1.28	1.04	1.11	1.41	1.14	0.52	0.70	0.88	0.74	0.66	0.76	0.80	0.76
Tap 1: 50-100 mL	1.05	1.40	1.50	1.34	0.81	1.03	0.98	0.98	0.68	1.01	0.90	0.87	0.34	0.53	0.68	0.56	0.58	0.53	0.48	0.52
Tap 1: 100-150 mL	0.65	0.90	1.17	0.90	0.89	0.93	0.87	0.91	0.93	0.98	0.88	0.85	0.27	0.35	0.40	0.35	0.47	0.43	0.37	0.41
Tap 2: 0-50 mL	1.07	1.48	1.56	1.40	1.23	1.40	1.36	1.36	1.16	1.18	1.27	1.19	0.63	0.77	0.99	0.84	0.80	0.82	0.86	0.83
Tap 2: 50-100 mL	0.95	1.46	1.49	1.34	0.89	1.03	1.11	1.03	1.03	1.02	1.20	1.05	0.41	0.54	0.75	0.60	0.56	0.54	0.61	0.57
Tap 2: 100-150 mL	0.59	0.74	0.97	0.76	0.93	0.93	1.05	0.96	0.93	0.98	1.04	0.98	0.29	0.40	0.59	0.46	0.49	0.51	0.49	0.50
Tap 3: 0-50 mL	1.24	1.72	1.44	1.53	1.09	1.50	1.70	1.47	1.03	1.17	1.51	1.20	0.41	0.62	0.90	0.70	0.62	0.72	0.82	0.74
Tap 3: 50-100 mL	1.15	1.51	0.78	1.24	0.81	1.12	1.32	1.11	1.00	1.05	1.34	1.09	0.36	0.50	0.76	0.59	0.55	0.54	0.61	0.57
Average				1.24				1.14				1.05				0.60				0.61

5.4   Scaling analysis

To collect scaling for analysis, segments of the pipe were removed from the systems and replaced with new ones. The segments were carefully selected, to be further away from the taps to minimize impacts of changing pipes on the sampling results and ensuring the same segment is not replaced twice. The pipe segments were left to dry at room temperature for at least 48 h. The scaling was removed from the pipe segments using a stainless steel spatula, weighed and acid digested for mass composition. Table 5.5 summarizes the mass percentage of lead, zinc and copper in pipe scaling collected at different phases of the experiment. The sum of lead, zinc and copper mass in the scaling is assumed to be 100% and the percentage reported in Table 5.5 represent the relative abundance of each metal with respect to the sum.

Table 5.5 Mass percentage of lead, zinc and copper in pipe scaling

System	Phase	Pb (%)	Zn (%)	Cu (%)
A	Conditioning phase	1.1	93.0	5.9
	Orthophosphate addition	1.9	39.1	59.0
	No orthophosphate addition	1.2	43.0	55.8
B	Free Chlorine = 8 mg/l as CL_2	3.6	87.5	8.9
	Monochloramine = 2 mg/ L as Cl_2	1.9	83.2	14.9
C	Monochloramine = 4 mg/L as Cl_2	2.4	76.4	21.2
	Flushing cycle 2	2.6	54.4	43.0

The scale collected during the conditioning phase from System A on Day 100 contained high levels of zinc (Table 5.5). This suggests the occurrence of dezincification of brass fittings, a form of galvanic corrosion where zinc is preferentially being corroded over other metals such as copper and lead. High lead levels were also observed during the conditioning phase. Zhang and Edwards [39] reported that waters with a high tendency to cause dezincification in brass can induce higher rates of lead release as well. Figure 5.10 shows that the scale formed is white in colour.
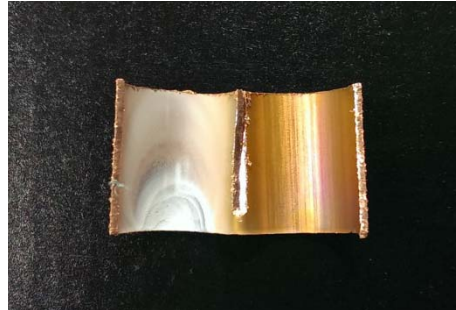
Figure 5.10 Scale formation on a copper pipe segment of System A during conditioning phase.

Figure 5.11 shows bluish-green scale formation on a copper pipe segment from System A during and after orthophosphate addition. Both scales contained similar chemical composition (Table 5.5) but when compared to the scale collected during conditioning phase, they contained significantly more copper and less zinc. Copper corrosion products such as copper hydroxide, carbonate and phosphate, are likely to be present as evident by the bluish-green coloration of the scale. Phosphate minerals have a much lower solubility compared to carbonate or hydroxide minerals (Table 5.2). Compared to other samples from systems B and C, the proportion of copper in the scale is higher for flow system A. The addition of orthophosphate could have caused more precipitation of copper ions.
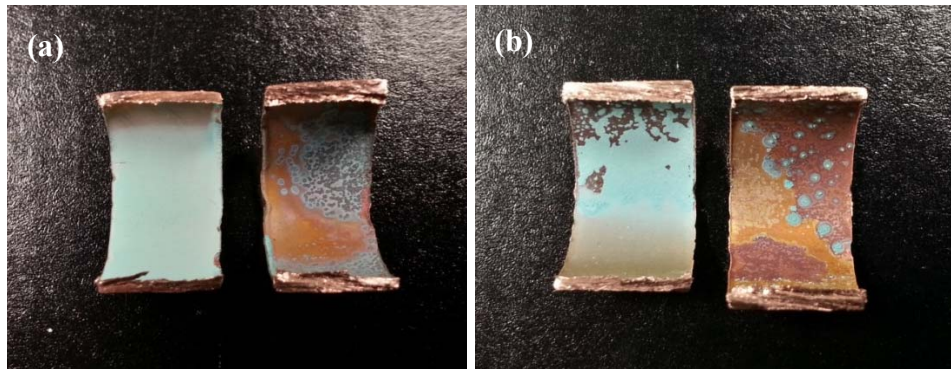
Figure 5.11 Scale formation on a copper pipe segment of System A (a) during orthophosphate (1 mg/L as P) addition and (b) after orthophosphate addition has stopped.

After a pipe segment was removed for scaling analysis, "blue water" was collected during sampling over the next week. This phenomenon was only observed in System A. Under normal flushing during sampling, such a phenomenon was not observed. A clear, colorless filtrate was obtained when the 'blue water' was filtered using a 0.45 micron pore size nylon membrane (Figure 5.12). This suggests that the blue colorization is due to the predominant presence of copper minerals rather than soluble copper ions. "Blue water" is usually the result of excessive copper corrosion by-products which are a result of increasing copper solubility and scale instability [98]. Possible copper mineral species include copper carbonate, copper phosphate and cupric hydroxide. However, the blue colorization was most likely due to copper phosphate since only "blue water" was observed for this flow system where orthophosphate is added. The formation of "blue water" also reveals that copper phosphate may be loosely attached to the pipe surface because normal flushing during sampling did not produce similar result. Physical disturbance such as changing pipes can easily detach the scale from the pipe surface. This finding supports the occurrence of peaks seen in total copper release during orthophosphate addition (Figure 5.2). Due to the formation of "blue water", it should be cautious when using orthophosphate for corrosion control within the premise distribution system due to aesthetic reasons. If orthophosphate addition were implemented, it will be necessary to have a

filtration system before the water leaves the tap. Further studies may be conducted to examine means to mitigate the formation of "blue water" with respect to the optimum dose of orthophosphate.

Figure 5.12 Samples collected, before (right) and after filtration (left), from System A after replacement of pipe segment.

In System B, total copper concentrations increased when the chemicals added are switched form free chlorine to monochloramine (Figure 5.5). Table 5.5 shows that the composition of copper in the scales increased from 8.9% to 14.9% during the disinfectant switch. Hence, changes in the composition of scales can reflect the trends in the release profiles. Similar to total lead and zinc release (Figures 5.4 and 5.6) profiles, lead composition remained low below 5% while zinc composition remained relatively unchanged during the disinfectant switch. The white scale is made up of predominantly zinc minerals such as $Zn(OH)_2$, $ZnCl_2$ and $ZnCO_3$ (Figure 5.13). Reddish-brown precipitate would be expected if lead(IV) oxide were formed during the chlorination phase. However, no such precipitate was observed.

In System C, the increase of copper in the scale from 21.2% to 43.0% during chlorine flushing was in agreement with the increasing total copper release shown in Figure 5.8. The higher copper content in the scale during chlorine flushing gave rise to a slight blue coloration which was absent when only monochloramine was used (Figure 5.14). Total lead and zinc levels remained unchanged during

119

chlorine flushing (Figures 5.7 and 5.9). Lead content in the scale did not show significant change, but zinc content showed a decrease from 76.4% to 55.4% to accommodate the increase in copper content. In both Systems B and C, a switch in disinfectants resulted in an increase in copper release and this was reflected in the increased copper content of the scale.
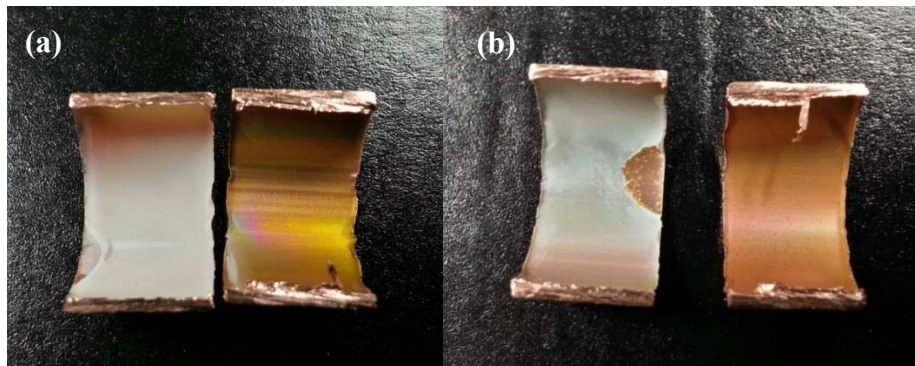
Figure 5.13 Scale formation on a copper pipe segment of System B in the presence of (a) free chlorine (8 mg/L as Cl_2) and (b) monochloramine (2 mg/L as Cl_2).

Figure 5.14 Scale formation on a copper pipe segment of System C in the presence of (a) monochloramine (4 mg/L as Cl_2) and (b) free chlorine (2 mg/L as Cl_2).

5.5　Summary

In this chapter, a modified sampling protocol using smaller sampling volume was proposed and evaluated. The sampling protocol could detect lead contamination and locate the source of lead release more effectively than existing protocols. "Lead-free" brass fittings were identified as the source of lead contamination in this study. Elevated lead levels, far exceeding the WHO guideline value of 10 μg/L, persisted for as long as five months in new systems. Physical disturbances, such as renovation works, could cause short-term spikes in lead release. Orthophosphate was able to suppress total lead release, but caused "blue water" problem. Total lead levels were suppressed when either free chlorine or monochloramine was first introduced to the system. A change in disinfectant did not yield expected rise in lead levels. Total copper and for all three flow systems were well within WHO guideline values throughout the duration of the study.

Chapter 6

Conclusions and recommendations

6.1   Conclusions

In this thesis, the influence of water parameters on galvanic corrosion of lead and the role of orthophosphate in inhibition of lead release in drinking water distribution systems were investigated. The conclusions of this thesis are summarized as below:

(1) Role of orthophosphate as an inhibitor of lead release

With orthophosphate addition, transient peaking of soluble Pb(II) concentration was observed within the first 24 h and can be easily missed out. The peaking and stablization of soluble Pb(II) concentration can be explained based on the dynamics between the rates of PbO_2 reductive dissolution and chloropyromorphite ($Pb_5(PO_4)_3Cl$) precipitation. This finding provides insights to how orthophosphate reduces lead levels under drinking water conditions and highlights the potential risk of short-term elevated lead concentrations. Intensive monitoring following the disinfectant changeover may be required to determine the overall lead exposure when using orthophosphate as a corrosion inhibitor.

(2) Galvanic corrosion of lead in drinking water

In stagnant conditions, reducing pH and increasing either chloride or sulfate concentrations promoted soluble lead release with little precipitation observed. The effect of chloride concentration on soluble lead release was similar to that of sulfate at the same molar concentration and the chloride-to-sulfate mass ratio (CSMR) did not provide a good indication for soluble lead release. In completely-mixed conditions, higher total lead releases were observed than stagnant ones for the same solution composition. The mixing caused an initial rapid release of soluble lead followed by a gradual decrease. This lead peak coincided with the

formation of a layer of white scaling which inhibited galvanic corrosion and suppressed soluble lead levels. More precipitates were observed in the presence of chloride than sulfate under the same molar concentration. The precipitates were identified to be cerussite and hydrocerussite. The findings suggest that distribution systems that have waters containing high levels of chloride may periodically experience lead contamination issues in the form of particulate lead when lead solids are formed and detached. This lead contamination scenario is more dynamic and harder to control.

In the presence of galvanic corrosion, soluble lead release increased while soluble copper release decreased as initial free chlorine or monochloramine concentration increased and the rate of disinfectant decay was slower. Free chlorine caused more lead release than monochloramine when there was no galvanic corrosion. When galvanic corrosion existed, however, monochloramine resulted in more lead release than free chlorine. Distribution systems using monochloramine is more susceptible to lead contamination due to galvanic corrosion than those using free chlorine.

When there was galvanic corrosion, total lead release increased with increasing orthophosphate concentrations while soluble lead release decreased. The faster total lead release was likely driven by the precipitation of lead phosphate minerals. Particulate lead contributed over 96% to total lead concentrations. The lead phosphate precipitates can control soluble lead levels and when immobilized, they should not cause lead contamination issues.

(3) Lead release in simulated premise drinking water distribution systems
A modified sampling protocol using smaller sampling volume was proposed and evaluated. The sampling protocol could detect lead contamination and locate the source of lead release more effectively than existing protocols. "Lead-free" brass fittings were identified as the source

123

of lead in this study. Elevated lead levels persisted for as long as five months in new systems. Physical disturbances, such as renovation works, could cause short-term spikes in lead release. Orthophosphate was able to suppress total lead release, but caused "blue water" problem. Total lead levels were suppressed when either free chlorine or monochloramine was first introduced to the system.

6.2   Recommendations

The results presented in this thesis provided insights to how lead behaves in drinking water, particularly its release by galvanic corrosion and inhibition by orthophosphate addition. Relevant issues such as sampling protocol and lead contamination in premise drinking water systems were investigated as well to give a more comprehensive understanding on lead contamination issues in drinking water. More future studies are required to provide essential information currently lacking in the literature.

(1) Effects of orthophosphate in oxidation of lead(II) carbonate in chlorinated solution

The presence of orthophosphate has been shown to inhibit PbO_2 formation from chlorination of Pb(II) ions [61]. Hydroxypyromorphite was formed instead. However, the role of orthophosphate in lead release from lead carbonate has not been studied. The presence of orthophosphate may prevent lead release from lead carbonate by phosphate adsorption to form a protective layer against free chlorine. In this case, hydroxypyromorphite may not be formed. Research should be conducted to investigate the role of orthophosphate in controlling soluble lead levels during the chlorination of lead carbonate. Solid surface analysis and solid phase characterization may be required to distinguish between orthophosphate adsorption and precipitation.

(2) Effects of orthophosphate in reduction of lead(IV) oxide in monochloraminated solution in the presence of NOM

Both orthophosphate and natural organic matter (NOM) can promote monochloramine decay which can consequently increase lead release from PbO_2 [20, 72]. Orthophosphate may have a synergistic effect with NOM on monochloramine decay causing more short-term lead release. Research should be conducted to investigate the synergistic effect between NOM and monochloramine on the reductive dissolution of PbO_2 in the presence of orthophosphate.

(3) Role of dissolved oxygen in galvanic corrosion in drinking water

Dissolved oxygen acts as an electron acceptor and will be reduced to form hydroxide ions at the cathode in galvanic corrosion. In the absence of dissolved oxygen, it is expected that other species in water such as H^+ will act as the electron acceptor. However, it is not known if changes in reaction pathway can reduce the rate of galvanic corrosion. Future studies should be conducted to investigate the role of dissolved oxygen on the rate of galvanic corrosion.

(4) Pretreatment of brass fittings before installation

Lead found on brass fittings is primarily due to surface contamination [31, 32]. A simple pretreatment such as submerging them in water before installation in real system can significantly reduce the amount of available lead that can potentially be released into the drinking water. However, the findings showed that elevated lead levels persisted for as long as 5 months when brass fittings were used was used in premise distribution systems. Hence, it will be necessary for future research to develop optimum cost-saving methods to remove surface lead from the brass fittings in the shortest time possible.

(5) Effects of aged pipes in lead release in premise drinking water distribution systems

New pipes have been employed in this study and the findings showed that elevated lead levels persisted for as long as five months in system. Aged pipes can be used in similar studies to examine the effect of scaling on lead release.

REFERENCES

1.   Bellinger, D.; Leviton, A.; Sloman, J.; Rabinowitz, M.; Needleman, H.L.; Waternaux, C. Low-level Lead Exposure and Children's Cognitive Function in the Preschool Years. *Pediatrics*. **1991**, 87 (2), 219-227.

2.   Weizsaecker, K. Lead toxicity during pregnancy. *Primary Care Update for OB/GYNS*. **2003**. 10 (6), 304-309.

3.   Papanikoloaou, N.C.; Hatzidaki, E.G.; Boonsalee, S.; Txanakakis, G.N.; Tsatsakis, A.M. Lead Toxicity update. A brief Review. *Med. Sci. Monit*. **2005**, 11, RA329-336.

4.   US Environmental Protection Agency. Prohibition on use of lead pipes, solder and flux. *Federal Register*. **1987**, 52, 20674.

5.   US Environmental Protection Agency. Maximum Contaminant Level Goals and National Primary Drinking Water Regulations for Lead and Copper. *Federal Register*. **1991**, 56, 26460-26564.

6.   US Environmental Protection Agency. National Primary Drinking Water Regulations for Lead and Copper: Short-Term Regulatory Revisions and Clarifications. *Federal Register*. **2007**, 72 (195), 57819-57820.

7.   World Health Organization (WHO). Water Sanitation and Health: Guidelines for drinking-water quality, 4th ed., **2011**.

8.   Schock, M.R.; Wagner, I.; Oliphant, R. The corrosion and solubility of lead in drinking water. Chapter 4 in *Internal Corrosion of Water Distribution Systems*, 2nd ed.; American Water Works Association Research Foundation/DVGW-TZW Cooperative Research Report, **1996**.

9.   Davidson, C.M.; Peters, N.J.; Britton, A.; Brady, L.; Gradliner, P.E.; Lewis, B.D. Surface analysis and depth profiling of corrosion products formed in lead pipes used to supply low alkalinity drinking water. *Water Sci. Technol*. **2004**, 49 (2), 49-54.

10.   Lytle, D.A.; Schock, M.R. Formation of Pb(IV) oxides in chlorinated water. *J. American Water Works Assoc*. **2005**, 97 (11), 102-114.

11. Schock, M.R.; Hyland, R.N.; Welch, M.M. Occurrence of contaminant accumulation in lead pipe scales from domestic drinking-water distribution systems. *Environ. Sci. Technol.* **2008**, 42, 4285-4291.

12. Kim, E.J.; Herrera, J.E. Characteristics of lead corrosion scales formed during drinking water distribution and their potential influence on the release of lead and other contaminants. *Environ. Sci. Technol.* **2010**, 44, 6054-6061.

13. Renner, R. Plumbing the depths of D.C.'s drinking water crisis. *Environ. Sci. Technol.* **2004**, 38 (12), 224A-227A.

14. Edwards, M.; Dudi, A. Role of chlorine and chloramines in corrosion of lead-bearing materials. *J. American Water Works Assoc.* **2004**, 96(10), 69-81.

15. Edwards, M.; Triantafyllidou, S.; Best, D. Elevated blood lead in young children due to lead-contaminated drinking water: Washington, DC, 2001-2004. *Environ. Sci. Technol.* **2009**, 43, 1618-1623.

16. Renner, R. Out of plumb when water treatment causes lead contamination. *Environ. Health Perspectives* **2009**, 117(12), A542-A547.

17. Lin, Y.P.; Valentine, R.L. Release of Pb(II) from monochloramine-mediated reduction of lead oxide (PbO_2). *Environ. Sci. Technol.* **2008**, 42, 9137-9143.

18. Lin, Y.P.; Valentine, R.L. Reduction of lead oxide (PbO_2) and release of Pb(II) in mixtures of natural organic matter, free chlorine and monochloramine. *Environ. Sci. Technol.* **2009**, 43, 3872-3877.

19. Dryer, D.J.; Korshin, G.V. Investigation of the reduction of lead dioxide by natural organic matter. *Environ. Sci. Technol.* **2007**, 41, 5510-5514.

20. Lin, Y.P.; Valentine, R.L. The release of lead from the reduction of lead oxide (PbO_2) by natural organic matter. *Environ. Sci. Technol.* **2008**, 42 (3), 760-765.

21. Xie, Y.; Wang, Y.; Giammar, D.E. Impact of chlorine disinfectants on dissolution of the lead corrosion product PbO_2. *Environ. Sci. Technol.* **2010**, 44, 7082-7088.

22. Xie, Y.; Wang, Y.; Singhal, V.; Giammar, D.E. Effects of pH and carbonate concentration on dissolution rates of the lead corrosion product PbO_2. *Environ. Sci. Technol.* **2010**, 44, 1093-1099.

23. Renner, R. Reaction to the solution: lead exposure following partial service line replacement. *Environ. Health Perspectives* **2010**, 118(5), A202-A208.

24. Health Canada. Minimizing exposure to lead from drinking water distribution systems. H128-1/07-513E, Water Talk, Canada, **2007**. Available online at http://www.hc-sc.gc.ca/ewh-semt/alt_formats/hecs-sesc/pdf/pubs/water-eau/lead-plomb-eng.pdf

25. DWI. Lead in drinking water. Drinking Water Inspectorate, London, **2010**. Available online at http://dwi.defra.gov.uk/consumers/advice-leaflets/lead.pdf

26. US Environmental Protection Agency. Reducing lead in drinking water: a benefit analysis. *Office of Policy and Evaluation*. Draft final report, **1986**, EPA-230-09-86-019.

27. LEAD. Lead in drinking water in Australia: hazards associated with lead based solder on pipes. The LEAD Group Inc., Australia, **2013**. Available online at http://www.lead.org.au/lanv8n1/l8v1-11.html

28. Edwards, M., Triantafyllidou, S. Chloride-to-sulfate mass ratio and lead leaching to water. *J. American Water Works Assoc.* **2007**, 99(7), 96-109.

29. Willison, H.; Boyer, T.H. Secondary effects of anion exchange on chloride, sulfate, and lead release: Systems approach to corrosion control. *Water Res.* **2012**, 46, 2385-2394.

30. Kimbrough, D.E. Brass corrosion as a source of lead and copper in traditional and all-plastic distribution systems. *J. American Water Works Assoc.* **2007**, 99(8), 70-76.

31. Elfland, C.; Scardina, P.; Edwards, M. Lead-contaminated water from brass plumbing devices in new buildings. *J. American Water Works Assoc.* **2010**, 102(11), 66-76.

32. CDA. Alloy Data Sheet, Envirobrass (SeBiLOY), Non-Leaded Red Brass and Yellow Brass Casting Alloys, A1032-95/00. Copper Development Association Inc., New York, **2000**. Available online at http://www.copper.org/applications/industrial/PDF_files/sebiloy.PDF

33. Lytle, D.A.; Schock, M.R. Stagnation time, composition, pH, and orthophosphate effects on metal leaching from brass. EPA/600/R-96-103, Washington, **1996**.

34. ISO. International standard (ISO 8044), Corrosion of metals and alloys: basic terms and definitions. **1991**.

35. Perez, N. Electrochemistry and corrosion science. Kluwer Academic Publishers: USA, **2004**.

36. Atkins, P.; Paula, J.D. *Physical Chemistry*, 8th ed.; Oxford, Freeman, and Co.: United States and Canada, **2006**.

37. Oliphant, R.J. Summary report on the contamination of potable water by lead from soldered joints. 125E, *Water Res. Centre*, Wiltshire, England, **1983**.

38. Gregory, R. Galvanic corrosion of lead solder in copper pipework. *Water & Envir. J.* **1990**, 4(2), 112-118.

39. Zhang, Y.; Edwards, M. Zinc content in brass and its influence on lead leaching. *J. American Water Works Assoc.* **2011**, 103(7), 76-83.

40. Nguyen, C.K.; Stone, K.R.; Edwards, M.A. Chloride-to-sulfate mass ratio: Practical studies in galvanic corrosion of lead solder. *J. American Water Works Assoc.* **2011**, 103(1), 81-92.

41. Triantafyllidou, S., Edwards, M. Galvanic corrosion after simulated small-scale partial lead service lead replacements. *J. American Water Works Assoc.* **2011**, 103(9), 85-99.

42. St. Clair, J.; Stamopoulos, C.; Edwards, M. Technical note: increased distance between galvanic lead:copper pipe connections decreases lead release. *Corrosion* **2012**, 68(9), 779-783.

43. Nguyen, C.K.; Stone, K.R.; Dudi, A.; Edwards, M.A. Corrosive microenvironments at lead solder surfaces arising from galvanic corrosion with copper pipe. *Environ. Sci. Technol.* **2010**, 44, 7076-7081.

44. Jones, D.A. Principles and prevention of corrosion, 2nd ed. Pearson Education, Inc.: Singapore, **2005**.

45. Snoeyink, V.L., Wagner, I. Principles of corrosion of water distribution systems. In internal corrosion of water distribution systems, 2nd ed. Denver, Colo.: AwwaRF and AWWA, **1996**.

46. Reiber, S. Galvanic stimulation of corrosion on lead-tin solder-sweated joints. *J. American Water Works Assoc.* **1991**, 83(7), 83-91.

47. Liu, H.; Korshin, G.V.; Ferguson, J.F. Investigation of the kinetics and mechanisms of the oxidation of cerussite and hydrocerussite by chlorine. *Environ. Sci. Technol.* **2008**, 42, 3241-3247.

48. Liu, H.; Korshin, G.V.; Ferguson, J.F. Interactions of Pb(II)/Pb(IV) solid phases with chlorine and their effects on lead release. *Environ. Sci. Technol.* **2009**, 43, 3278-3284.

49. Wang, Y.; Xie, Y.; Li, W.; Wang, Z., Giammar, D.E. Formation of lead (IV) oxides from lead(II) compounds. *Environ. Sci. Technol.* **2010**, 44, 1093-1099.

50. Zhang, Y.; Lin, Y.P. Determination of PbO_2 formation kinetics from the chlorination of Pb(II) carbonate solids via direct PbO_2 measurement. *Environ. Sci. Technol.* **2011**, 45 (6), 2338-2344.

51. Arnold, Jr., R.B.; Edwards, M. Potential reversal and the effects of flow pattern on galvanic corrosion of lead. *Environ. Sci. Technol.* **2012**, 46, 10941-10947.

52. Boyd, G.R.; Reiber, S.H.; McFadden, M.S.; Korshin, G.V. Effects of changing water quality on galvanic coupling. *J. American Water Works Assoc.* **2012**, 104(3), 45-46.

53. Wang, Y.; Jing, H.; Mehta, V.; Welter, G.J.; Giammar, D.E. Impact of galvanic corrosion on lead release from aged lead service lines. *Water Res.* **2012**, 46, 5049-5060.

54. Cartier, C.; Arnold Jr., R.B.; Triantafyllidou, S.; Prévost, M.; Edwards, M. Effect of flow rate and lead/copper pipe sequence on lead release from service lines. *Water Res.* **2012**, 46, 4142-4152.

55. Boffardi, B.P. Potable water treatment and monitoring for corrosion and scale control. *Jour. NEWWA*. **1988**, 102(6), 111.

56. Edwards, M.; Mcneill, L.S. Effect of phosphate inhibitors on lead release from pipes. *J. American Water Works Assoc.* **2002**, 94(1), 79-90.

57. Hayes, C.; Aertgeerts, R.; Barrott, L.; Becker, A.; Benoliel, M.J.; Croll, B.; Edwards, M.; Gari, D.; Hoekstra, E.; Jung, M.; Postawa, A.; Ruebel, A.; Russell, L.; Schock, M.; Skubala, N.; Witszak, S.; Tielemans, M.; Zabochnicka-Swiatek, M. Best practice guide on the control of lead in drinking water, ed. Hayes, C. IWA Publishing: London, **2010**.

58. Nriagu, J.O. Lead orthophosphates-IV formation and stability in the environment. *Geochim. Cosmochim. Acta*. **1974**, 38, 887-898.

59. Stumm, W. Chemistry of the solid-water interface: processes at the mineral-water and particle-water interface in natural systems. John Wiley & Sons, Inc.: Canada, **1992**.

60. Nriagu, J.O. Lead orthophosphates-II stability of chloropyromorphite at 25°C. *Geochim. Cosmochim. Acta*. **1973**, 37, 367-377.

61. Lytle, D.A.; Schock, M.R.; Scheckel, K. The inhibition of Pb(IV) oxide formation in chlorinated water by orthophosphate. *Environ. Sci. Technol.* **2009**, 43, 6624-6631.

62. Schock, M.R.; Lytle, D.A., Sandvig, A.M.; Clement, J.; Harmon, S.M. Replacing polyphosphate with silicate to solve lead, copper, and source water iron problems. *J. American Water Works Assoc.* **2005**, 97(11), 84-93.

63. Zhang, P.; Ryan, J. Transformation of Pb(II) from cerussite to chloropyromorphite in the presence of hydroxyapatite under varying conditions of pH. *Environ. Sci. Technol.* **1999**, 33, 625-630.

64. Zhang, P.; Ryan, J.; Bryndzia L.T. Pyromorphite formation from goethite adsorbed lead. *Environ. Sci. Technol.* **1997**, 31, 2673-2678.

65. Zhang, P.; Ryan, J. Formation of chloropyromorphite from galena (PbS) in the presence of hydroxyapatite. *Environ. Sci. Technol.* **1999**, 33, 618-624.

66. Scheckel, K.G.; Ryan, J. Effects of aging and pH on dissolution kinetics and stability of chloropyromorphite. *Environ. Sci. Technol.* **2002**, 36, 2198-2204.

67. Sandvig, A.; Kwan, P.; Kirmeyer, G.; Maynard, B.; Mast, D.; Trussell, R.; Trussell, S.; Cantor, A.; Prescott, A. Contribution of service line and plumbing fixtures to lead and copper rule compliance issue. AwwaRF, Denver, **2008**.

68. Hoekstra, E.J.; Hayes, C.R.; Aertgeerts, R.; Becker, A.; Jung, M.; Postawa, A.; Russell, L.; Witczak, S. Guidance on sampling and monitoring for lead in drinking water. Luxembourg, European Commission, Joint Research Centre, Institute for Health and Consumer Protection, **2009**.

69. van den Hoven, T.; Slaats, N. Lead monitoring. Analytical methods for drinking water, advances in sampling and analysis. (Quevaullier, P.; Thompson, K.C., editors) Wiley & Sons, Oxford, UK, **2006**.

70.   Hayes, C.R.; Incledion, S.; Balch, M. Experience in Wales (UK) of the optimization of ortho-phosphate dosing for controlling lead in drinking water. *J. Water & Health* **2008**, 6(2), 177-185.

71.   Government of Ontario. Ontario Regulation 399/07. Safe Drinking Water Act, 2002 – Amended to O. Reg. 170/03. Drinking Water System. Ont., Canada, **2007**.

72.   Ministere du Développement durable, de I'Environnement et des. Parcs (MDDEP). Reglement sur la Qualite de l'eau Potable . Québec, **2005**.

73.   Valentine, R.L.; Jafvert, R.L. General acid catalysis of monochloramine disproportionation. *Environ. Sci. Technol.* **1988**, 22, 691-696.

74.   Housing & Development Board. Annual Report, Key statistics, **2012**. Available online at http://www10.hdb.gov.sg/eBook/AR2012/keystatistics.html

75.   Triantafyllidou, S.; Parks, J.; Edwards, M. Lead particles in potable water. *J. American Water Works Assoc.* **2007**, 99(6), 107-117.

76.   Public Utility Board. *Handbook on Application For Water Supply.* Singapore, **2009**.

77.   APHA, AWWA and WEF. *Standard Methods for the Examination of Water and Wastewater*. Washington, D.C.: American Public Health Association, American Water Works Association, and Water Environment Federation. **2012**.

78.   Valentine, R.L.; Ozekin, K.; Vikesland, P.J. Chloramine decomposition in distribution system and model waters. *AWWARF* and *AWWA*. **1998**, Denver, CO.

79.   Committee on Public Water Supply Distribution Systems: Assessing and Reducing Risks. Public Water Supply Distribution Systems: Assessing and Reducing Risks: First Report; National Research Council of the National Academies, National Academies Press: Washington, DC, **2005**.

80.   Thomas, J.M.; Tricker, M.J. Electronic structure of the oxides of lead. *J. Chem. Soc., Faraday Trans. 2*. **1975**, 71, 329-336.

81.   Payne, D.J.; Egdell, R.G.; Law, D.S.L.; Glans, P.A.; Learmonth, T.; Smith, K.E.; Guo, J.; Walsh, A.; Watson, G.W. Experimental and theoretical study of the electronic structures of α-PbO and β-PbO$_2$. *J. Mater. Chem*. **2007**, 17, 267-277.

82. Eighmy, T.T.; Shaw, E.L.; Eusden, J.D.Jr; Francis, C.A. Chloropyromorphite ($Pb_5(PO_4)_3Cl$) by XPS: an environmentally important secondary mineral. *Surface Science Spectra*. **1998**, 5, 122-129.

83. ICDD. Powder diffraction file: PDF-4. Newton Square, PA. **2002**.

84. Gustafsson, J.P. Visual MINTEQ, ver. 3.0. Stockholm, Sweden. **2012**.

85. Morel, F.M.M.; Hering, J.G. Principles and application of aquatic chemistry. Wiley-Interscience: New York, **1993**, 374.

86. Xie, L.; Giammar, D.E. Equilibrium solubility and dissolution rate of the lead phosphate chloropyromorphite. *Environ. Sci. Technol.* **2007**, 41, 8050-8055.

87. Martinez, C.E.; Jacobson, A.R.; Mcbride, M.B. Lead phosphate minerals: solubility and dissolution by model and natural ligands. *Environ. Sci. Technol.* **2004**, 38, 5584-5590.

88. Dudi, A. Reconsidering lead corrosion in drinking water: Product testing, direct chloramines attack and galvanic corrosion. Master's Thesis, Virginia Tech, Blacksburg, VA, **2004**.

89. Reiber, S.; Dufresne, L. Effects of external currents and dissimilar metal contact on corrosion of lead from lead service lines. Final report to US Environmental Protection Agency, Region 3, Philadelphia, **2006**.

90. Birks, N.; Pettit, F.A. Erosion-corrosion and wear. *Journal De Physique IV*, 667-676.

91. Liu, H.; Schonberger, K.D.; Korshin, G.V.; Ferguson, J.F.; Meyerhofer, P.; Desormeaux, E.; Luckenbach, H. Effects of blending of desalinated water with treated surface drinking water on copper and lead release. *Water Res.* **2010**, 44, 4057-4066.

92. Xie, Y.; Giammar, D.E. Effects of flow and water chemistry on lead release rates from pipe scales. *Water Res.* **2011**, 45, 6525-6534.

93. Schock, M.R.; Lytle, D.A.; Clement, J.A. Effect of pH, DIC, orthophosphate and sulfate on drinking water cuprosolvency. EPA/600/R-95-085, USEPA, Office of Research & Development, Cincinnati, **1995**.

94. Yohai, L.; Schreiner, W.H.; Vazquez, M.; Valcarce, M.B. Surface characterization of copper, zinc and brass in contact with tap water inhibited with phosphate ions. *Applied Surf. Sci.* **2011**, 257, 10089-10095.

95. Zhang, X., Pehkonen, S. O., Kocherginsky, N., Ellis, G. A. Copper corrosion in mildly alkaline water with disinfectant monochloramine. *Corr. Sci.* **2002**, 44(11), 2507-2528.

96. Zhang, Y.; Edwards, M. Effects of pH, chloride, bicarbonate and phosphate on brass dezincification. *J. American Water Works Assoc.* **2011**, 103(4), 90-102.

97. Nguyen, C.K.; Powers, K.A.; Raetz, M.A.; Parks, J.L.; Edwards, M.A. Rapid free chlorine decay in the presence of $Cu(OH)_2$: Chemistry and practical implications. *Water Res.* **2011**, 45(16), 5302-5312.

98. Schock, M.; Sandvig, A. Long-term effects of orthophosphate treatment on copper concentration. *J. American Water Works Assoc.* **2009**, 101(7), 71-82.